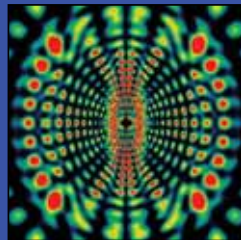


Quantum transport in chaotic and disordered systems

Andreas Buchleitner

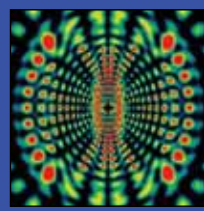
Quantum optics and statistics

Institute of Physics, Albert Ludwigs University of Freiburg



**Nonlinear Dynamics
in Quantum Systems**

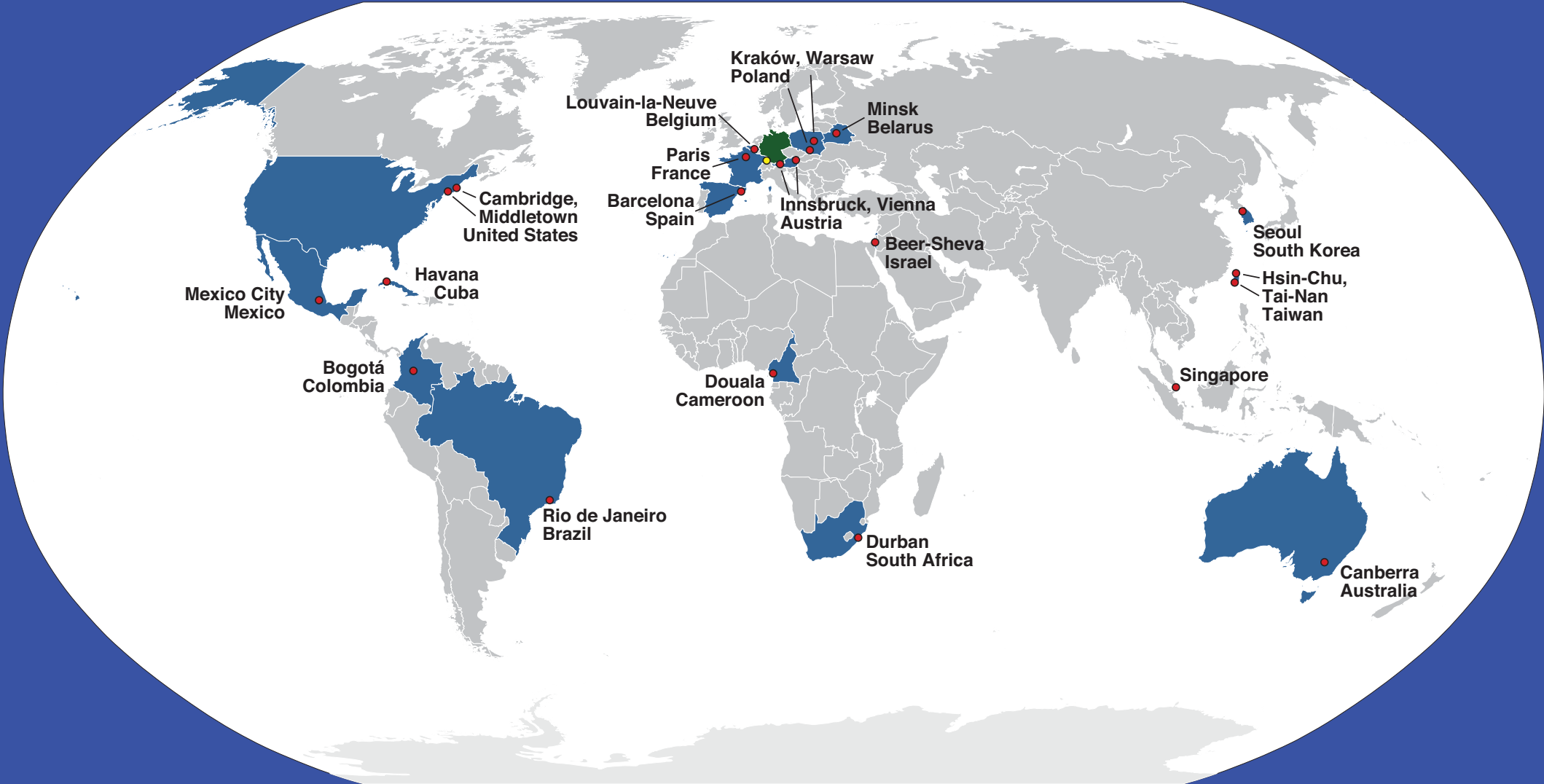
Tainan, 27-29 August 2010



Nonlinear Dynamics in Quantum Systems



In Collaboration with . . .



funded by DFG, DAAD, AvH and VolkswagenStiftung

Key words

transport

chaos

disorder

Chaos, disorder, complexity

Given a state

$$|\Psi\rangle = \sum_j c_j |\phi_j\rangle,$$

the number

$$W = \exp \left(- \sum_j |c_j|^2 \ln |c_j|^2 \right)$$

provides a good measure of complexity, where W has to be minimized over the choice of the basis set $\{|\phi_j\rangle\}$.

Strict determinism – absence of complexity

Given x_0 and v_0 at time t_0 , and the forces acting on the particle, we can completely reconstruct/predict its past/future. . .

The particle's state really is its trajectory $x(t), v(t)$ for all times t



de facto, there is no evolution – no time arrow – time just a parameter

Ubiquity of deterministic chaos/complexity

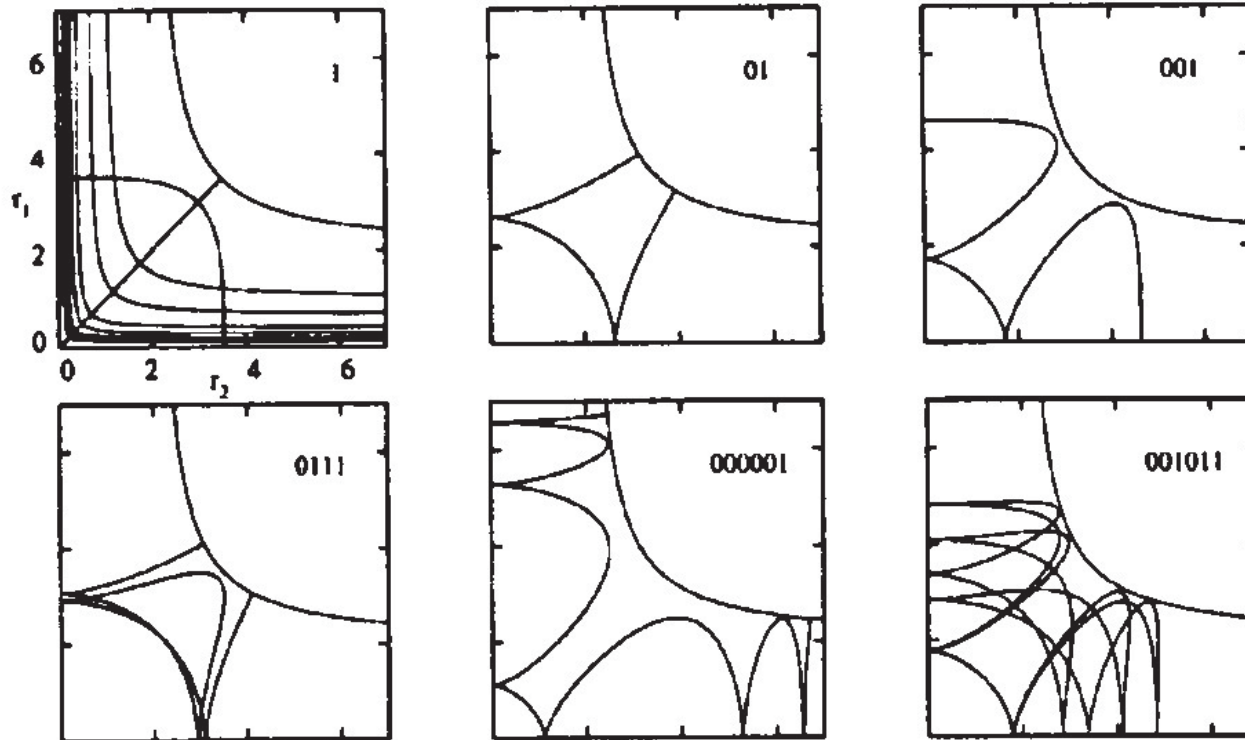
. . . implies . . .

- exponential sensitivity to perturbations
- need of exponentially many observations to unambiguously characterize an individual trajectory
- **intrinsic uncertainty** on the state if only finite number of observations available

e.g., **double pendulum**

Symbolic code of helium

(electrons in the helium atom – map trajectories on binary code)



vice versa, exponentially unstable **trajectories encode “complex” information**

in particular: the spectrum

the more complex, the longer the code

Ingredients for complexity in quantum systems

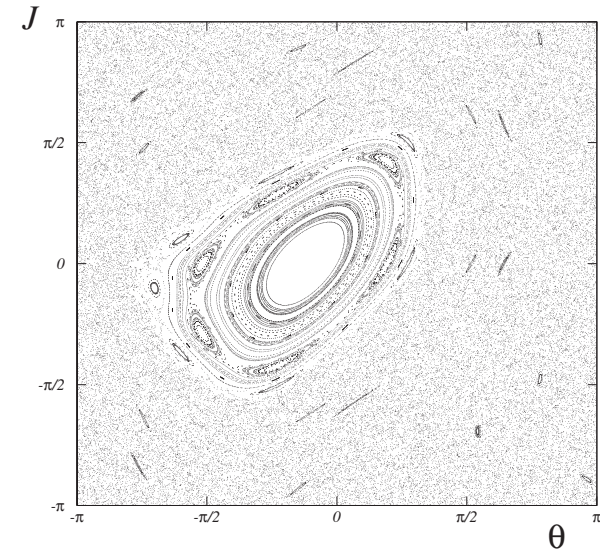
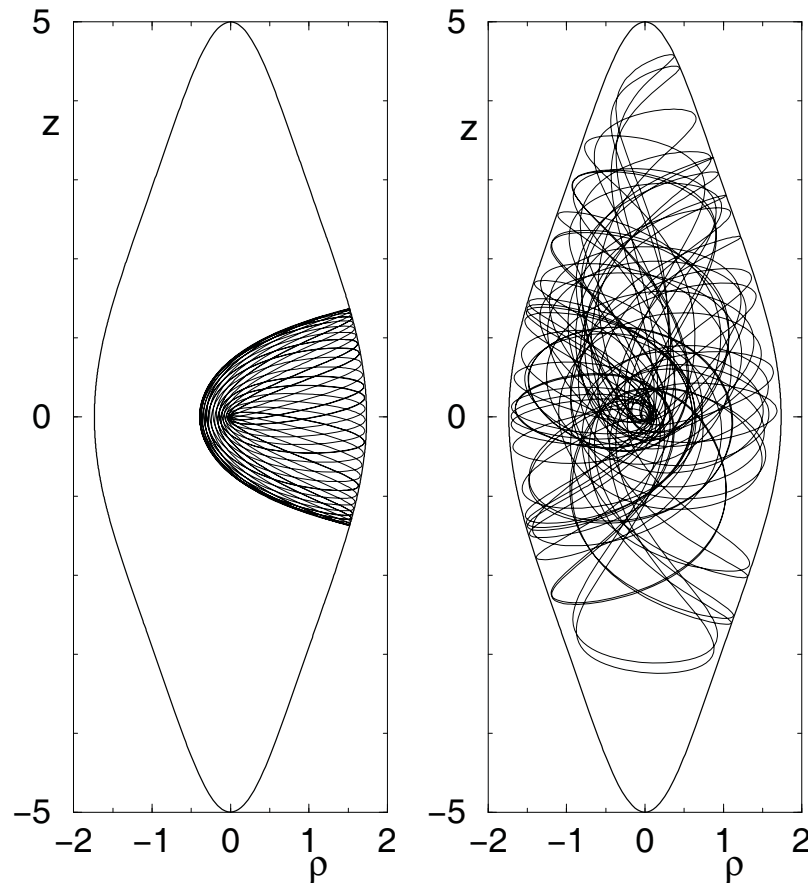
- strong coupling of few degrees of freedom (chaos)
- disorder (solid state)
- many-particle interactions (nuclear physics)
- high density of states (semiclassics)

Dynamical Chaos

– e.g., atomic hydrogen in a static magnetic field $\parallel \hat{z}$ –

near integrable

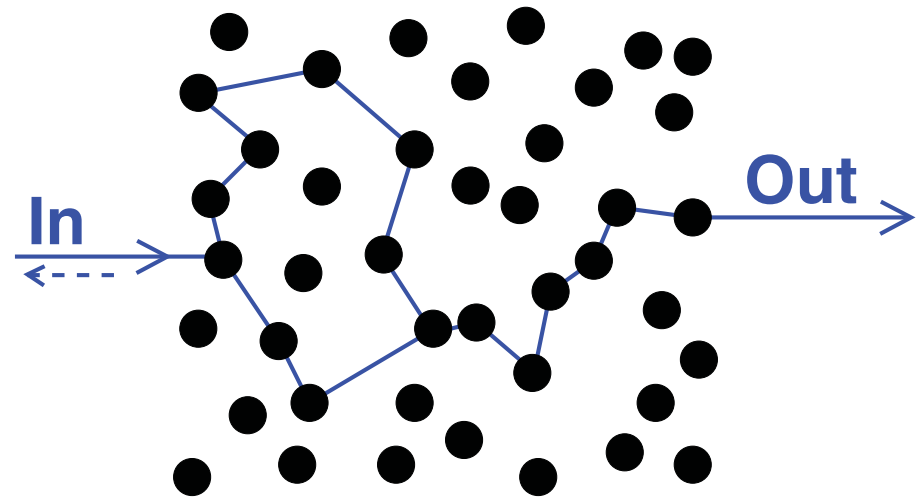
chaotic



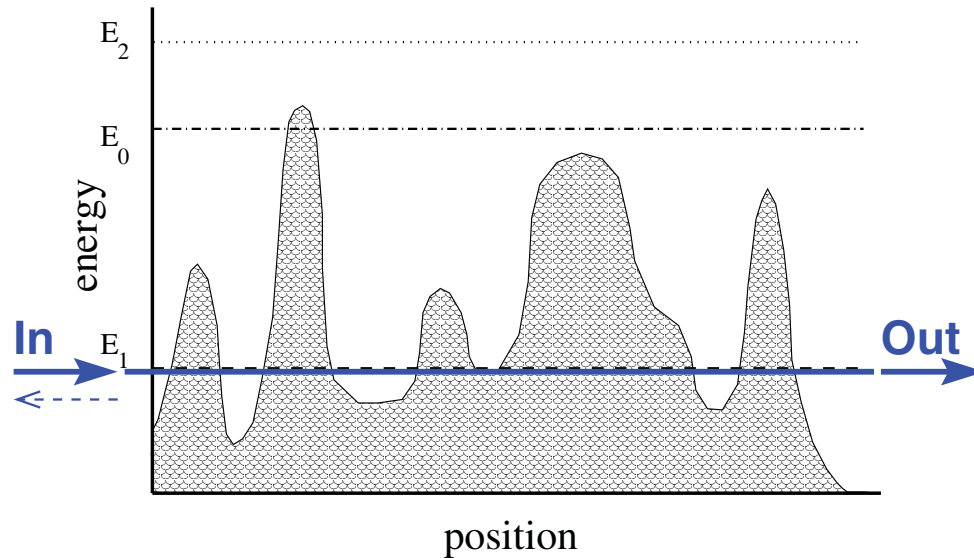
[Delande & Gay, 1986]

Wave propagation in disordered media

- light scattering on a disordered medium
 - milk
 - Saturn's rings
 - (ultra) cold atoms
- **interference effects despite disorder!**
(*distinct* from double slit with jitter!)



Transmission across disordered potentials



strong/Anderson localization

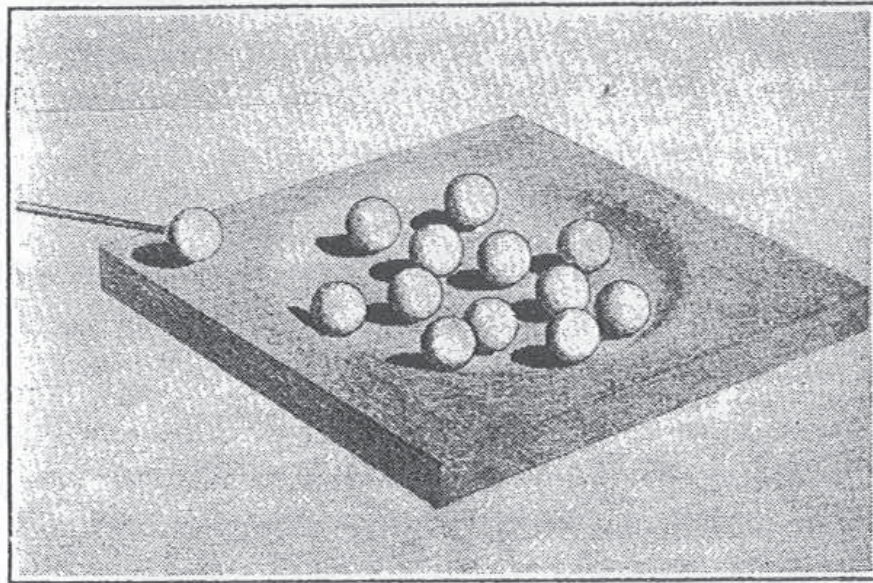
– would like to do this with BEC's in optical lattices –

- metal-insulator transition in disordered solids [Anderson 1958]
- exponentially localized states – localization length ξ , sample length L
- in general: no microscopic control on disorder
- seek statistical predictions on transmission properties

Many particle interactions – then and now

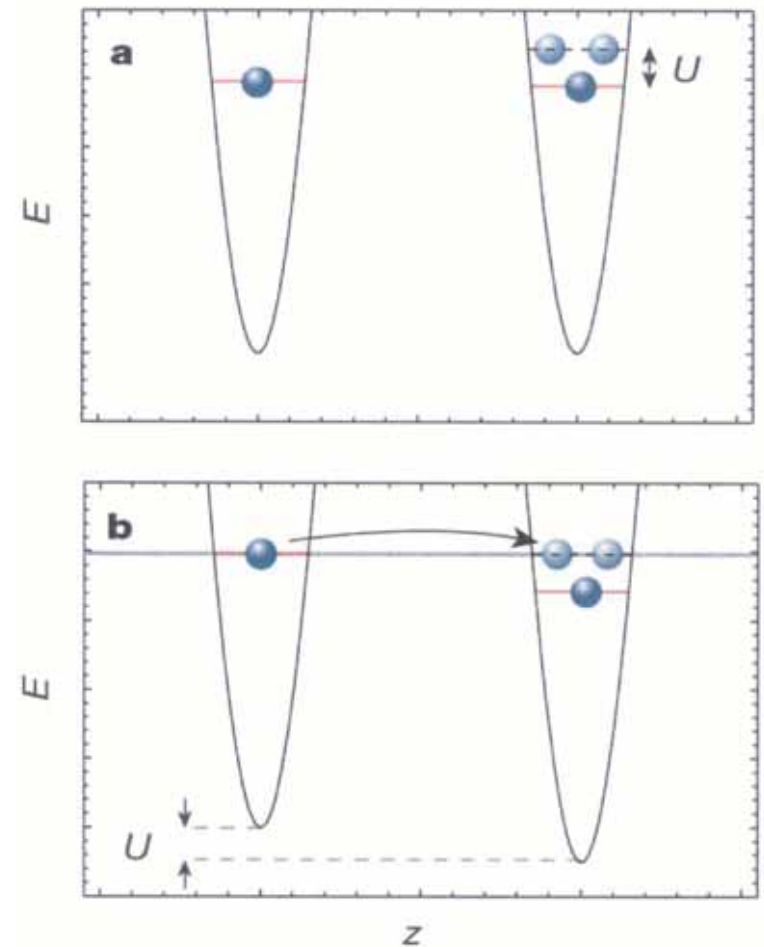
$$H_B = -\frac{J_B}{2} \left(\sum_l a_{l+1}^\dagger a_l + h.c. \right) + \frac{W_B}{2} \sum_l n_l (n_l - 1)$$

compound nuclei

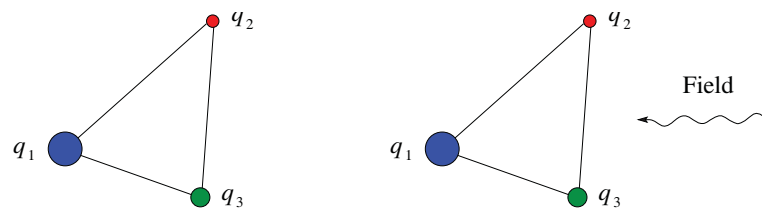


[N. Bohr, 1936]

ultracold atoms



[Greiner et al., 2002]



Non-integrable

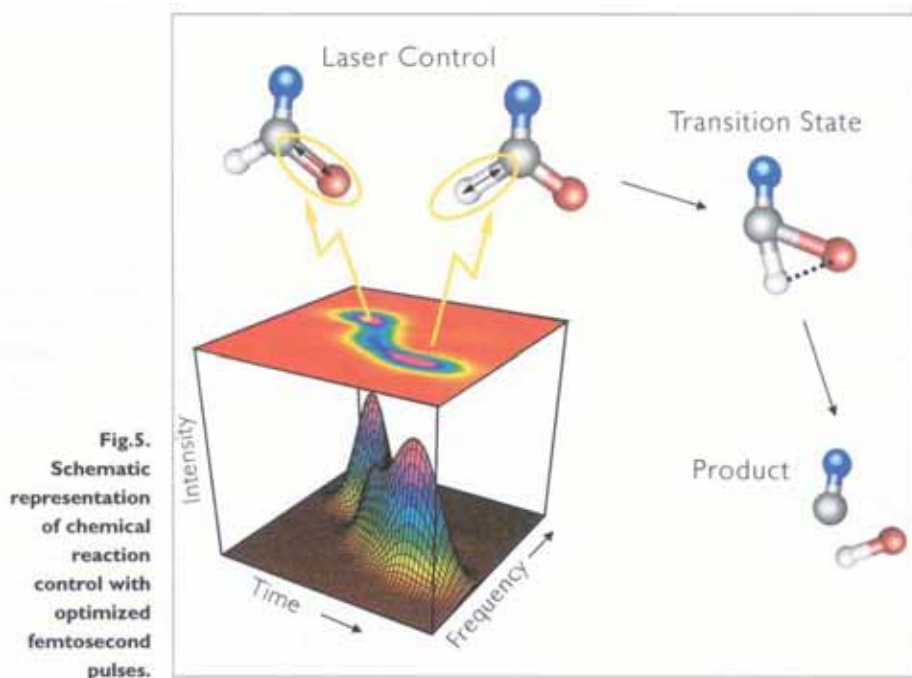
New phenomena

driven helium

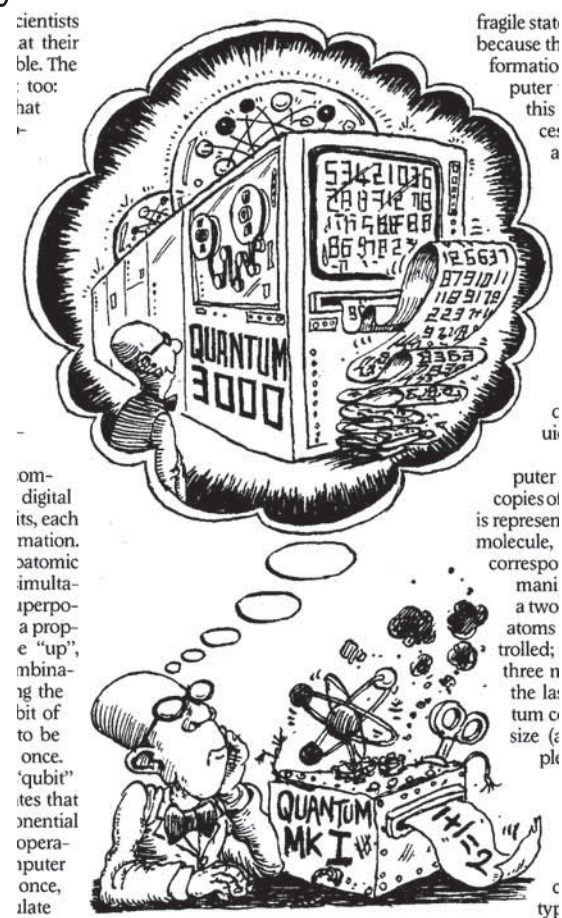
Vision: Quantum Control of/through Complexity

complex dynamics generates new and robust quantum phenomena

similar questions in apparently remote areas



[L. Kurtz, LMU München 2001]



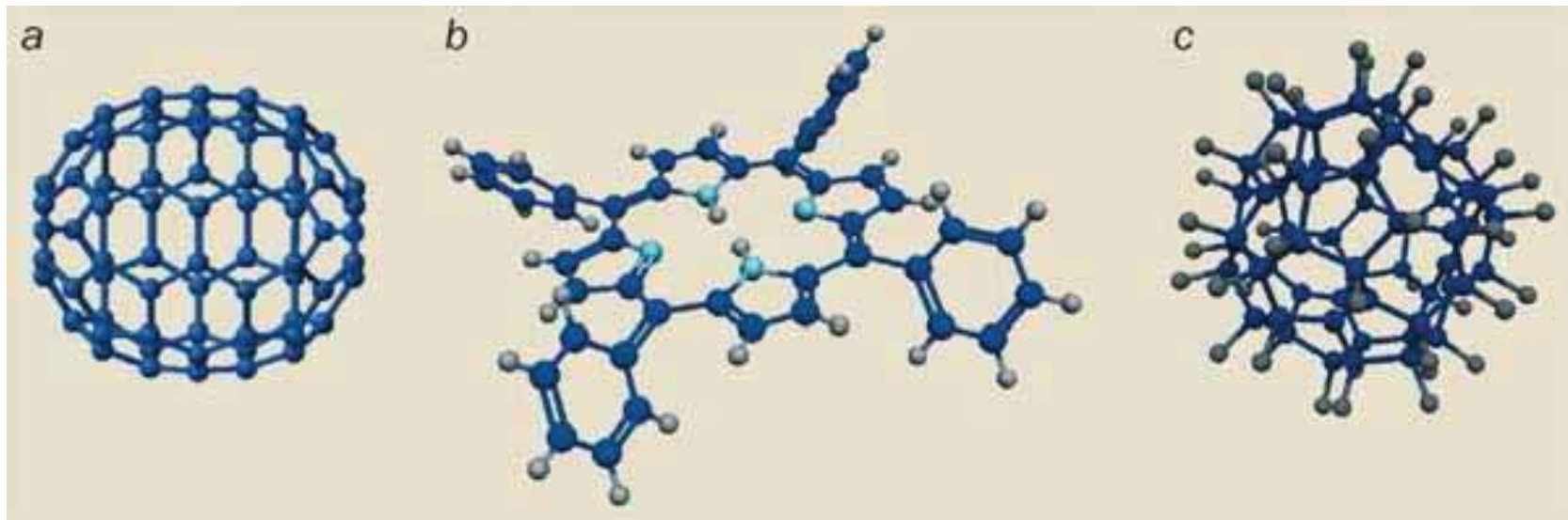
[The Economist, *Quantum Dreams*, 10/3/2001]

Complexity in AMO physics

– the boring times are over . . .

Emergence of novel phenomena induced by

- deterministic chaos • many particle interactions • disorder • noise
- interference • entanglement • decoherence



[Hornberger et al., Physics World 2005]

Guiding principle/challenge for theory:

The quest for quantitative precision is as arduous as it is important.

Bertrand Russell, ABC of Relativity

Roadmap

- **Nonlinear resonances: from helium to Bose-Hubbard**

Peter Schlagheck & Javier Madroño & Pierre Lugan & Klaus Zimmermann & Soeren Roerden & Maximilian Schmidt & Celsus Bouri

- Matter wave transport in periodic optical potentials

Alexey Ponomarev & Javier Madroño & Hannah Venzl & Alexej Schelle & Andrey Kolovsky & Stefan Hunn & Moritz Hiller & Tobias Zech & Lewin Stein & Sandro Wimberger & Dominik Hörndlein & Vivian Franca

- Photon transport in disordered atomic samples

Vyacheslav Shatokhin & Thomas Wellens & Cord A. Müller & Tobias Geiger & Felix Eckert & Nicolas Cherroret & Jochen Zimmermann & Scott Sanders

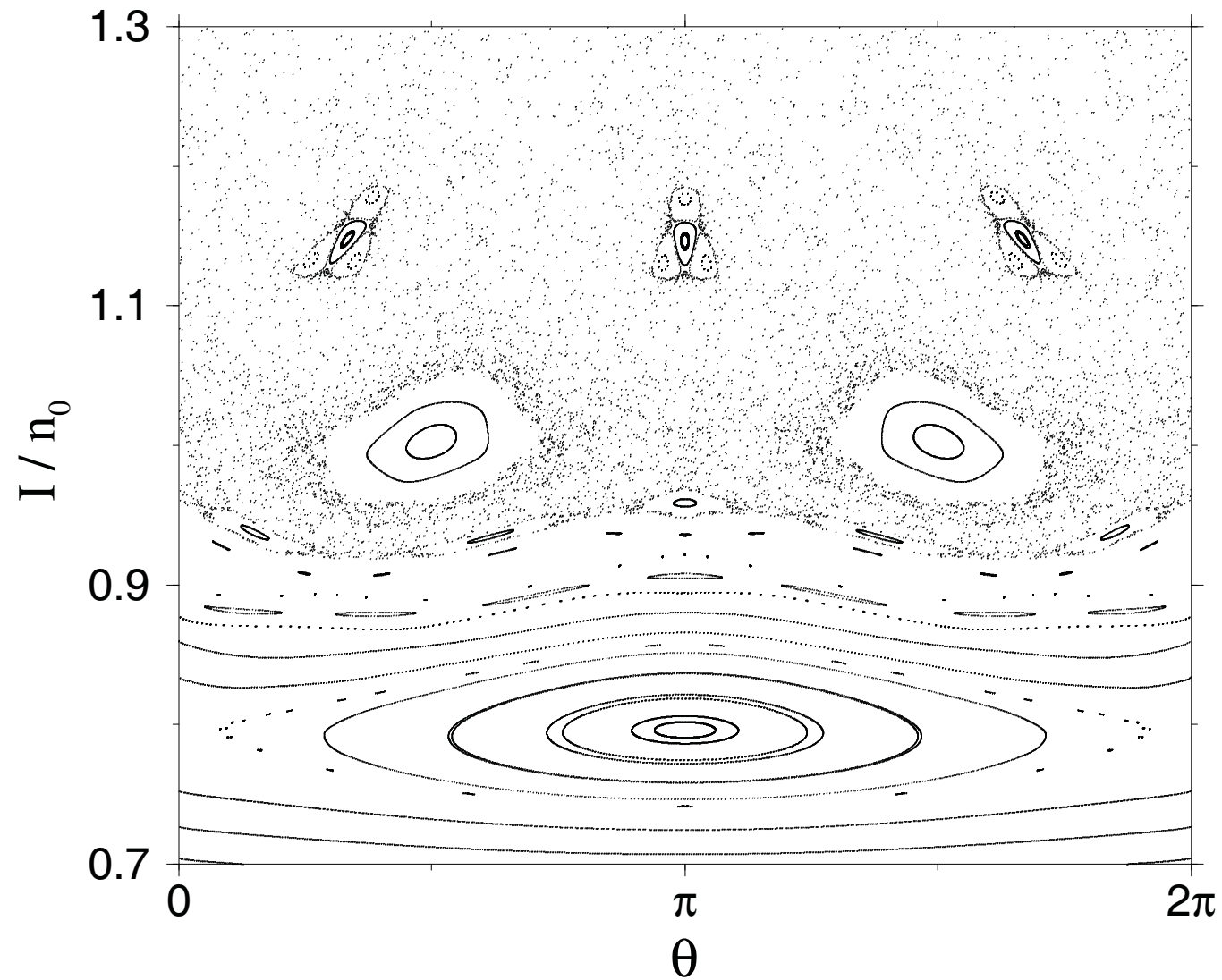
- Energy transport in strongly driven Rydberg systems

Andreas Krug & Sandro Wimberger & Javier Madroño & Alexej Schelle

- Quantum transport in biological functional units

Torsten Scholak & Thomas Wellens & Simeon Sauer & Florian Mintert & Fernando de Melo & Markus Tiersch

Tool: Nonlinear resonances



Nonlinear resonances in many-particle dynamics. . .

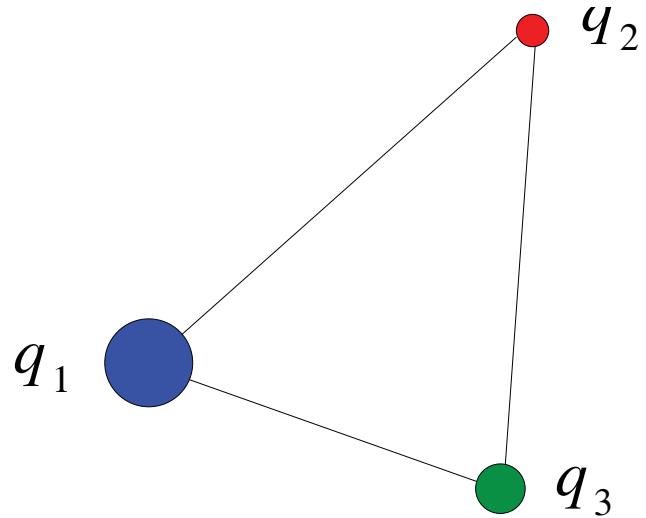
I Helium

II A digression – Nondispersive wave packets in single particle dynamics

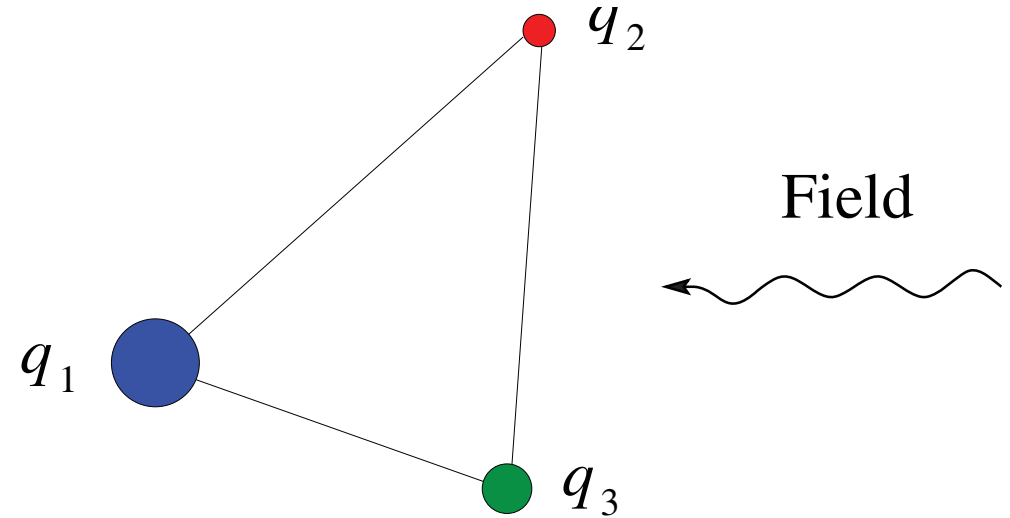
III Back to Helium

IV Bose-Hubbard

From “naked” to periodically driven Helium



Non-integrable



New phenomena

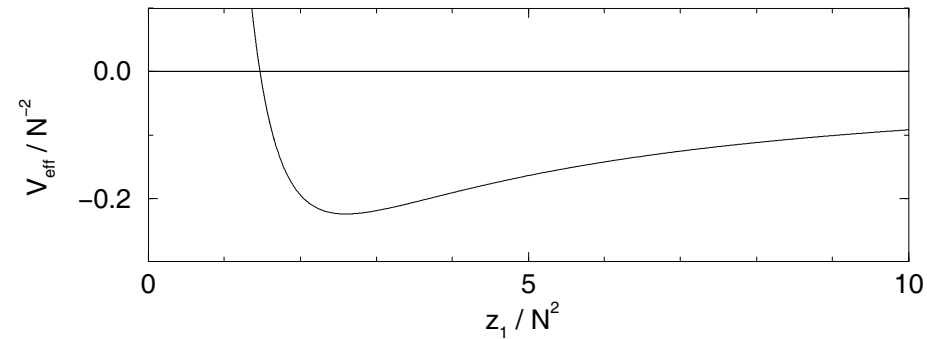
What is special about Helium?

- minimal many-particle interaction
- mixed, regular-chaotic, **high dimensional** phase space [Richter et al., 1993]
- “dirty”, i.e. additional complication:
open system – decay through multiple continua
[Tanner et al, 2000]
- **ABUNDANT EXPERIMENTAL DATA**

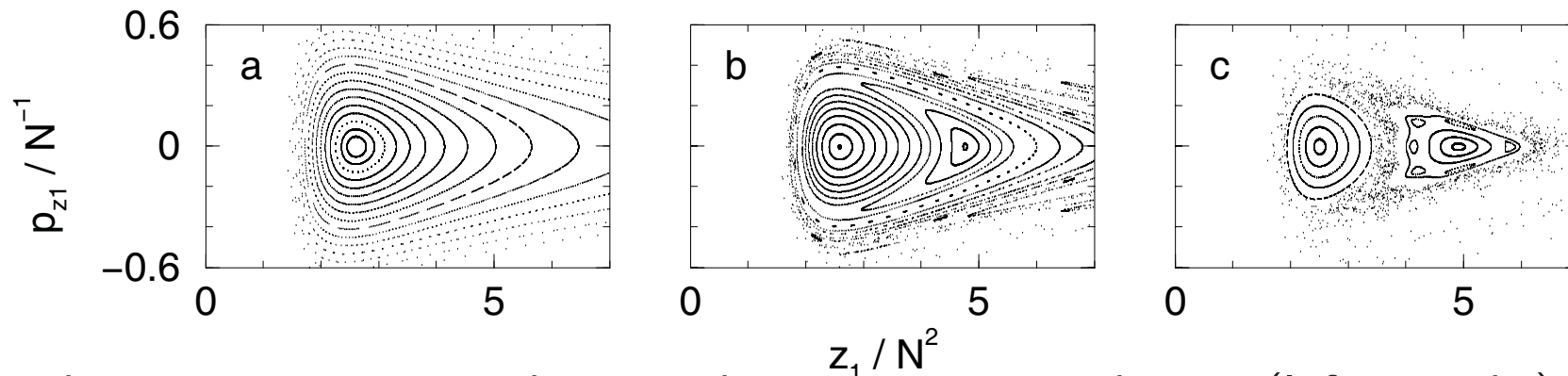
Island of stability: the frozen planet



lives on a well defined adiabatic potential [Ostrovsky & Prudov, 1995]



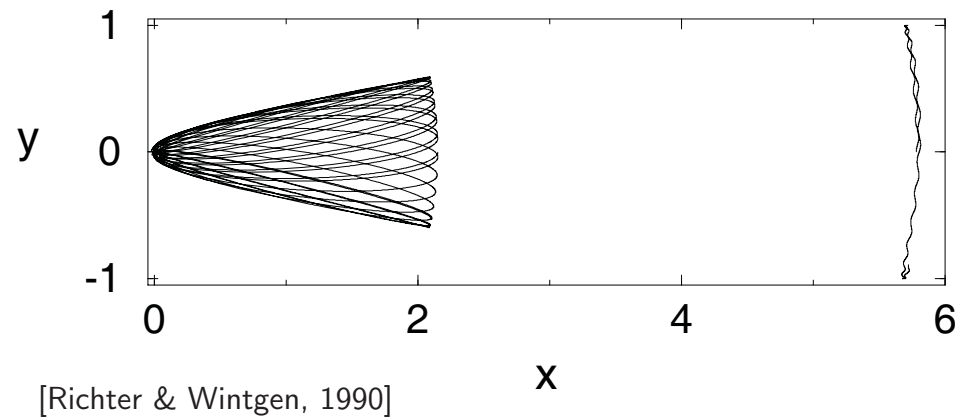
with a phase space structure reflecting the countourlines thereof



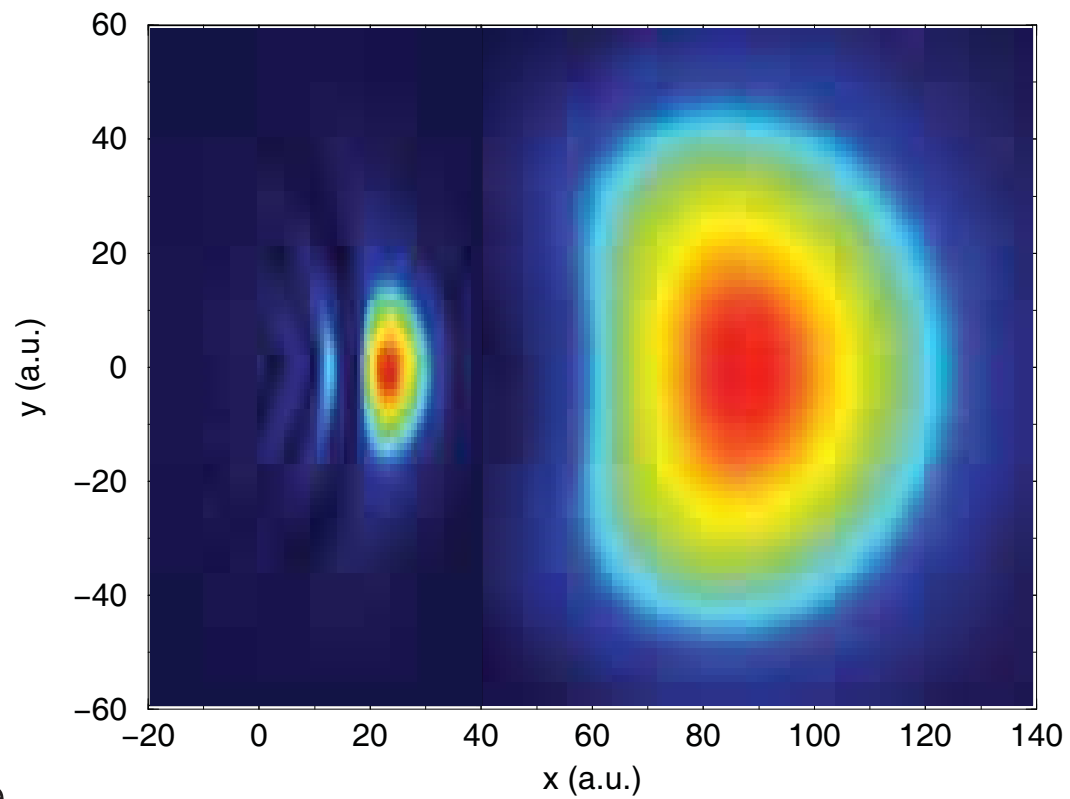
phase space metamorphosis under near resonant driving (left to right)

Quantum mechanical eigenstate vs. stable classical trajectory

typical classical trajectory



quantum eigenstate

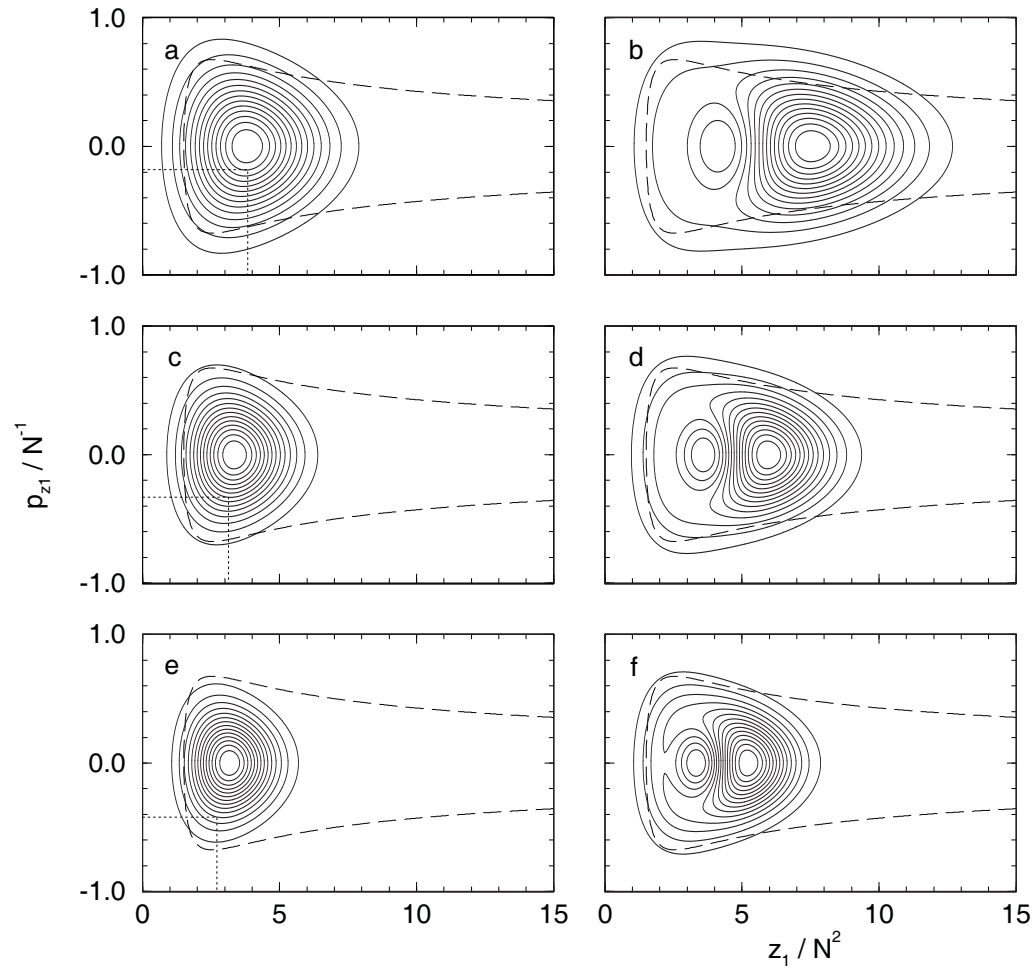


Dimension matters!

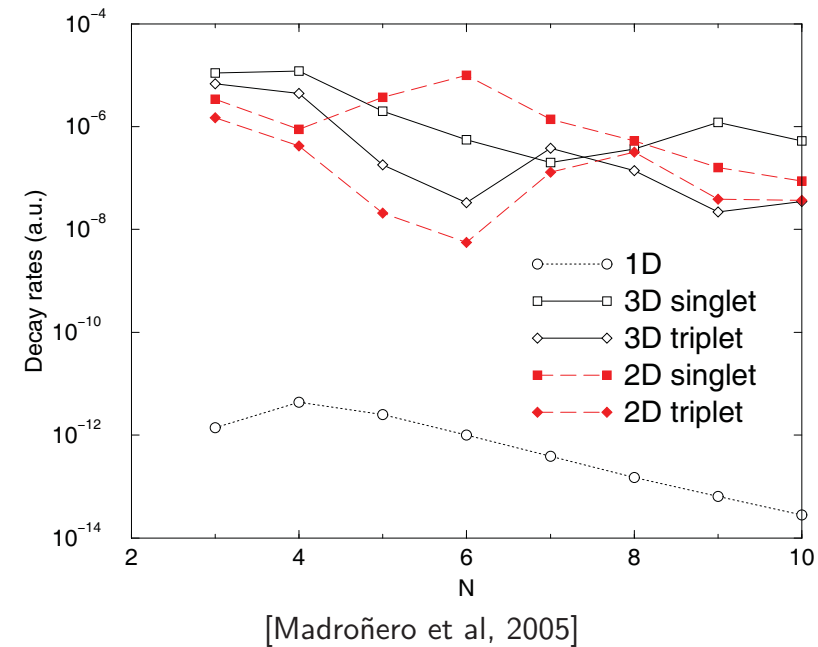
→ Classical trapping of quantum eigenstate ←

→ only if the island has size \hbar an eigenstate can settle there ←

phase space projections

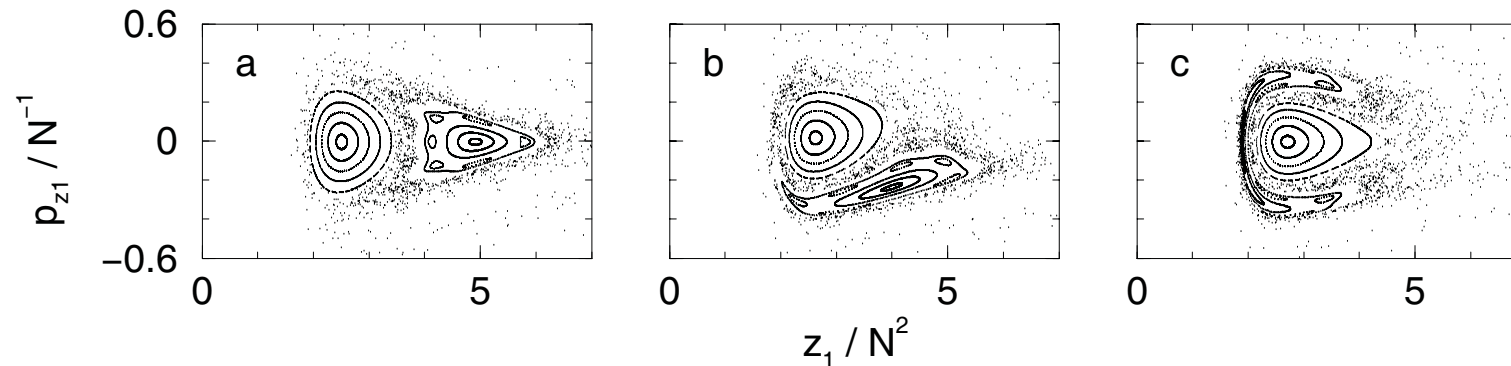


tunneling lifetimes

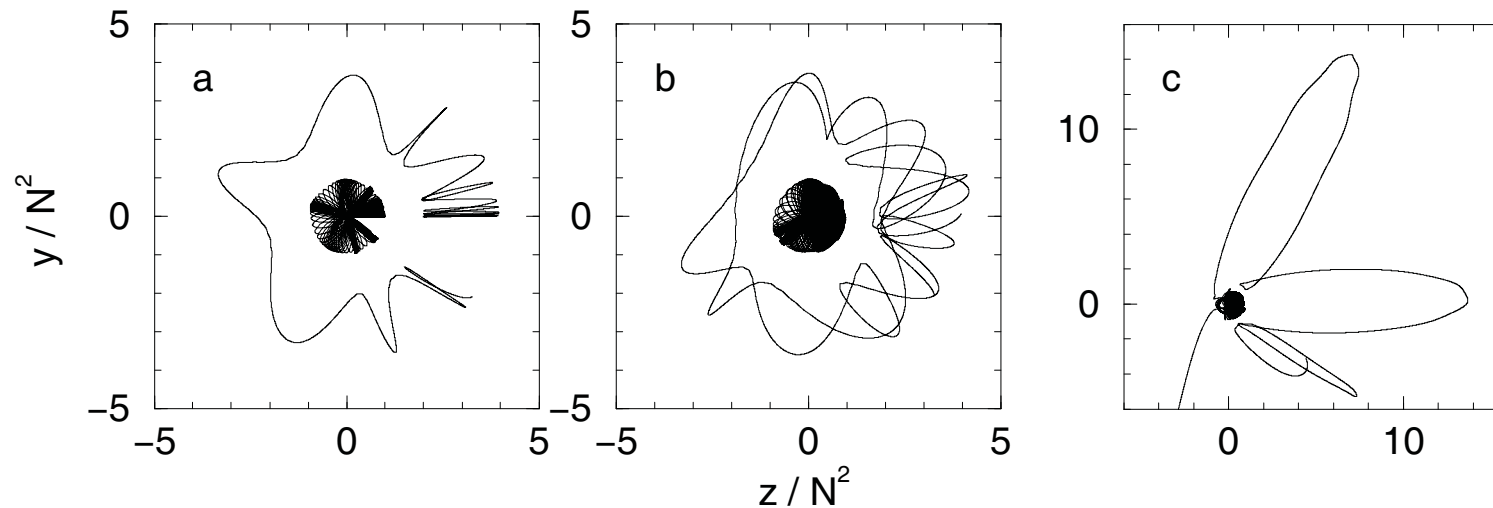


Collinear stability, transverse instability under driving

Under near-resonant driving of the **collinear configuration**, the phase space structure develops stable (elliptic) structures which reflect the periodicity of the drive – $\omega t = 0, \pi/2, \pi$, from left to right! [Schlagheck, -, 1998, 2003]



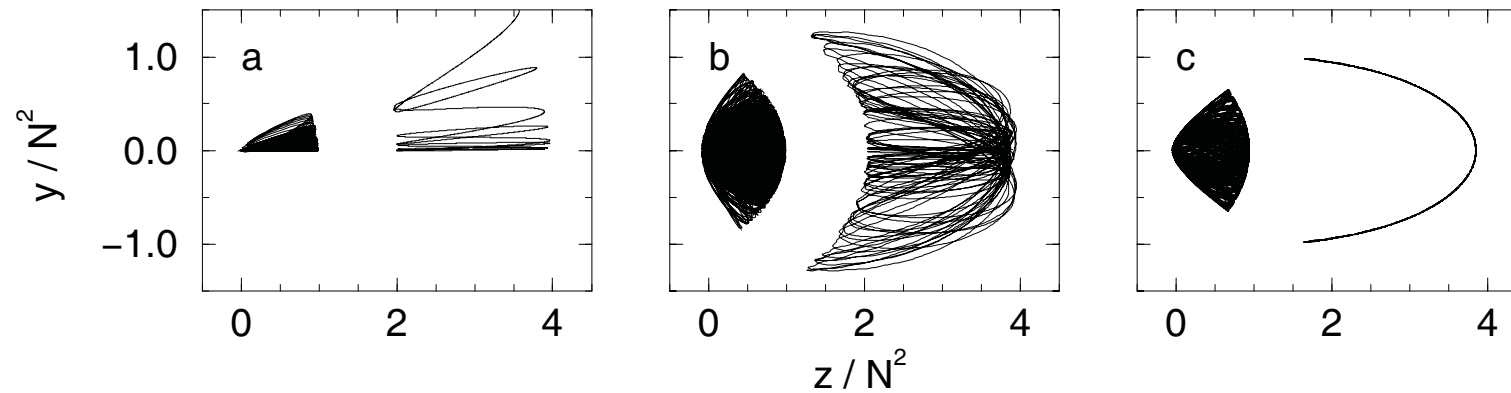
However, when we admit transverse deviations, the classical dynamics turns unstable!



Transverse stabilization by additional static field

The transverse instability can be overcome by applying an additional static electric field along the axis of the configuration

[Schlagheck, - 1998, 2003]



(classical 3D simulation)

Nonlinear resonances in many-particle dynamics. . .

I Helium

II A digression – Nondispersive wave packets in **single particle** dynamics

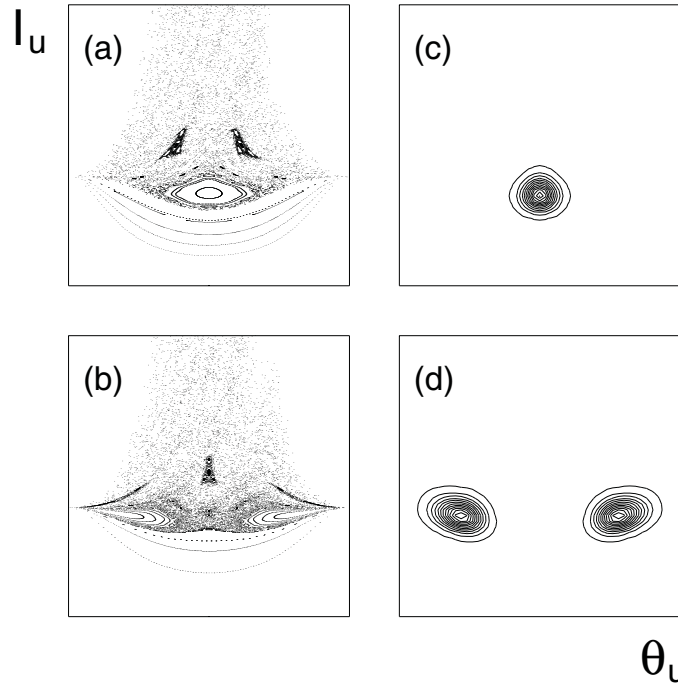
III Back to Helium

IV Bose-Hubbard

Islands of stability host non-dispersive quantum wave packets

– 1D , single electron example –

phase space projection of a Floquet eigenstate – $2\pi/\omega$ -periodic driving!!!

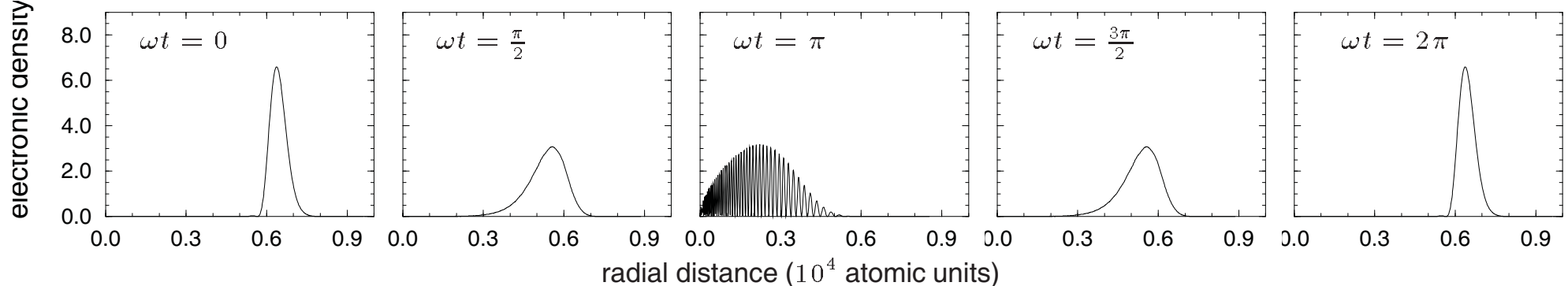


$$F = 0.035/n^4, \quad \omega = 1.0/n^3, \quad n = 57$$

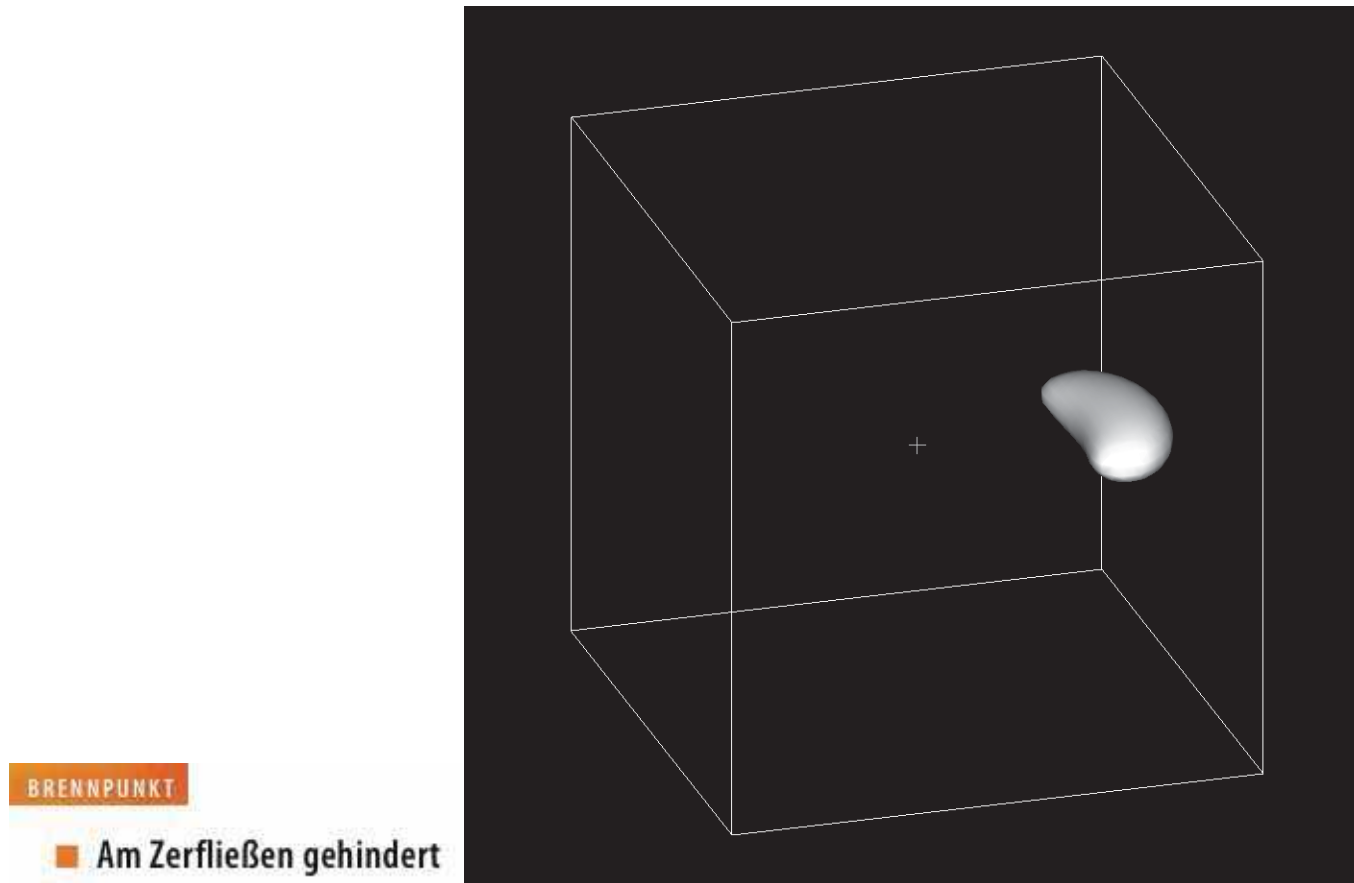
no dispersion – lifetimes $\Gamma_\epsilon^{-1} \simeq 10^6 \times \frac{2\pi}{\omega}$

[-, 1993, Delande, -, 1994]

Floquet state in configuration space



Arbitrary control in 3D – wave packet on circular trajectory



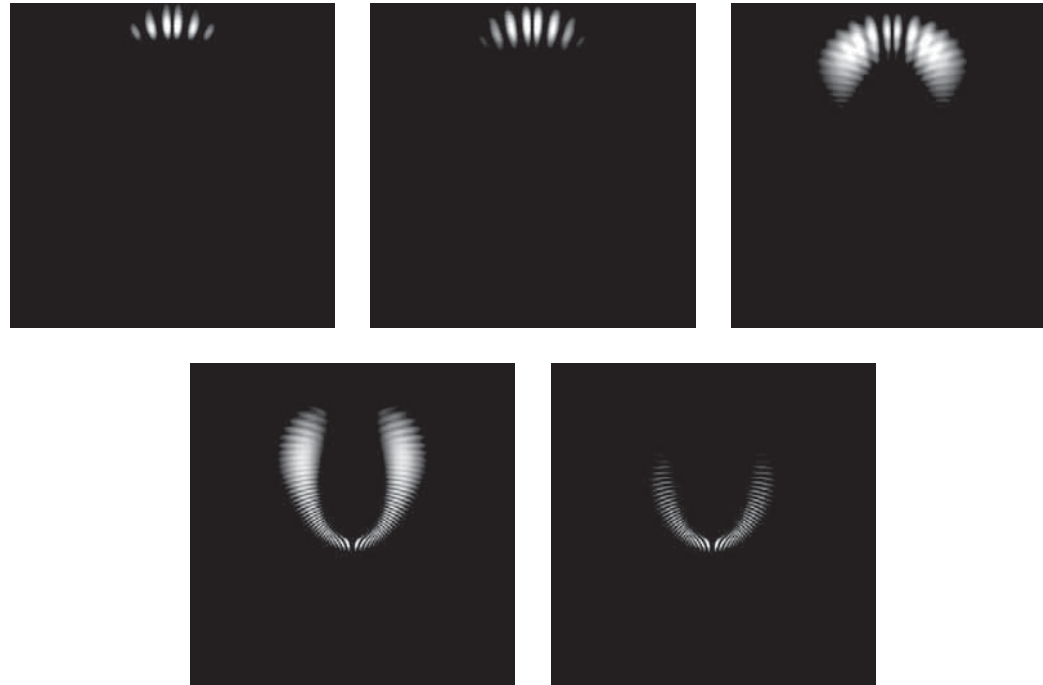
control through circularly polarized e-m field, $\rho, z = \pm 10000$ a.u.

[Białynicki-Birula, Kaliński & Eberly, 1994; Brunello, Uzer & Farelly, 1996; Zakrzewski, Delande, -, 1995]

EXPERIMENTS: [Maeda et al., 2009; Mestayer et al., 2009]

isovalue plots of the electronic density

Wave packet on elliptic trajectory



linearly polarized control field, rotational symmetry around z-axis,
snapshots at different phases of Kepler cycle

$\rho, z = \pm 3500$ a.u.

[-, Sacha, Delande & Zakrzewski, 1998]

isovalue plots of the electronic density

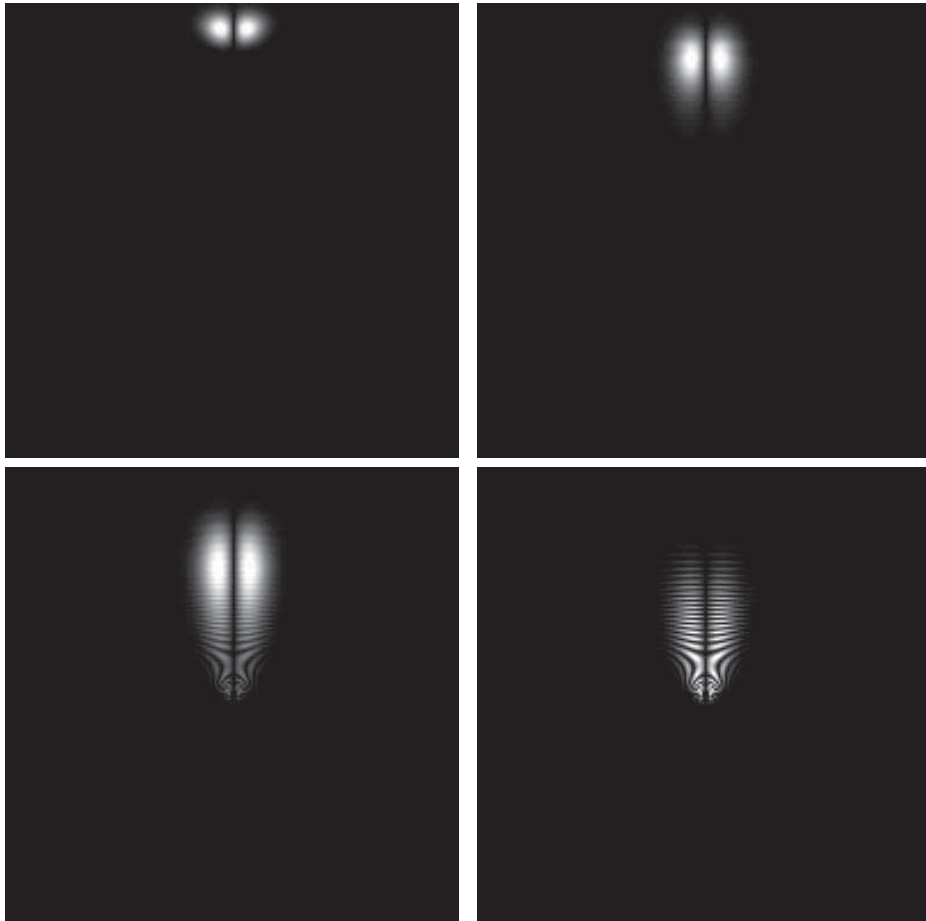
Experimental evidence

position-sensitive detection

[Maeda & Gallagher & Co, 2004-2009]

experimental life time

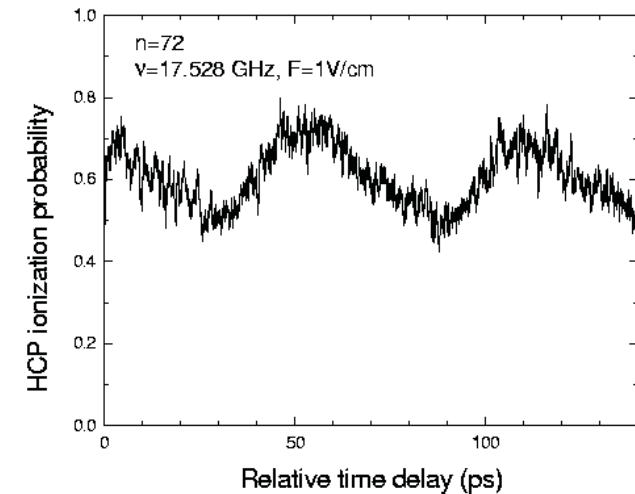
≥ 15000 Kepler orbits!



control by linearly polarized e-m and parallel static electric field,
snapshots at different phases of Kepler cycle

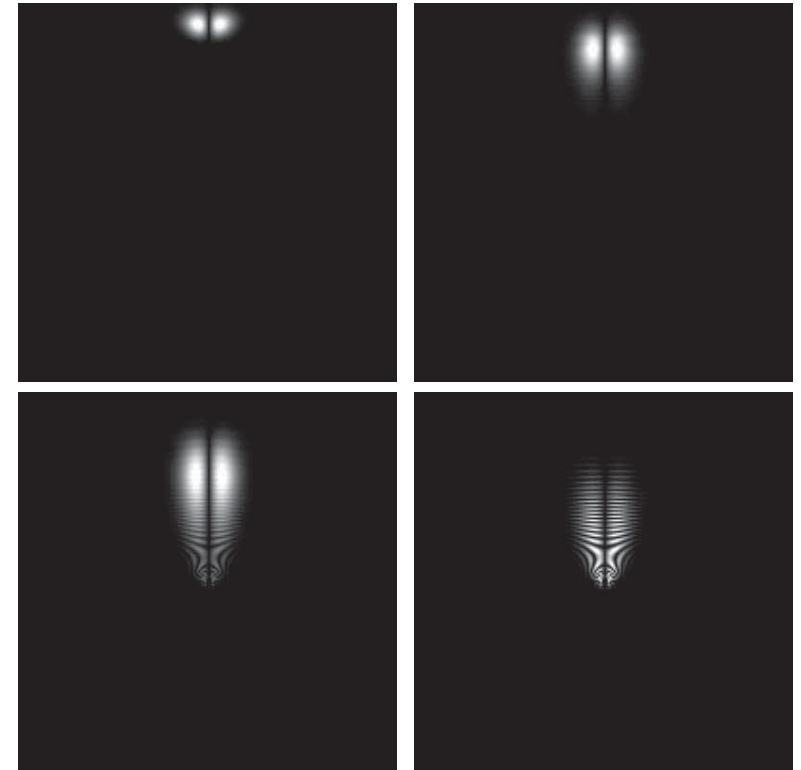
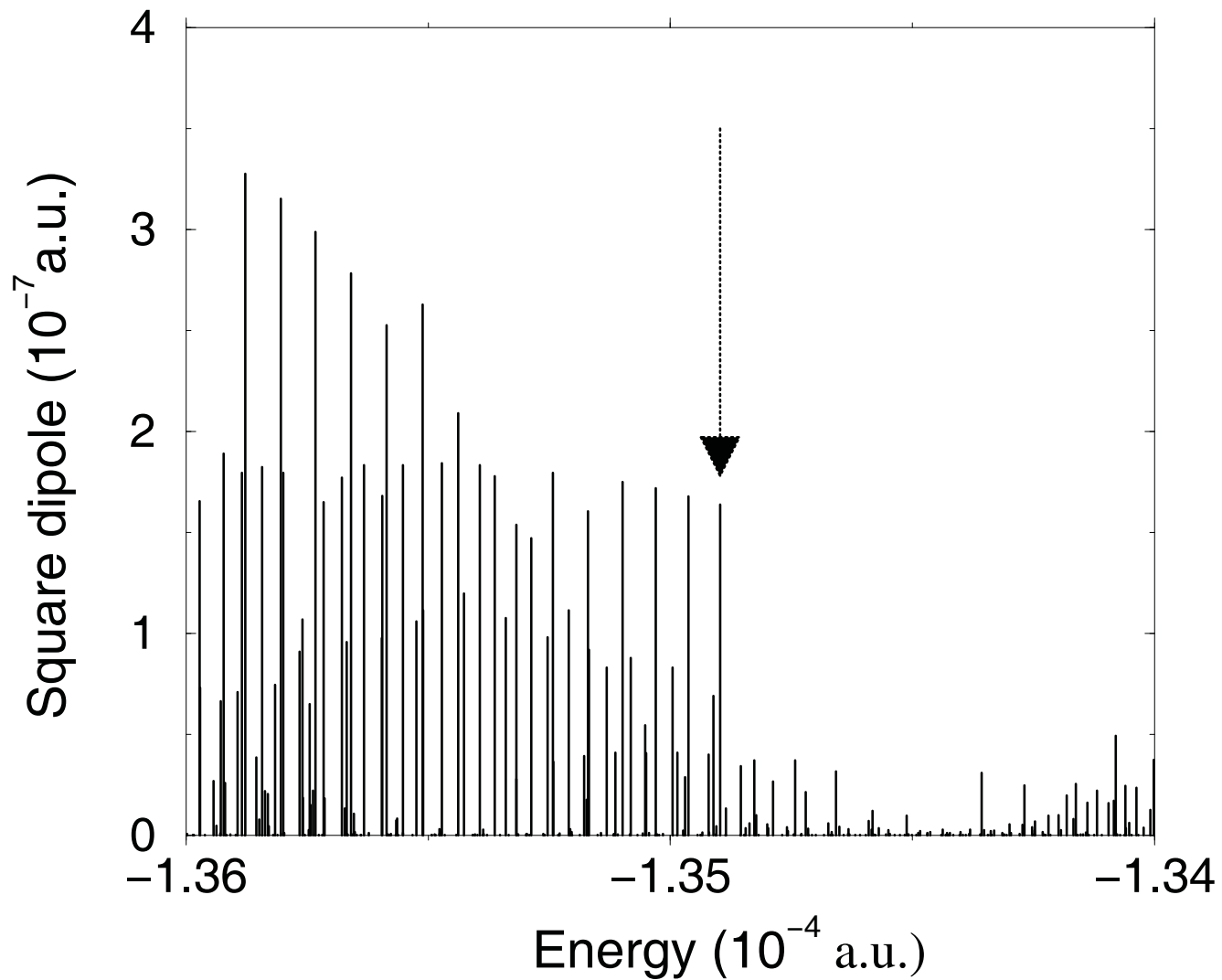
$\rho, z = \pm 10000$ a.u.

[-, Delande & Zakrzewski, 2002]



Clear spectroscopic signature

Floquet spectroscopy of the dressed atom



Remember the “simple example” . . .

. . . of the harmonic oscillator



nach demjenigen Gesetz, das sich für einen Massenpunkt mit der Energiefunktion (1) aus der gewöhnlichen Mechanik ergeben würde. Die Amplitude, in x gemessen, ist A , in q gemessen also

$$a = \frac{A}{2\pi} \sqrt{\frac{h}{m\nu_0}}. \quad (11)$$

Für die Energie eines Massenpunktes m , der mit dieser Amplitude und mit der Frequenz ν_0 oszilliert, ergibt die gewöhnliche Mechanik

$$2\pi^2 a^2 \nu_0^2 m = \frac{A^2}{2} h \nu_0 \quad (12)$$

d. i. nach (6), gerade $n h \nu_0$, wo n die mittlere Quantenzahl der herausgegriffenen Gruppe. Die „Korrespondenz“ ist also auch in dieser Hinsicht eine vollkommene.

Der zweite Faktor in (9) ist im allgemeinen sowohl von x als auch von t eine sehr rasch veränderliche Funktion vom Absolutbetrag ≤ 1 , welche

ständig — doch möchte ich an dieser Stelle hierauf nicht näher eingehen.

Unsere Wellengruppe hält dauernd zusammen, breitet sich nicht im Laufe der Zeit auf ein immer größeres Gebiet aus, wie man es sonst, z. B. in der Optik, gewohnt ist. Das will freilich hier im eindimensionalen nicht viel sagen, ein Buckel auf einer Seite verhält sich ganz ähnlich. Man erkennt aber leicht, daß sich durch Multiplikation von zwei bzw. drei Ausdrücken wie (4), der eine in x , der andere in y , der dritte in z geschrieben, auch der ebene bzw. der räumliche Oszillator darstellen läßt, d. h. eine ebene oder eine räumliche Wellengruppe, die auf einer harmonischen Ellipse umläuft¹⁾. Auch eine solche Wellengruppe bleibt dauernd beisammen, im Gegensatz z. B. zu einem Wellenpaket der klassischen Optik, das sich im Laufe der Zeit zerstreut. Der Unterschied dürfte davon herrühren, daß unsere Gruppe aus einzelnen diskreten harmonischen Komponenten aufgebaut ist, nicht aus einem Kontinuum von solchen.

Ich möchte schließlich noch erwähnen, daß eine

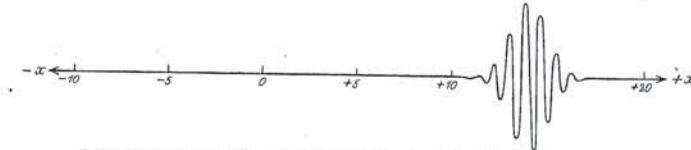


Fig. 2. Pendelnde Wellengruppe als undulationsmechanisches Bild des Massenpunktes.

viele tiefe und schmale Furchen in das Antlitz des ersten Faktors gräbt und so eine Wellengruppe daraus macht, deren Bild — nur ganz schematisch — in Fig. 2 wiedergegeben ist. Der Abszissenmaßstab der Fig. 2 ist natürlich viel kleiner als in Fig. 1; Fig. 2 müßte fünfmal vergrößert werden, um mit Fig. 1 direkt vergleichbar zu sein. Eine genauere Betrachtung des zweiten Faktors in (9) offenbart folgendes interessante Detail, das in der Fig. 2, die nur ein Stadium darstellt, nicht zum Ausdruck kommt. Die Anzahl und Breite der „Furchen“ oder „Wellchen“, welche den Massenpunkt durchsetzen, ist zeitlich veränderlich. Die Wellchen sind am zahlreichsten und schmalsten beim Durchgang durch die Mitte $x = 0$; sie werden völlig ausgegültet an den Umkehrstellen $x = \pm A$, weil dort nach (10) der $\cos 2\pi\nu_0 t = \pm 1$ und daher der $\sin 2\pi\nu_0 t = 0$ wird, so daß der zweite Faktor in (9) gar nicht von x abhängt. Die gesamte Ausdehnung der Wellengruppe („Dicke des Massenpunktes“) bleibt jedoch stets dieselbe. Die Veränderlichkeit der „Kräuselung“ ist als eine Abhängigkeit von der Geschwindigkeit aufzufassen und als solche nach allgemeinen undulationsmechanischen Gesichtspunkten vollkommen ver-

gemeinsame additive Konstante, sagen wir C , die eigentlich in (3) zu allen ν_n hinzuzufügen ist (entsprechend der „Ruhenergie“ des Massenpunktes) nichts wesentliches ändert. Es tritt nur in der eckigen Klammer in (9) der Addend $2\pi C t$ hinzu. Dadurch werden die Oszillationen innerhalb der Wellengruppe zeitlich sehr viel rascher, während das durch (10) beschriebene Pendeln der Gruppe als ganzer und ebenso ihre Kräuselung davon ganz unberührt bleiben.

Es läßt sich mit Bestimmtheit voraussehen, daß man auf ganz ähnliche Weise auch die Wellengruppen konstruieren kann, welche auf hochquantigen Keplerellipsen umlaufen und das undulationsmechanische Bild des Wasserstoffelektrons sind; nur sind die der rechen-technischen Schwierigkeiten größer als in dem hier behandelten, ganz besonders einfachen Schulbeispiel.

¹⁾ Es sei hier die interessante Bemerkung eingeschaltet, daß für den ebenen Oszillator die Quantenniveaus ganzzahlig, für den räumlichen dagegen wieder „halbzahlig“ werden. Ähnliches gilt für den Rotator. Die spektroskopisch so bedeutungsvolle Halbzahligkeit hängt also mit der ungeraden Dimensionszahl des Raumes zusammen.

nach demjenigen Gesetz, das sich für einen Massenpunkt mit der Energiefunktion (1) aus der gewöhnlichen Mechanik ergeben würde. Die Amplitude, in x gemessen, ist A , in q gemessen also

$$\alpha = \frac{A}{2\pi} \sqrt{\frac{h}{m\nu_0}}. \quad (11)$$

Für die *Energie* eines Massenpunktes m , der mit dieser Amplitude und mit der Frequenz ν_0 oszilliert, ergibt die gewöhnliche Mechanik

$$2\pi^2 \alpha^2 \nu_0^2 m = \frac{A^2}{2} h \nu_0 \quad (12)$$

d. i. nach (6), gerade $n h \nu_0$, wo n die mittlere Quantenzahl der herausgegriffenen Gruppe. Die „Korrespondenz“ ist also auch in dieser Hinsicht eine vollkommene.

Der *zweite* Faktor in (9) ist im allgemeinen sowohl von x als auch von t eine sehr rasch veränderliche Funktion vom Absolutbetrag ≤ 1 , welche

ständig — doch möchte ich an dieser Stelle hierauf nicht näher eingehen.

Unsere Wellengruppe hält dauernd zusammen, breitet sich *nicht* im Laufe der Zeit auf ein immer größeres Gebiet aus, wie man es sonst, z. B. in der Optik, gewohnt ist. Das will freilich hier im eindimensionalen nicht viel sagen, ein Buckel auf einer Saite verhält sich ganz ähnlich. Man erkennt aber leicht, daß sich durch Multiplikation von zwei bzw. drei Ausdrücken wie (4), der eine in x , der andere in y , der dritte in z geschrieben, auch der *ebene* bzw. der *räumlichen* Oszillator darstellen läßt, d. h. eine ebene oder eine räumliche Wellengruppe, die auf einer harmonischen Ellipse umläuft¹⁾. Auch eine solche Wellengruppe bleibt dauernd beisammen, im Gegensatz z. B. zu einem Wellenpaket der klassischen Optik, das sich im Laufe der Zeit zerstreut. Der Unterschied dürfte davon herrühren, daß unsere Gruppe aus einzelnen *diskreten* harmonischen Komponenten aufgebaut ist, nicht aus einem *Kontinuum* von solchen.

Ich möchte schließlich noch erwähnen, daß eine

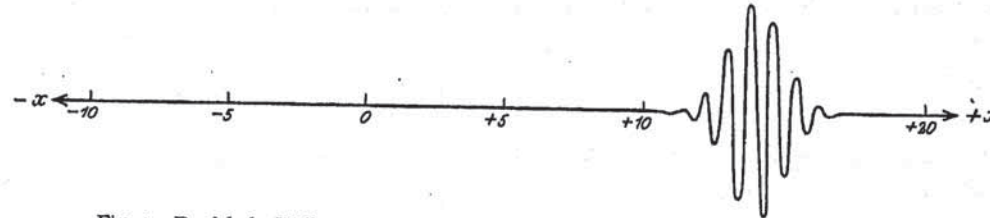


Fig. 2. Pendelnde Wellengruppe als undulationsmechanisches Bild des Massenpunktes.

Es läßt sich mit Bestimmtheit voraussehen, daß man auf ganz ähnliche Weise auch die Wellengruppen konstruieren kann, welche auf hochquantigen Keplerellipsen umlaufen und das undulationsmechanische Bild des Wasserstoffelektrons sind; nur sind da die rechen-technischen Schwierigkeiten größer als in dem hier behandelten, ganz besonders einfachen Schulbeispiel.

Status non-dispersive one particle wave packets

- **various experimental realizations**
 - **one electron Rydberg states** under periodic or delta-train driving
DONE (Univ. of Virginia and Rice Univ.)
 - **cold atoms** – atomic center of mass degree of freedom
- **can control shape and size of wave packet trajectory, even in real time**
- **experimental evidence so far “coarse grained”**
- **experimental evidence of very long life times**
- **theoretical understanding essentially complete**
(semiclassics, RMT, CAT, fully quantum)
- **two-electron wave packet experiments** under way (Virginia)

Nonlinear resonances in many-particle dynamics. . .

I Helium

II A digression – Nondispersive wave packets in single particle dynamics

III Back to Helium

IV Bose-Hubbard

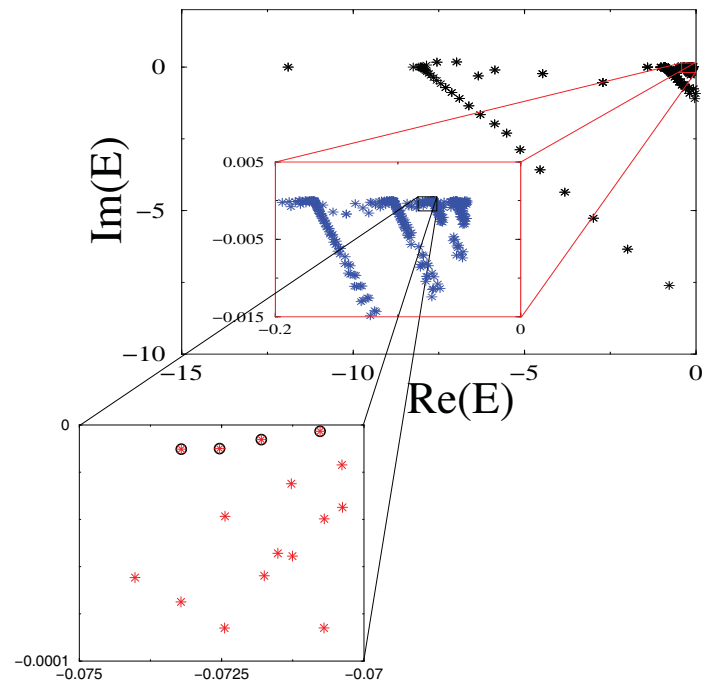
Do such wave packets exist in the two-electron system?

$$H = \frac{p_1^2 + p_2^2}{2} - \frac{Z}{r_1} - \frac{Z}{r_2} + \frac{1}{r_{12}} + F(x_1 + x_2) \cos \omega t$$

- Periodically time-dependent system
 - Floquet Theory
- Ionization Process
 - Complex Rotation
- Appropriate representation
 - Parabolic Coordinates
 - Oscillator quantum numbers
 - n_1, n_2, n_3, n_4
- Efficient and accurate numerical calculations
 - Parallel programming

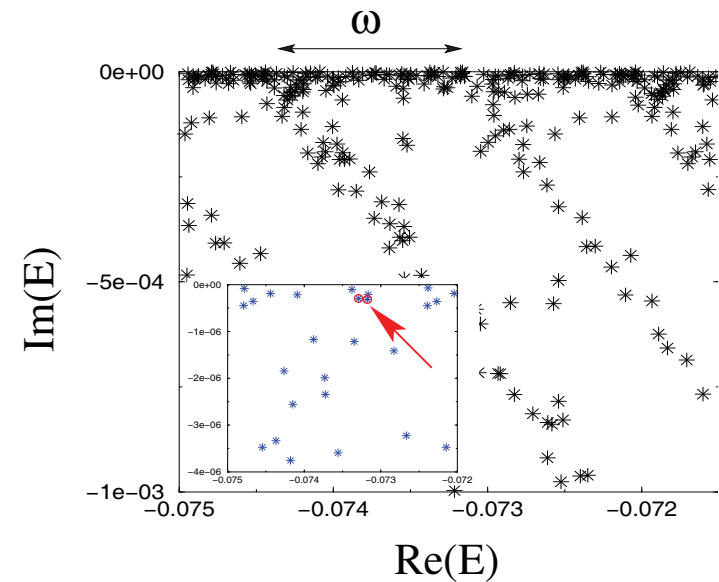
Spectrum in the complex plane

Spectrum of the 2D Helium atom



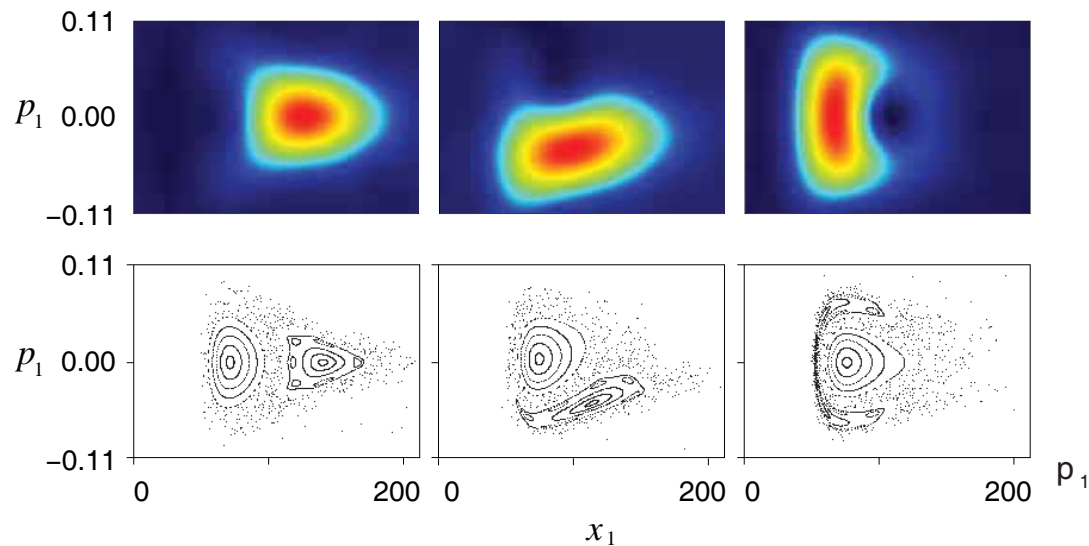
frozen planet states: $\langle \cos \theta_{12} \rangle \approx 1$.

Spectrum of the 2D driven Helium atom



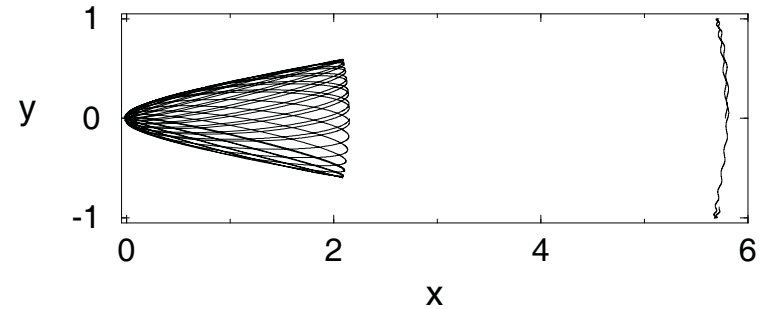
Nondispersive wave packets in driven 2D Helium

phase space
(projection along field polarization axis)

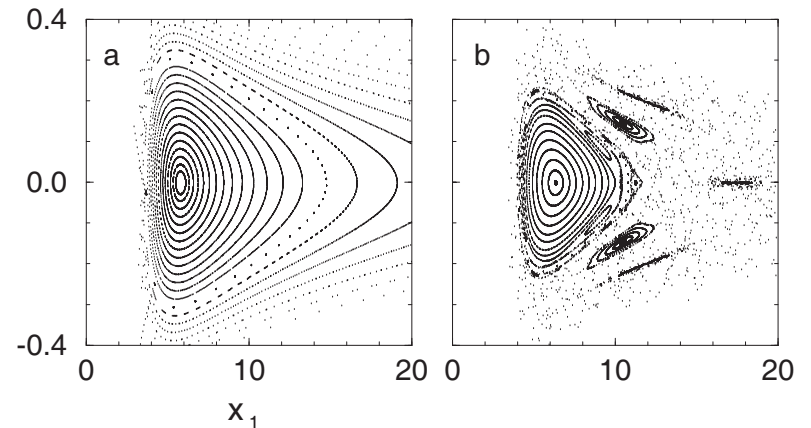


$\omega t = 0 \dots \pi/2 \dots \pi$ (left to right) $N = 6$
life times approx. several hundred field cycles

configuration space



projective phase space



[Schlagheck, -, 1998,2003]

[Madróñero, PhD thesis, LMU Munich, 2004]

! benchmark for semiclassics in high dimensions !

Nonlinear resonances in many-particle dynamics. . .

I Helium

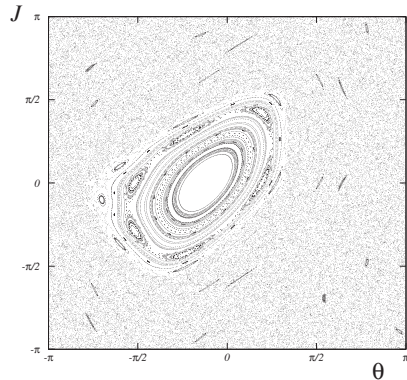
II A digression – Nondispersive wave packets in single particle dynamics

III Back to Helium

IV Bose-Hubbard

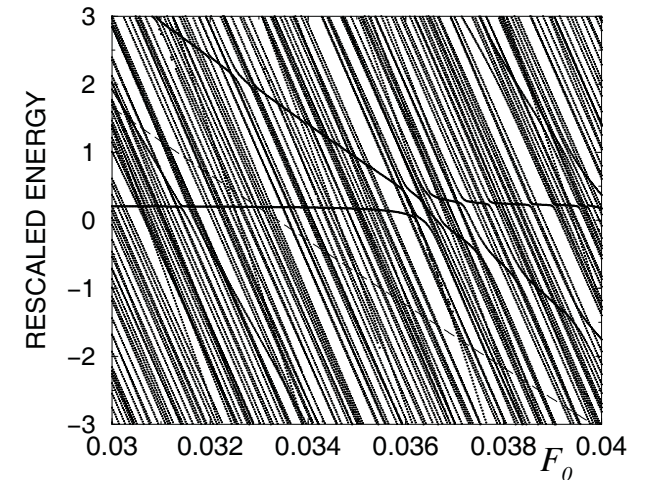
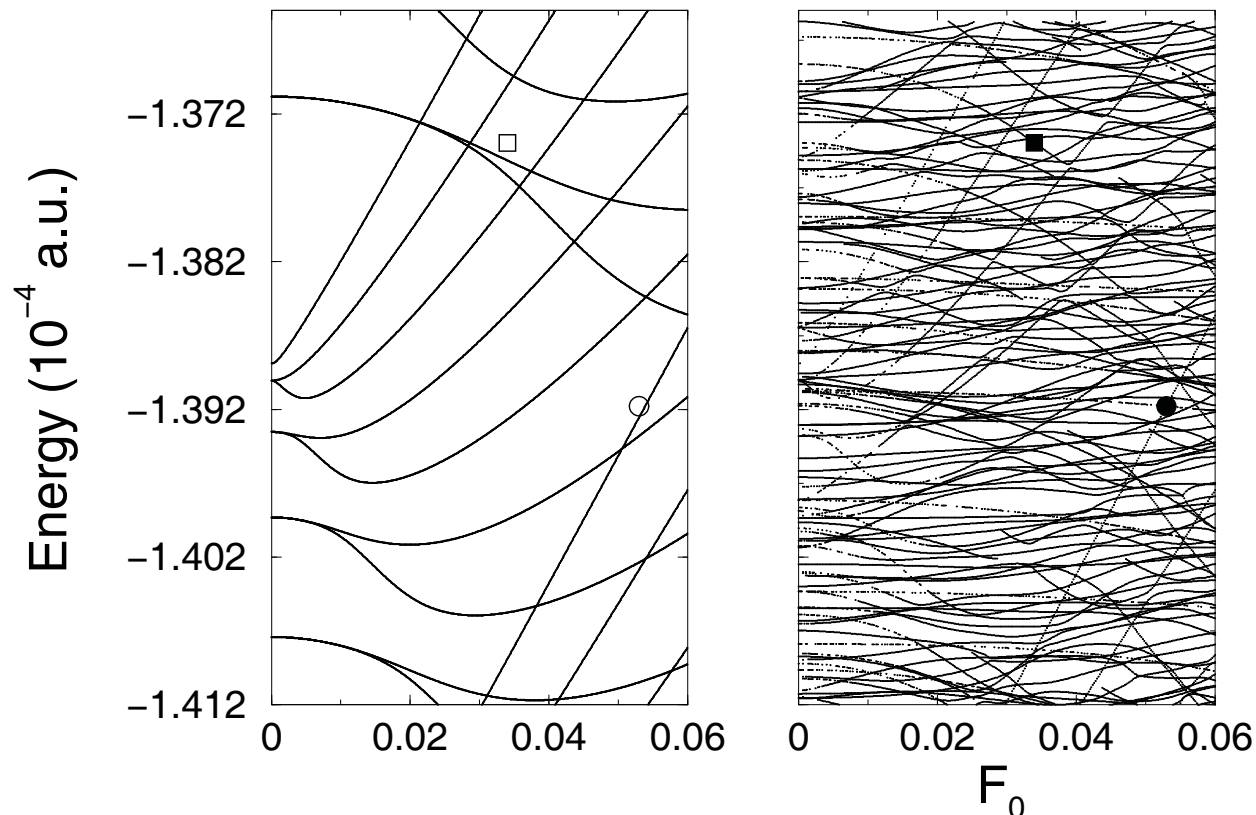
Nonlinear resonances in “level spaghetti”

KAM torus in “chaotic sea”



regular level structure embedded into irregular level dynamics – much alike regular island embedded into chaotic phase space

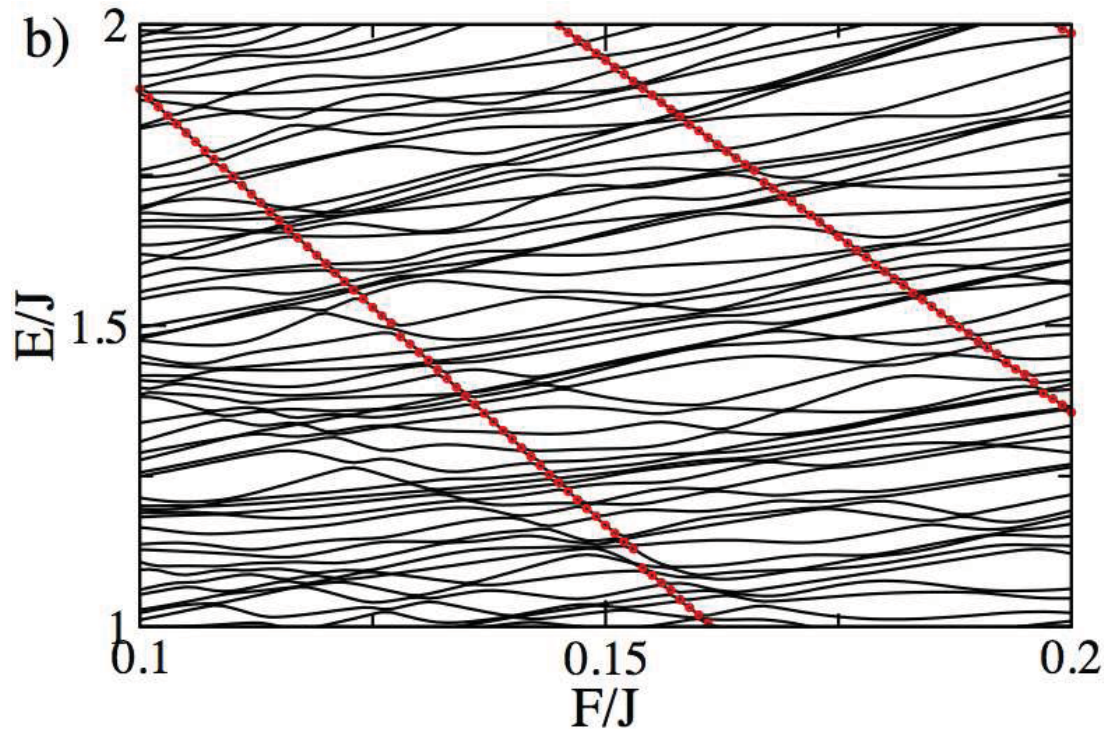
eigenvalues anchored to the island “go straight”!



[Zakrzewski et al., 1997]

Solitonic solutions in the tilted Bose Hubbard problem

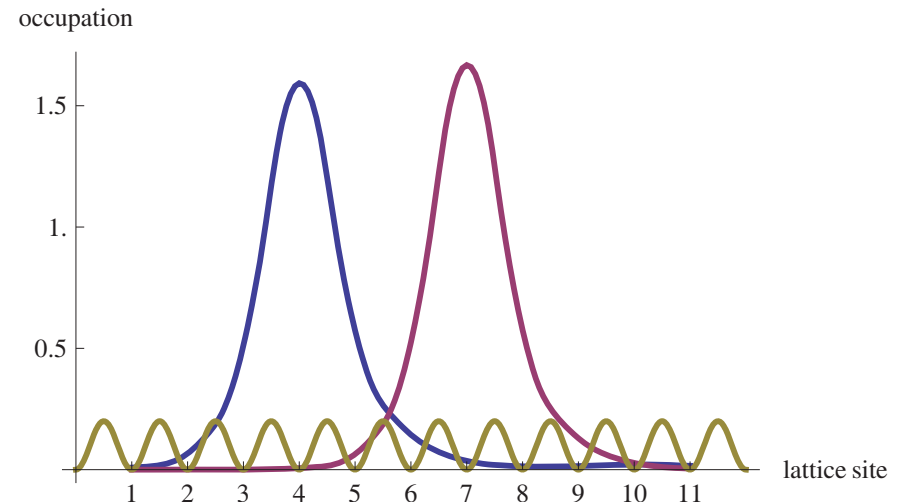
$$H = -\frac{J_B}{2} \left(\sum_l a_{l+1}^\dagger a_l + h.c. \right) + \frac{W_B}{2} \sum_l n_l(n_l - 1) + Fd \sum_l l n_l$$



$$N = 3, L = 11, J_B = 0.038, W_B = 0.032$$

- L solitonic states “screened” against chaotic background
- robust, strongly localized many particle configurations (more than 60 % of all atoms on one site)

[H. Venzl, T. Zech, B. Oleś, M. Hiller, F. Mintert, -, preprint]



What to take away . . .

- **trapping of quantum states** in classical nonlinear resonance island, garnished by finite tunneling rates which (indirectly) reflect the local phase space structure
- long lived (wave packet like) eigenstates are eligible for flexible and robust quantum control – **benchmark for semiclassics**
- similar phenomena naturally arise in the experimental manipulation of (interacting) cold matter – **without classical analog** –, and in molecular spectra
- **exact quantum treatment may turn prohibitive (without quantum computer)**
 - **quantitative semiclassics in high-dimensional phase space needed!**

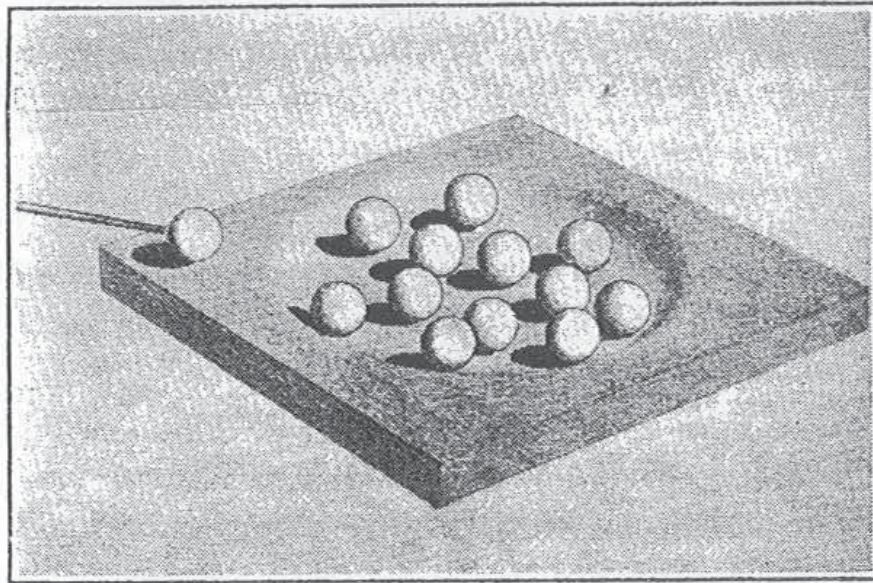
Roadmap

- **Nonlinear resonances: from helium to Bose-Hubbard**
Peter Schlagheck & Javier Madroño & Pierre Lugan & Klaus Zimmermann & Soeren Roerden & Maximilian Schmidt & Celsus Bouri
- **Matter wave transport in periodic optical potentials**
Alexey Ponomarev & Javier Madroño & Hannah Venzl & Alexej Schelle & Andrey Kolovsky & Stefan Hunn & Moritz Hiller & Tobias Zech & Lewin Stein & Sandro Wimberger & Dominik Hörndlein & Vivian Franca
- **Photon transport in disordered atomic samples**
Vyacheslav Shatokhin & Thomas Wellens & Cord A. Müller & Tobias Geiger & Felix Eckert & Nicolas Cherroret & Jochen Zimmermann & Scott Sanders
- **Energy transport in strongly driven Rydberg systems**
Andreas Krug & Sandro Wimberger & Javier Madroño & Alexej Schelle
- **Quantum transport in biological functional units**
Torsten Scholak & Thomas Wellens & Simeon Sauer & Florian Mintert & Fernando de Melo & Markus Tiersch

Many particle interactions – then and now

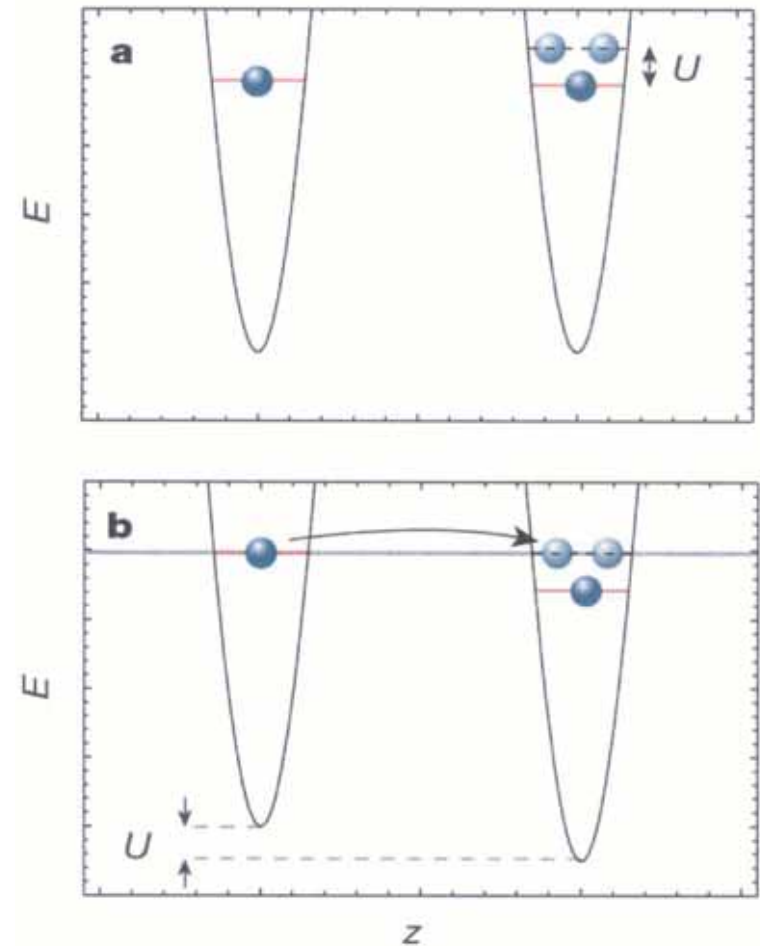
$$H_B = -\frac{J_B}{2} \left(\sum_l a_{l+1}^\dagger a_l + h.c. \right) + \frac{W_B}{2} \sum_l n_l (n_l - 1)$$

compound nuclei

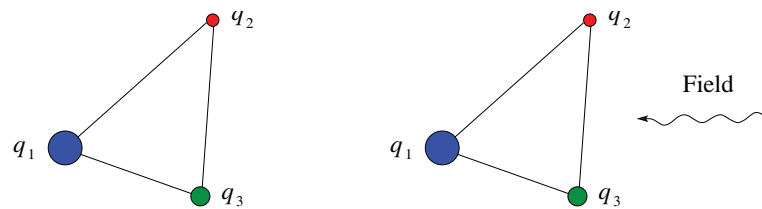


[N. Bohr, 1936]

ultracold atoms



[Greiner et al., 2002]



Non-integrable

New phenomena

driven helium

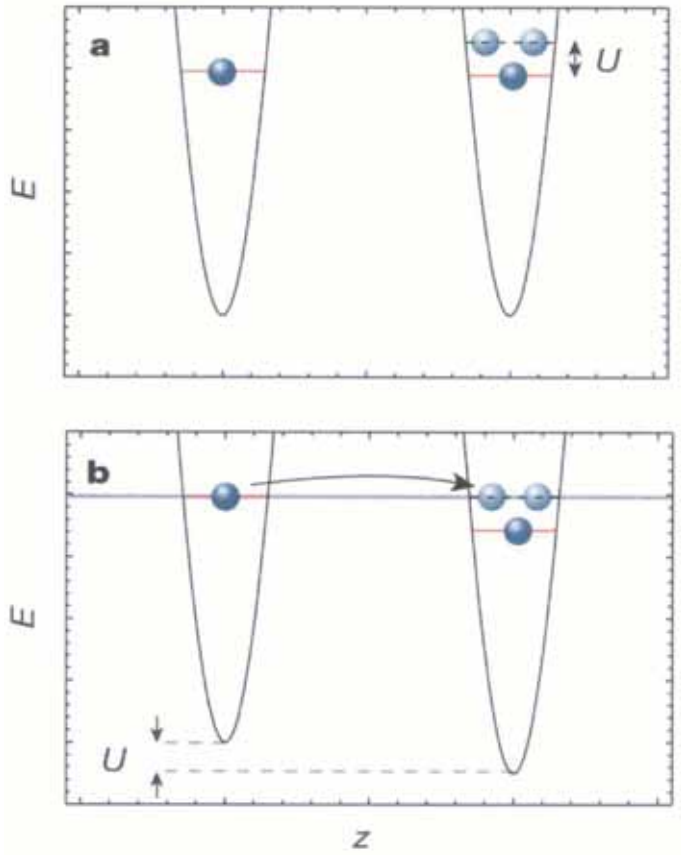
Controlled many-particle dynamics give rise to. . .

- **tunable spectral densities – from discrete to quasi continuous**
- tunable spectral statistics – from regular to chaotic
- tunable dynamics/entanglement – from periodic to irreversible/complex

all this in an experimentally realized, microscopic Hamiltonian

Tunable spectral densities in the Bose-Hubbard model

$$H_B = -\frac{J_B}{2} \left(\sum_l a_{l+1}^\dagger a_l + h.c. \right) + \frac{W_B}{2} \sum_l n_l(n_l - 1)$$



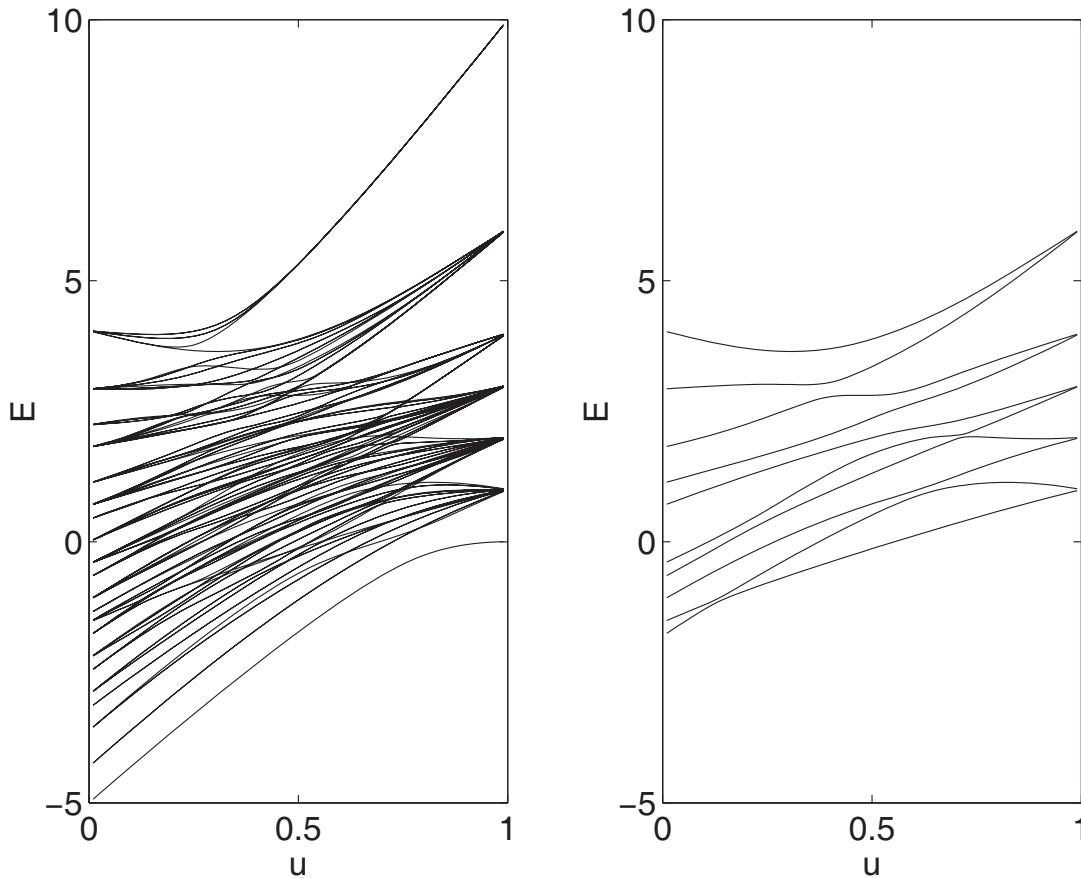
- Bose Einstein Condensate loaded into an optical lattice
- finite lattice size L , particle number N , filling factor $\bar{n} = N/L \simeq 1$, modelling with Bose-Hubbard Hamiltonian
- on-site energy W_B , hopping matrix element J_B
- **Hilbert space dimension**
 $\mathcal{N} = (N + L - 1)!/N!(L - 1)!$

Controlled many-particle dynamics give rise to. . .

- tunable spectral densities – from discrete to quasi continuous
- **tunable spectral statistics – from regular to chaotic**
- tunable dynamics – from periodic to irreversible/complex

all this in an experimentally realized, microscopic Hamiltonian

“Chaotic” spectrum of the unperturbed BH Hamiltonian



$$u \equiv W_B, J_B = 1 - u, L = N = 5$$

BH completely integrable for $J_B = 0$
(no hopping; Wannier eigenstates)

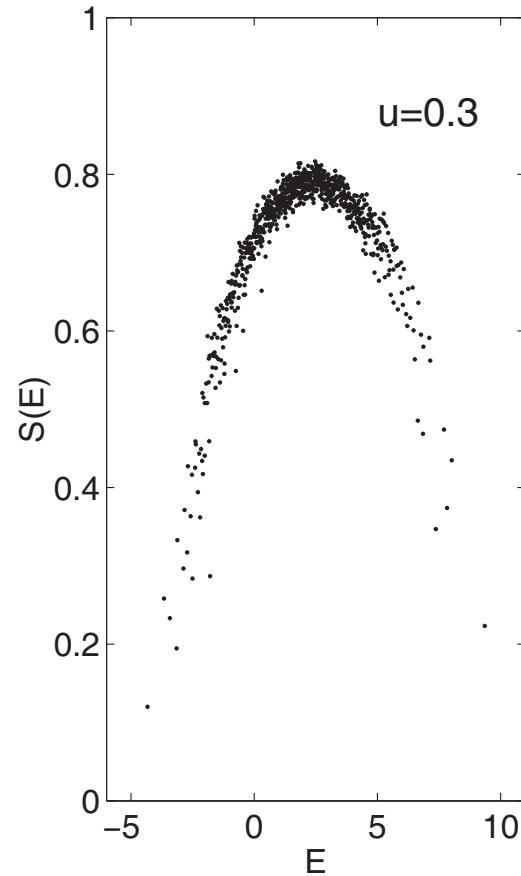
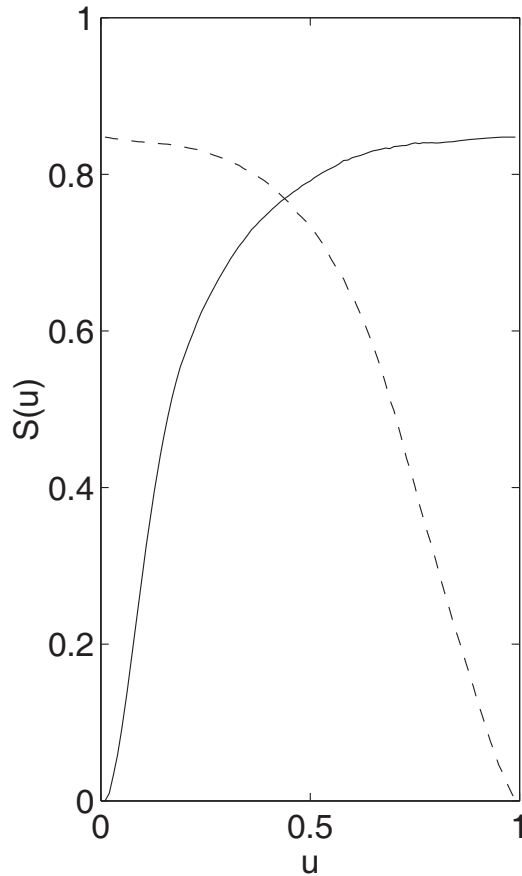
$$E_\mu = W_B \mu, \mu = \frac{1}{2} \sum_l n_l (n_l - 1)$$

and $W_B = 0$ (no interaction; Bloch waves)

$$E_\nu = -J_B \nu, \nu = \sum_k \cos\left(\frac{2\pi k}{L}\right) n_k$$

after removal of symmetries no crossings are left in the spectrum –
indication of nonintegrability of the spectral dynamics! –

Delocalization of eigenfunctions



entropy measures average delocalization of eigenstates (in a given, generic basis):

$$S(u) = \left\langle -\frac{1}{\log \mathcal{N}} \sum_{j=1}^{\mathcal{N}} |c_j|^2 \log(|c_j|^2) \right\rangle$$

entropy of individual eigenstates:

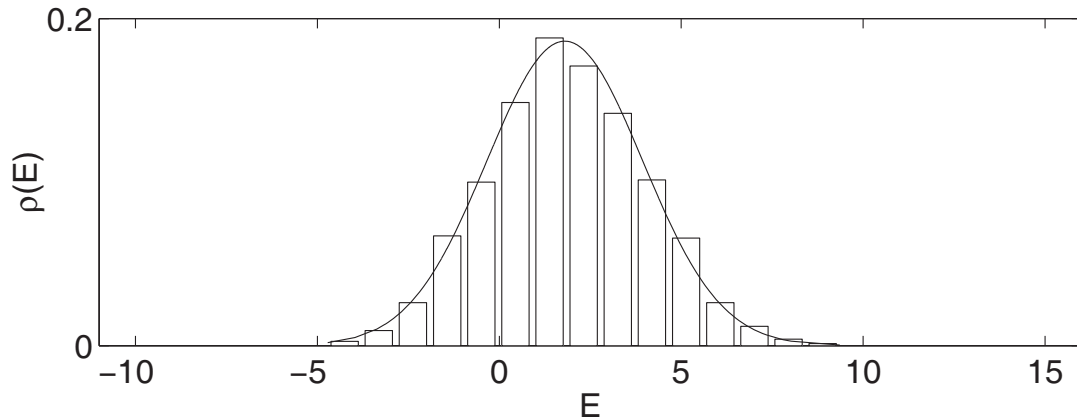
$$S(E) = \min[S^{(\nu)}(E), S^{(\mu)}(E)]$$

strong mixing for intermediate values of $0 < u < 1$, in the bulk of the spectrum!

left panel; solid: ν -basis, dashed: μ -basis

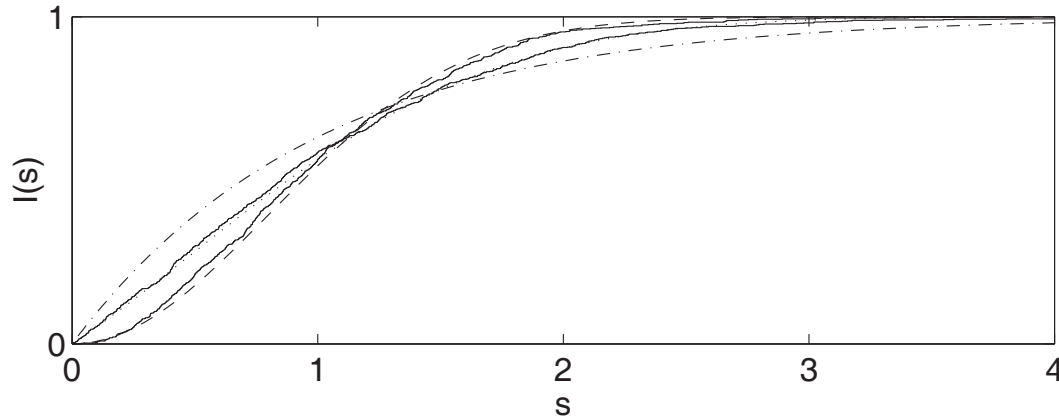
right: entropy of individual eigenstates at $u = 0.3$

Universal spectral statistics



density of states

$$\rho(E) \sim \exp[-(E - \bar{E})^2/\sigma^2]$$



integrated level spacing distribution

$$I(s) = \int_0^s P(s') ds'$$

faithfully follows Random Matrix prediction!

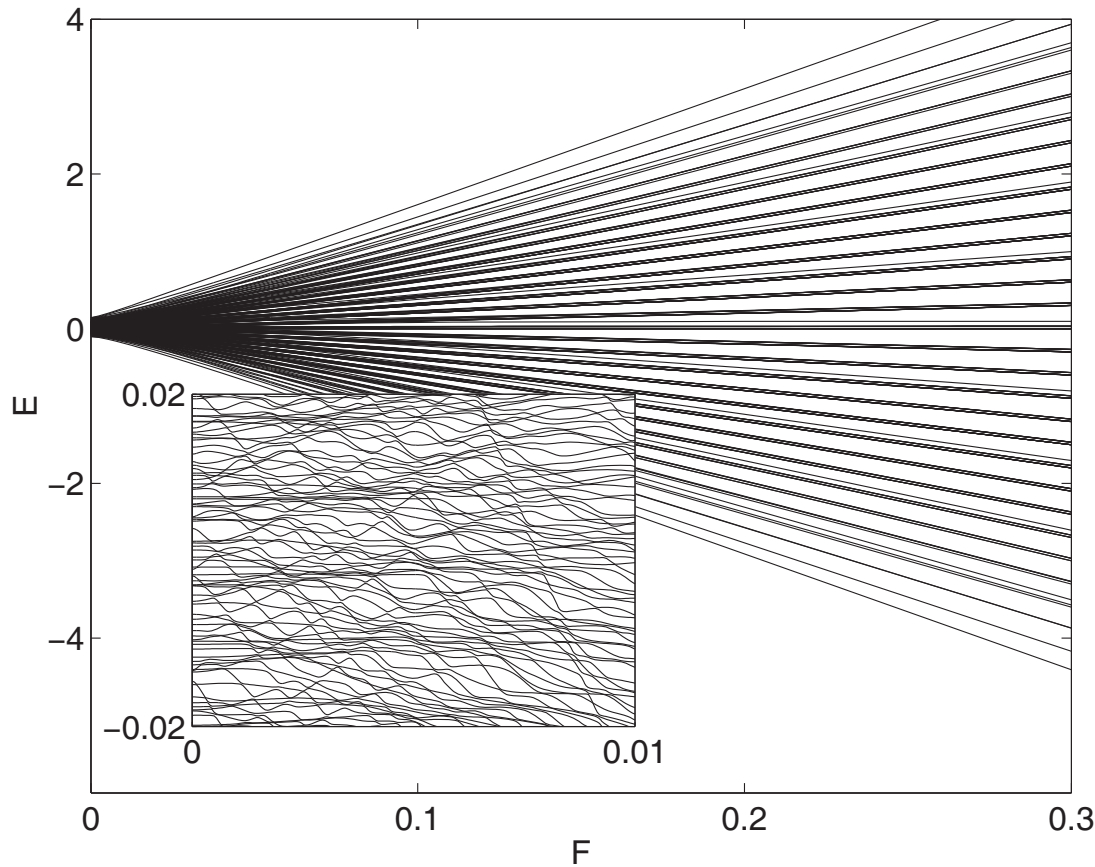
top: density of states

bottom: integrated level spacing distribution

$$L = N = 8, u = 0.3$$

Tuning the spectrum from regularity to complexity

$$H = -\frac{J_B}{2} \left(\sum_l a_{l+1}^\dagger a_l + h.c. \right) + \frac{W_B}{2} \sum_l n_l(n_l - 1) + Fd \sum_l n_l$$



$$[N = 3, L = 11, J_B = 0.038, W_B = 0.032]$$

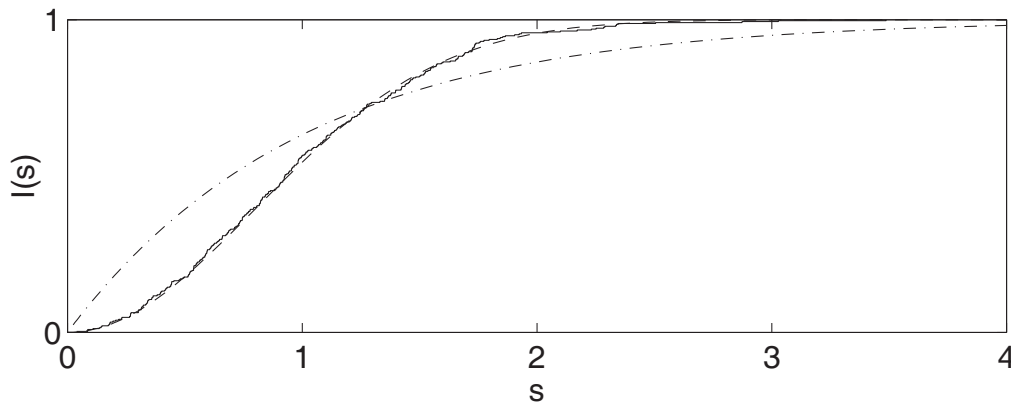
- Bose-Hubbard Hamiltonian under **static tilt**
- parametric spectral evolution

$$H(F)|\psi_j(F)\rangle = E_j(F)|\psi_j(F)\rangle$$

- spacings $s_j(F) = E_{j+1}(F) - E_j(F)$
- inset: **competing symmetries – “level spaghetti”**

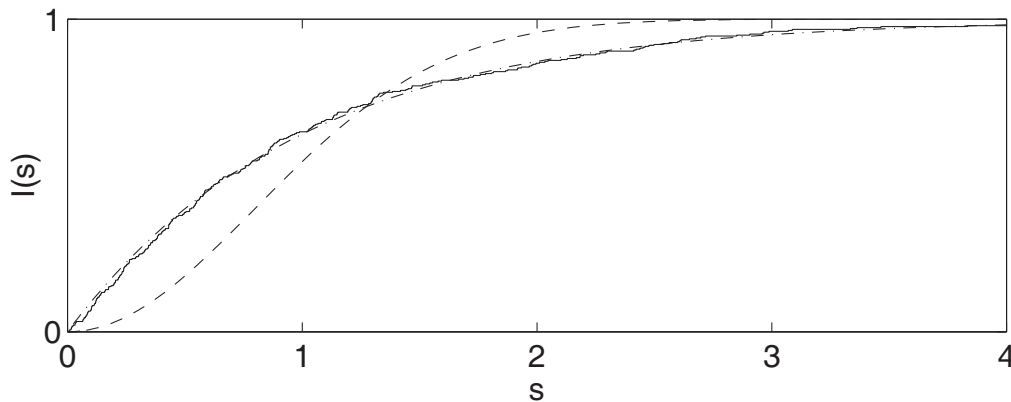
Regular/Poisson vs. chaotic/Wigner statistics

cumulated nearest neighbor distribution



- $I(s) = \int_0^s P(s') ds'$,
 $I(s)^{\text{Wigner}} = 1 - \exp(-\pi s^2/4)$

- **chaotic (Wigner)** spectrum for not too large static field (top, $F = 0.01$)



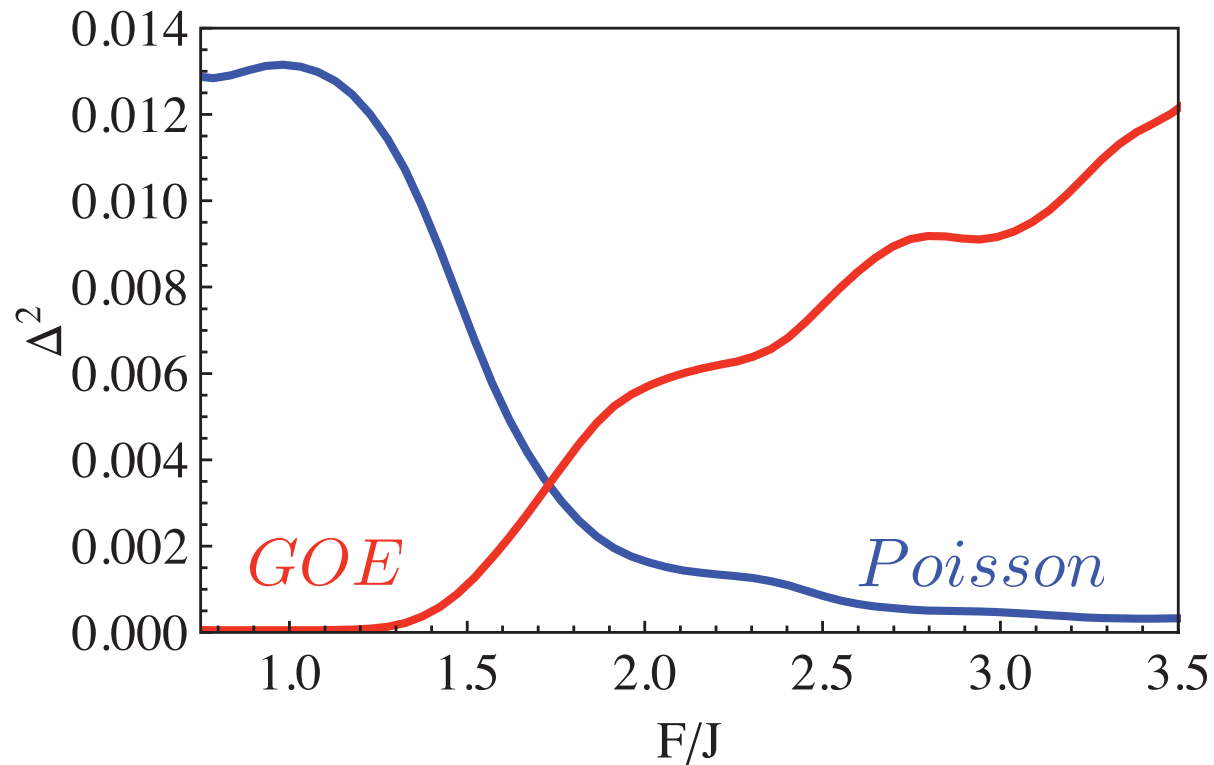
- $I(s)^{\text{Poisson}} = 1 - \exp(-s)$

- **regular (Poisson)** spectrum for strong tilt (Stark symmetry dominates, bottom, $F = 0.04$)

$[N = 3, L = 11, J_B = 0.038, W_B = 0.032]$

Tuning from chaotic to regular statistics

- **blue line:** deviation from Poisson – regularity
- **red line:** deviation from Wigner – chaos



sharp transition!

Controlled many-particle dynamics give rise to. . .

- tunable spectral densities – from discrete to quasi continuous
- tunable spectral statistics – from regular to chaotic
- **tunable dynamics – from periodic to irreversible/complex**

all this in an experimentally realized, microscopic Hamiltonian

Dynamical complexity from chaotic spectra

the spectrum generates the dynamical “code”

$$|\psi(t)\rangle = U(t)|\psi_0\rangle = \sum_j \exp(-iE_j t/\hbar) |\phi_j\rangle \langle \phi_j | \psi_0\rangle$$

“Width” $W = \exp\left(-\sum_j |c_j|^2 \ln |c_j|^2\right)$, $c_j = \langle \phi_j | \psi_0\rangle$
provides good measure of **complexity**.

[Blümel & Smilansky, 1988]

- The larger W , the harder to simulate!
- Poisson statistics \rightarrow small W
- Wigner statistics \rightarrow large W
- Note analogy to Schmidt numbers in entanglement theory!

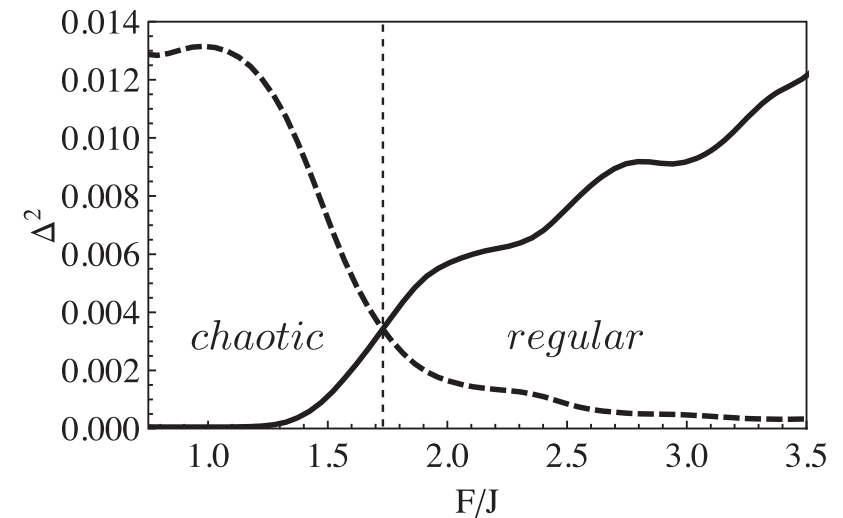
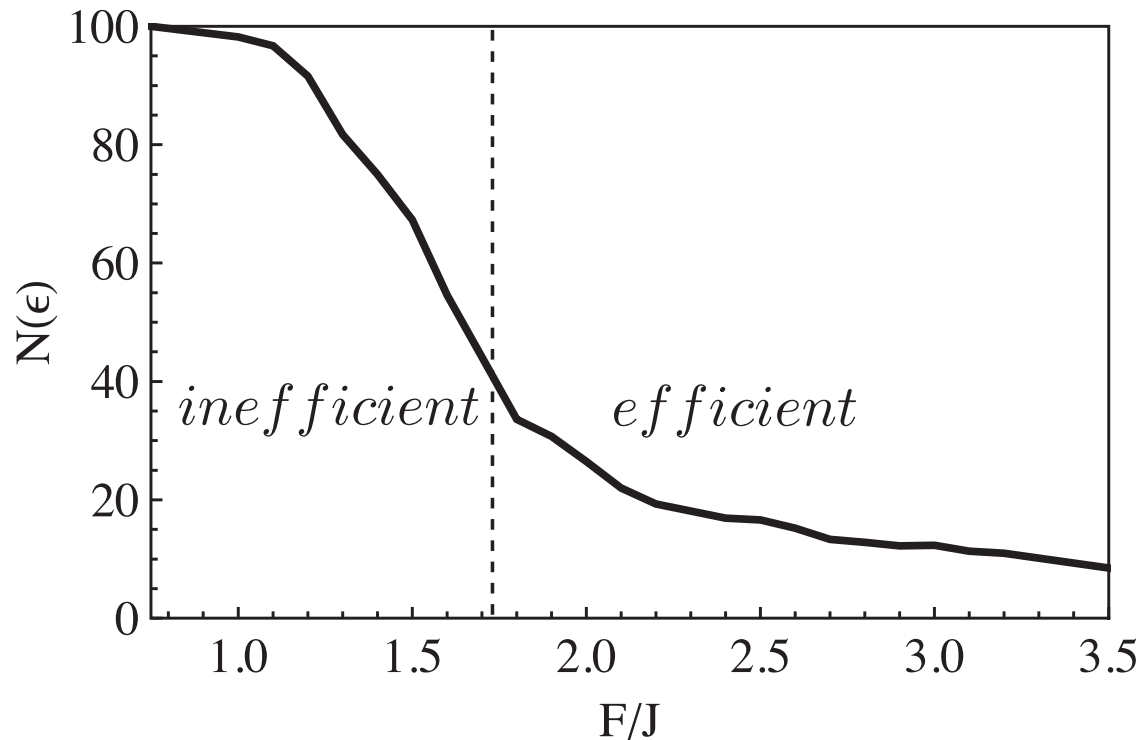
[Mintert et al., 2004]

Message I: “Chaos” entails inefficiency of t-DMRG

- Width $W \sim N(\epsilon)$ – number of **Schmidt coefficients** larger than $\epsilon = 0.01$; **t-DMRG simulation** for $N = 8$ particles initially placed at the centre of lattice with $L = 64$

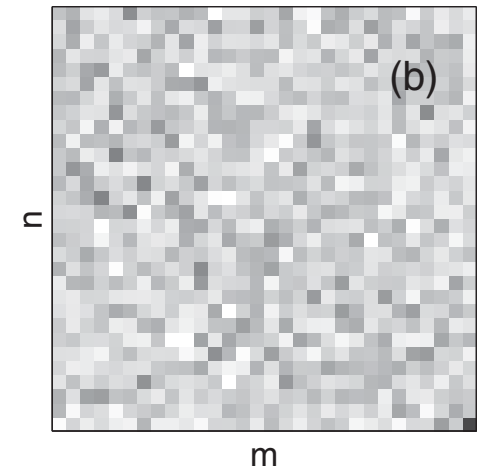
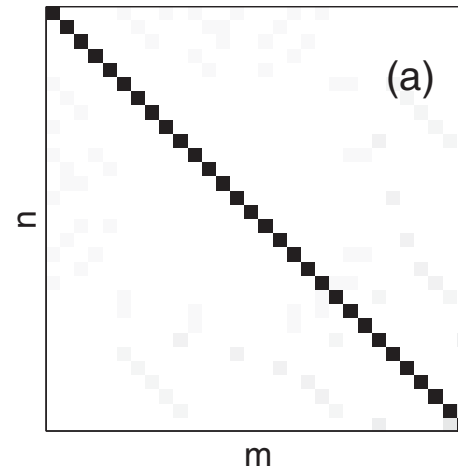
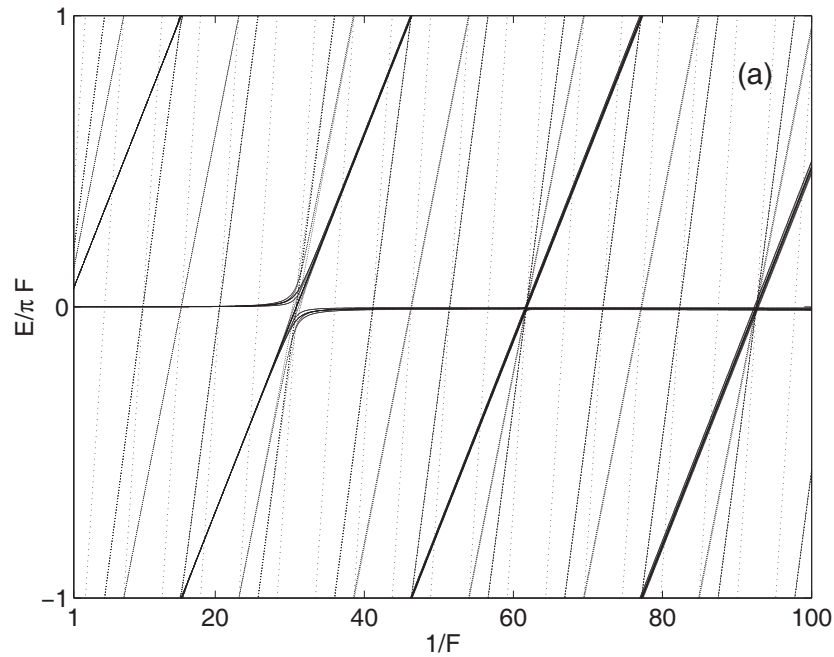
[Fannes et al., 1992; Vidal 2003]

- data for **bipartition with broadest distribution of Schmidt coefficients**

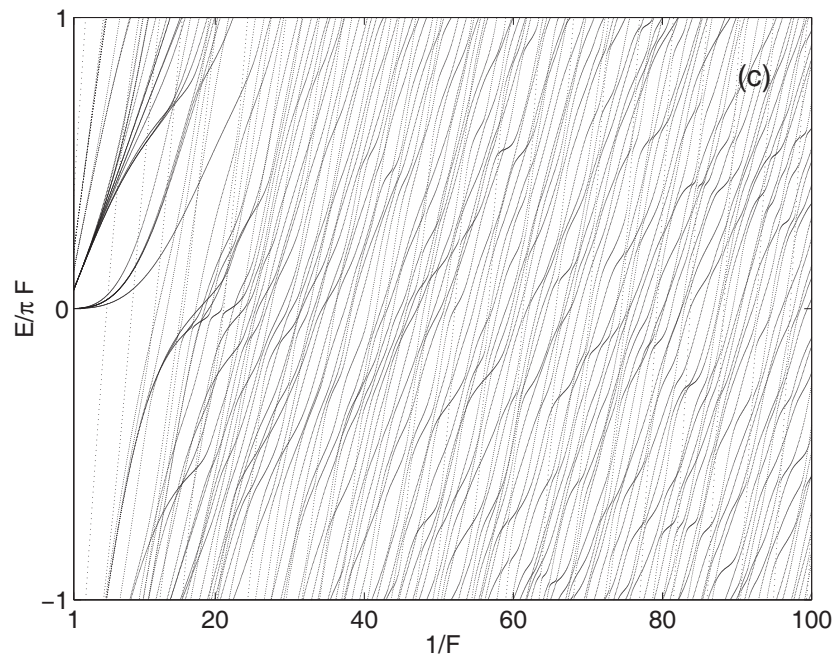


small F : basis saturates!

Spectrum of the Floquet-Bloch operator



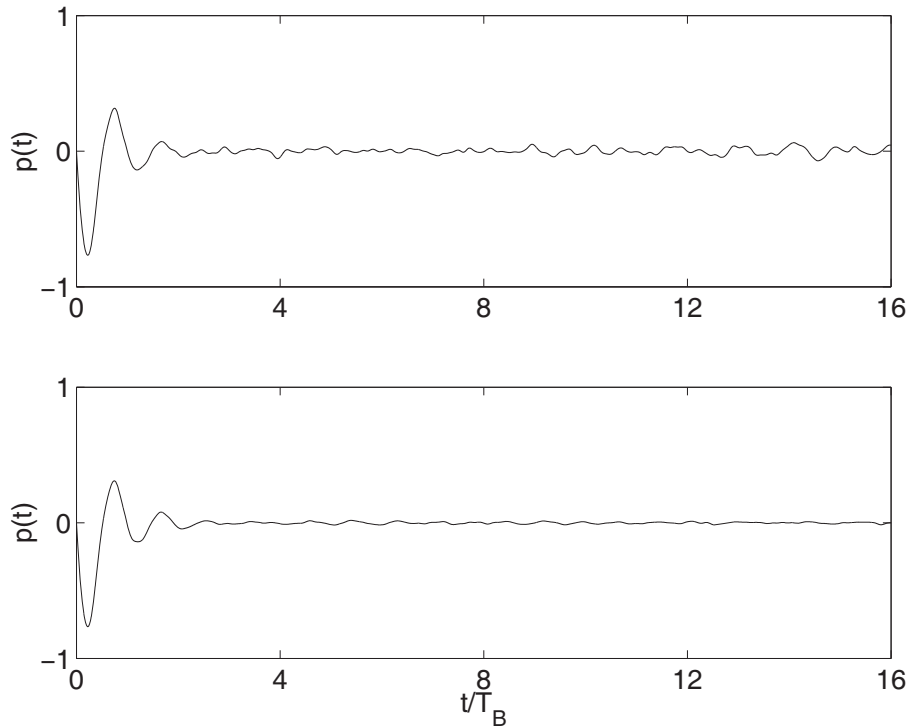
↑ matrix structure of Floquet-Bloch operator for strong ($F = 0.5$, (a)) and weak tilt ($F = 0.01$, (b)); $J_B = 0.038$, $W_B = 0.032$



← level dynamics of Floquet-Bloch operator for $J_B = 0.00076$ (top) and $J_B = 0.038$ (bottom) $N = 4$, $L = 7$

small J_B : $\exp(-iET_B) \simeq \exp(-i\mu W_B/Fd)$

Many particle induced decoherence



[A. Kolovsky & A.B., 2003]

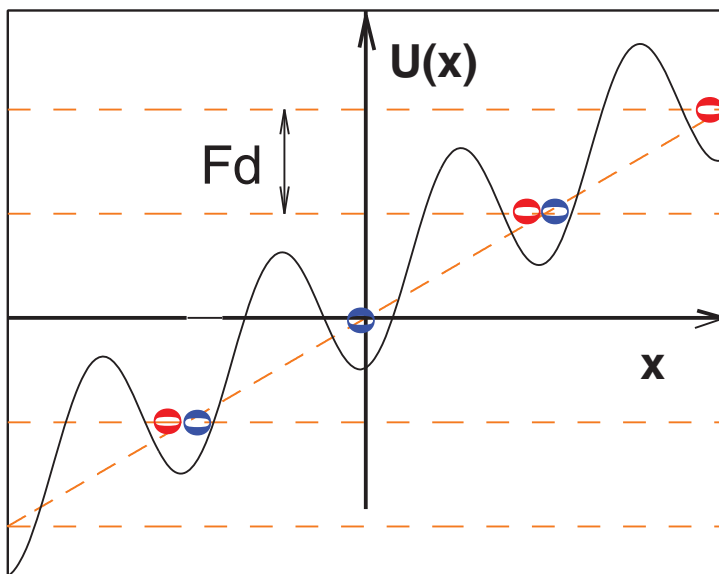
- average atomic momentum
 $p(t) = \text{tr} [\hat{p}\hat{\rho}(t)]$ – single particle density matrix $\hat{\rho}(t)$
- interaction-induced, rapid decay of Bloch oscillations!
- rapid convergence towards thermodynamic limit $N, L \rightarrow \infty$, $N/L = \text{const}$, N, L particle number and lattice size. $L = 7$ (top), $L = 9$ (bottom), $N/L = 1$.
- Hilbert space dimensions $\mathcal{N} = 1716$ (top), $\mathcal{N} = 24310$ (bottom)

Message II: The BH Hamiltonian as tunable environment

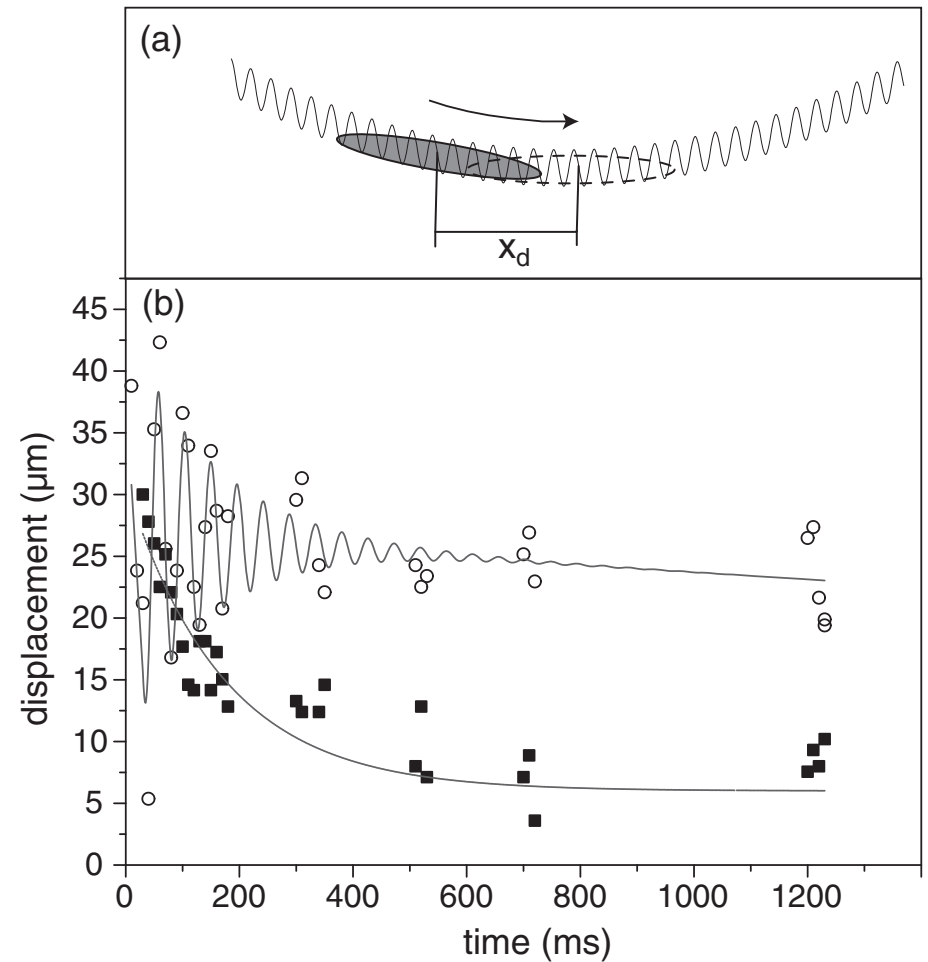
$$H = -\frac{J_F}{2} (\sum_l |l+1\rangle\langle l| + h.c.) + Fd \sum_l |l\rangle l \langle l| + H_B + W_{FB} \sum_l n_l |l\rangle\langle l|$$

Current needs

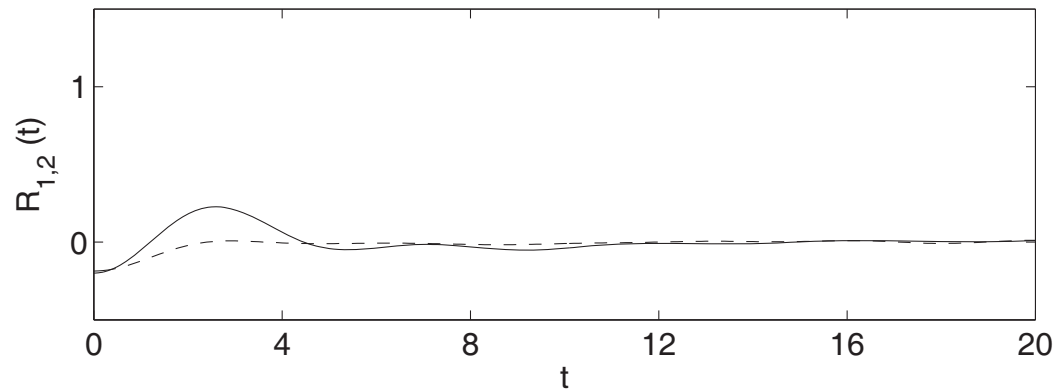
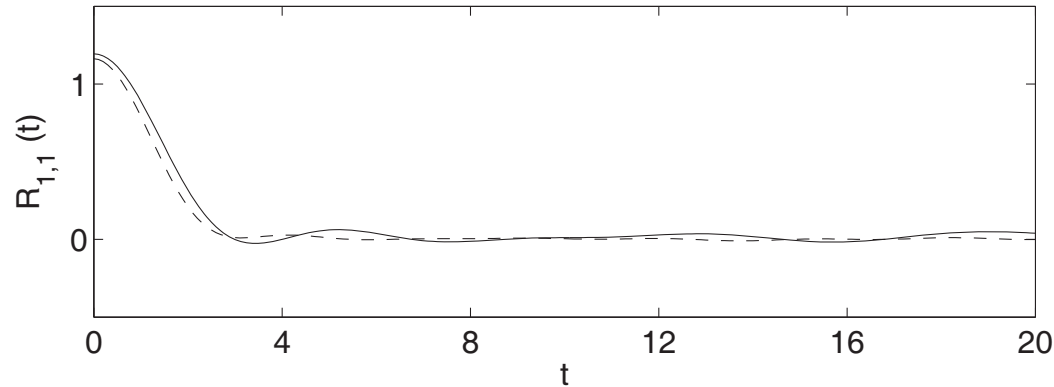
- external force – static field F
- *controlled* relaxation processes
 - Fermi-Boson collisions



experiments (relaxation hitherto uncontrolled)



System-bath separation and rapidly decaying bath correlations



← the boson-number cross-correlation functions decay on time scale $\tau \simeq 3\hbar/J_B$

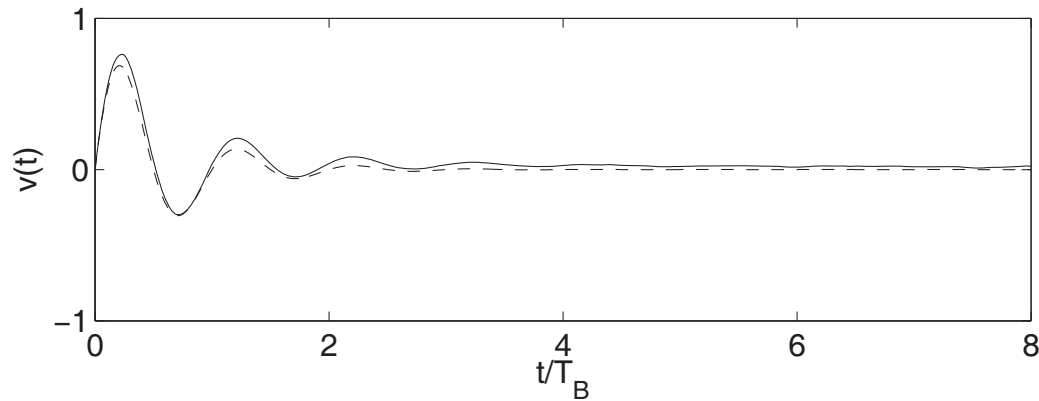
- for $\tau \ll T_B$, the bath is delta-correlated
- can derive master equation for fermionic degree of freedom, after tracing out the bosonic degree of freedom

$$R_{l,m}(t, t') = \text{Tr}[n_l(t)n_m(t')]$$

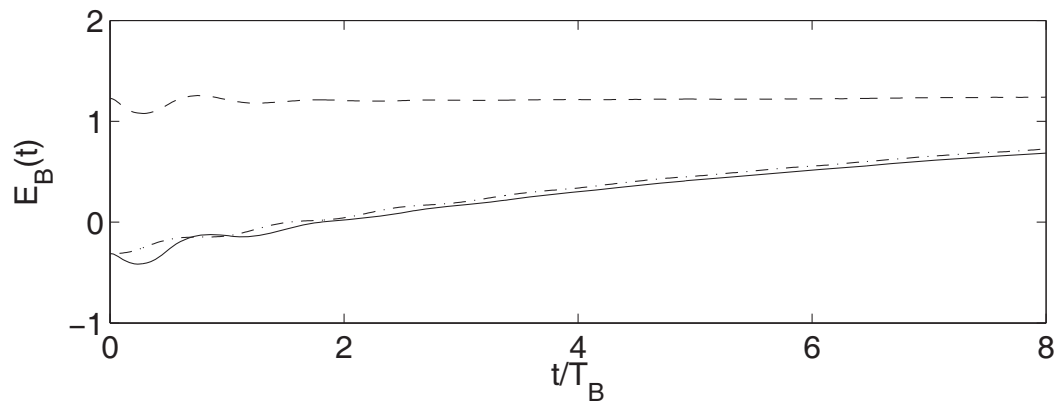
Interaction induced decay of fermionic Bloch oscillations

spin-polarized fermions interact with bosonic HB “bath”

only fermions experience static force



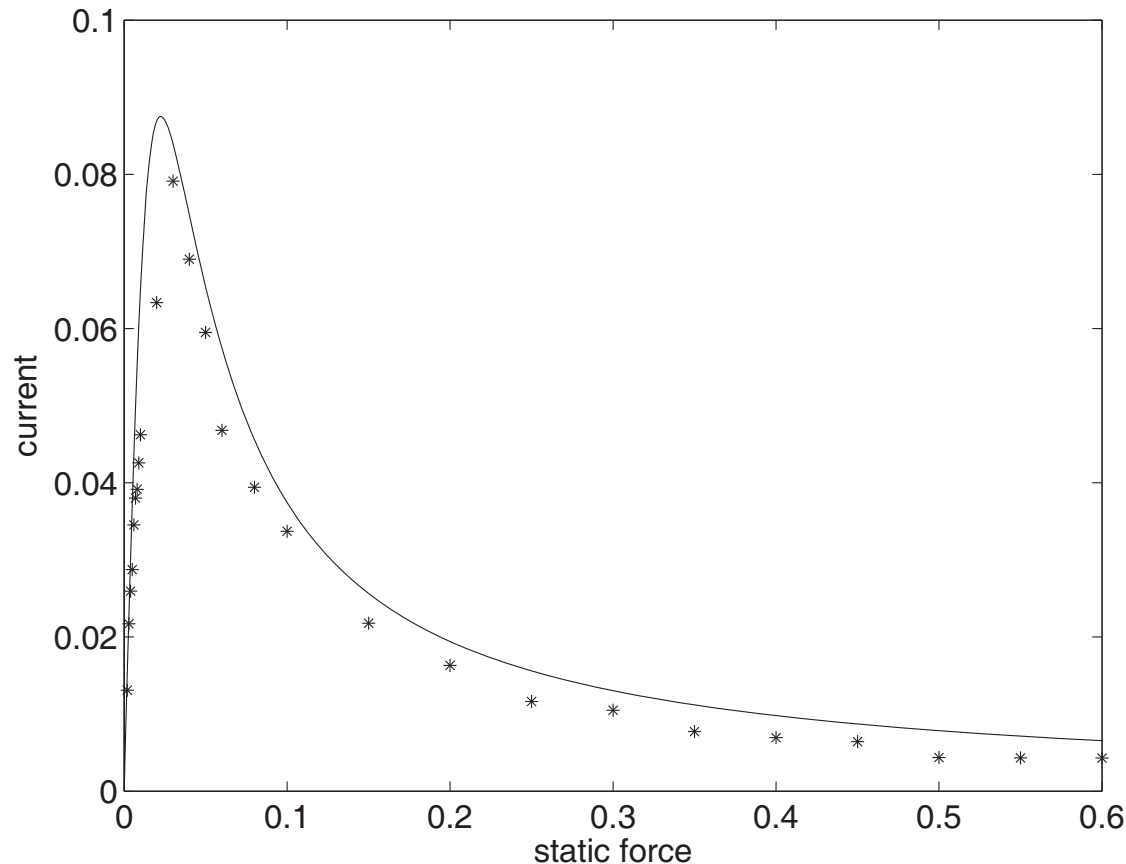
← fermionic Bloch oscillations decay
(described by master equation)



← heating of the bath, if bath initially non-thermalized/cold!

Directed atomic current across a 1D optical lattice

fermionic “current-voltage” characteristics across the lattice



- clear transition from Ohmic ($\bar{v} \sim Fd$) to negative differential conductance ($\bar{v} \sim 1/Fd$)
- in accord with phenomenological Esaki-Tsu relation for electron transport in semiconductor superlattices (full line)

$$\bar{v} = \frac{J_F d}{4\hbar} \frac{\omega_B/\gamma}{1 + (\omega_B/\gamma)^2}$$

engineered bath/decoherence, controlled relaxation rate $\gamma \simeq \frac{3\bar{n}^2 W_{\text{FB}}^2}{\hbar J_B}$

Literature (selection) & take-home message

- P.W. Anderson, *Concepts in Solids: Lectures on the Theory of Solids*, Addison-Wesley 1992;
- L. Pitaevski and S. Stringari, *Bose-Einstein Condensation*, Clarendon Press 2003;
- H. Ott et al., *Phys. Rev. Lett.* **92**, 160601 (2004);
- M. Köhl et al., *Phys. Rev. Lett.* **94**, 080403 (2005);
- C.-S. Chuu et al., *Phys. Rev. Lett.* **95**, 260403 (2005);
- Y. Takasu et al., *Phys. Rev. Lett.* **91**, 040404 (2003);
- O. Bohigas, in *Chaos and Quantum Physics*, Les Houches LII, ed. by M.-J. Giannoni, A. Voros, J. Zinn-Justin, North Holland 1991;
- L. Esaki and R. Tsu, *IBM J. Res. Dev.* **14**, 61 (1970);
- T.M. Fromhold et al., *Nature* **428**, 726 (2004);
- A. Ponomarev et al., *Phys. Rev. Lett.* **96**, 050404 (2006);
- J. Madroñero et al., *Adv. At. Mol. Opt. Phys.* (2006).

engineered bath, controlled current, microscopic Hamiltonian

Roadmap

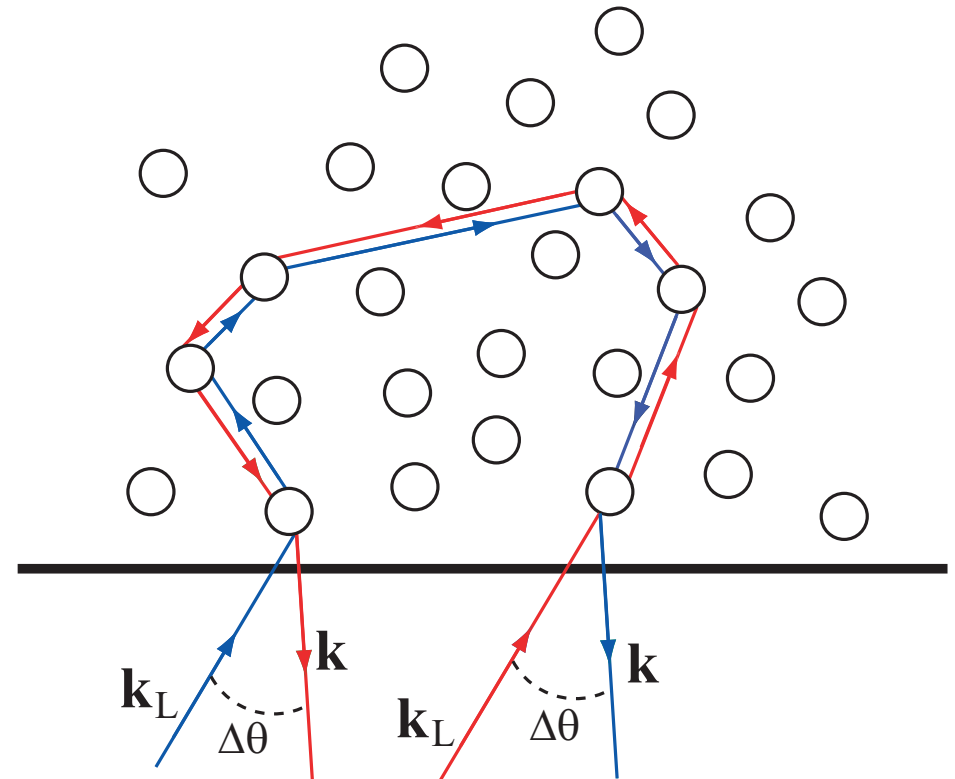
- **Nonlinear resonances: from helium to Bose-Hubbard**
Peter Schlagheck & Javier Madroñero & Pierre Lugan & Klaus Zimmermann & Soeren Roerden & Maximilian Schmidt & Celsus Bouri
- **Matter wave transport in periodic optical potentials**
Alexey Ponomarev & Javier Madroñero & Hannah Venzl & Alexej Schelle & Andrey Kolovsky & Stefan Hunn & Moritz Hiller & Tobias Zech & Lewin Stein & Sandro Wimberger & Dominik Hörndlein & Vivian Franca
- **Photon transport in disordered atomic samples**
Vyacheslav Shatokhin & Thomas Wellens & Cord A. Müller & Tobias Geiger & Felix Eckert & Nicolas Cherroret & Jochen Zimmermann & Scott Sanders
- **Energy transport in strongly driven Rydberg systems**
Andreas Krug & Sandro Wimberger & Javier Madroñero & Alexej Schelle
- **Quantum transport in biological functional units**
Torsten Scholak & Thomas Wellens & Simeon Sauer & Florian Mintert & Fernando de Melo & Markus Tiersch

Coherent backscattering of light (CBS)

- interference effect in disordered media
- survives disorder average
- enhanced backscattering intensity over a homogeneous background
- experimental tool to characterize diffuse scattering media

[Maret et al.]

- photon wave length λ much smaller than average distance of scatterers ℓ

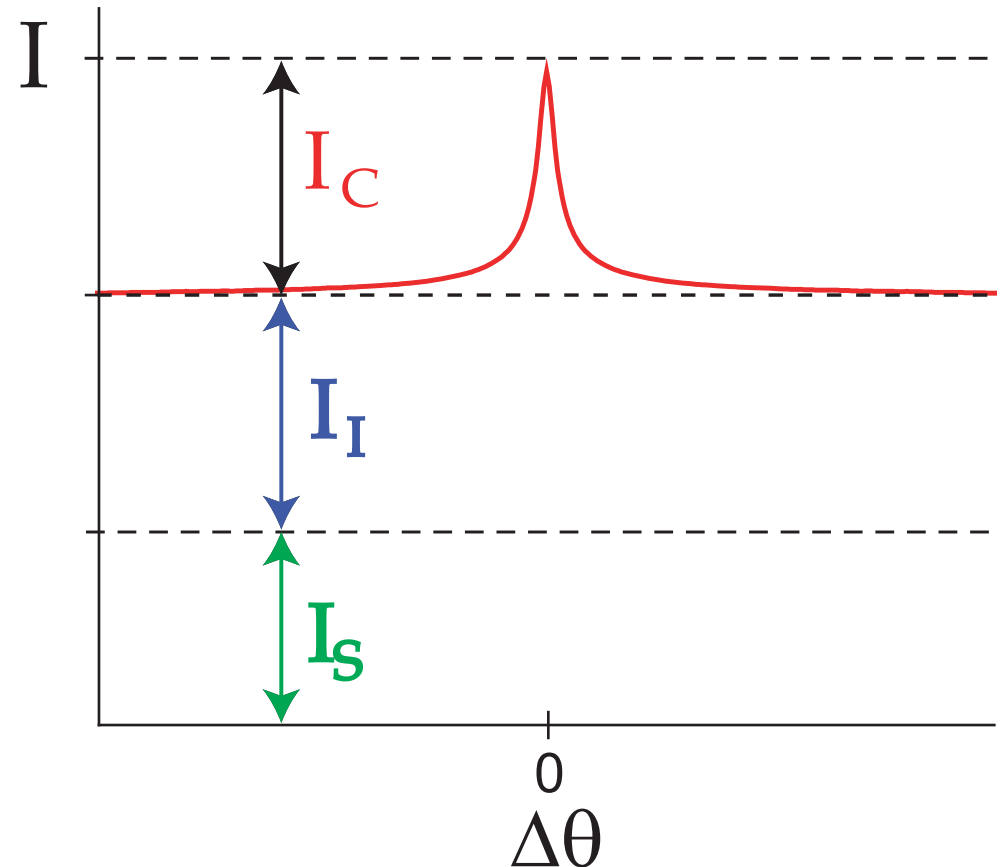


here: multiple photon scattering from cold atoms with internal electronic structure

The CBS cone

- interference effect stems from cross term of pairs of interfering amplitudes
- much as in double-slit interference
- in general, the CBS interference signal is only a *small* correction to the sum of single scattering and direct multiple scattering amplitudes

$$\alpha(\Delta\theta) = 1 + I_C(\Delta\theta)/(I_s + I_I)$$

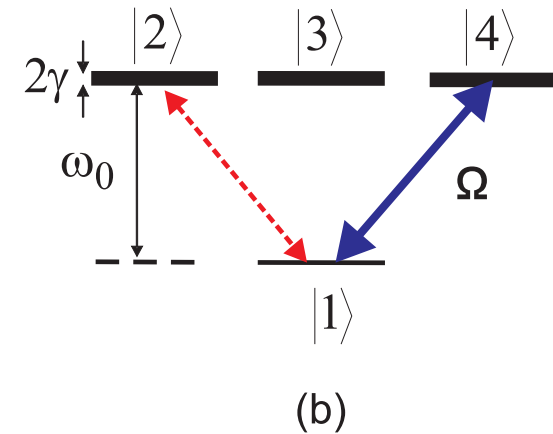
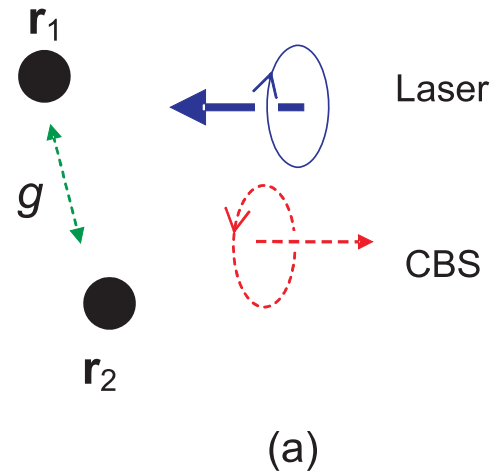


- background terms can be eliminated through observation in the appropriate polarization channel
- width of the cone encodes mean free path:

$$\Delta\theta \simeq 1/k\ell, \quad k = 2\pi/\lambda$$

Why CBS with cold atoms?

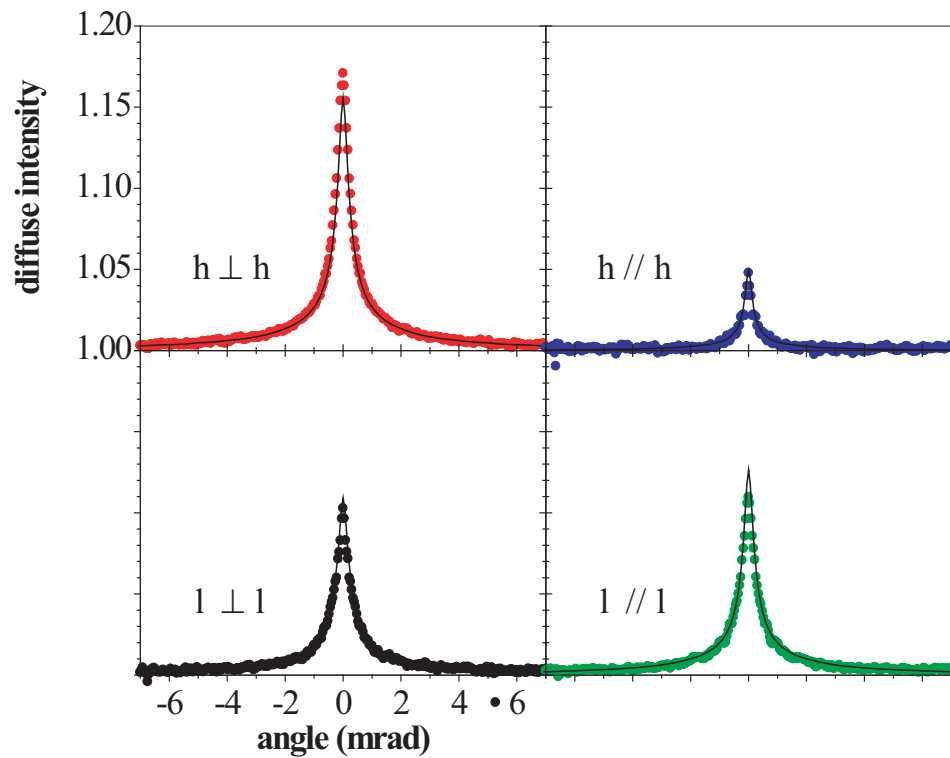
- point-like scatterers
- very good sample control (monodisperse, defect-free)
- tunable scattering properties (laser frequency vs. electronic transition frequencies)
- simple microscopic description



Experimental results at small injected intensities

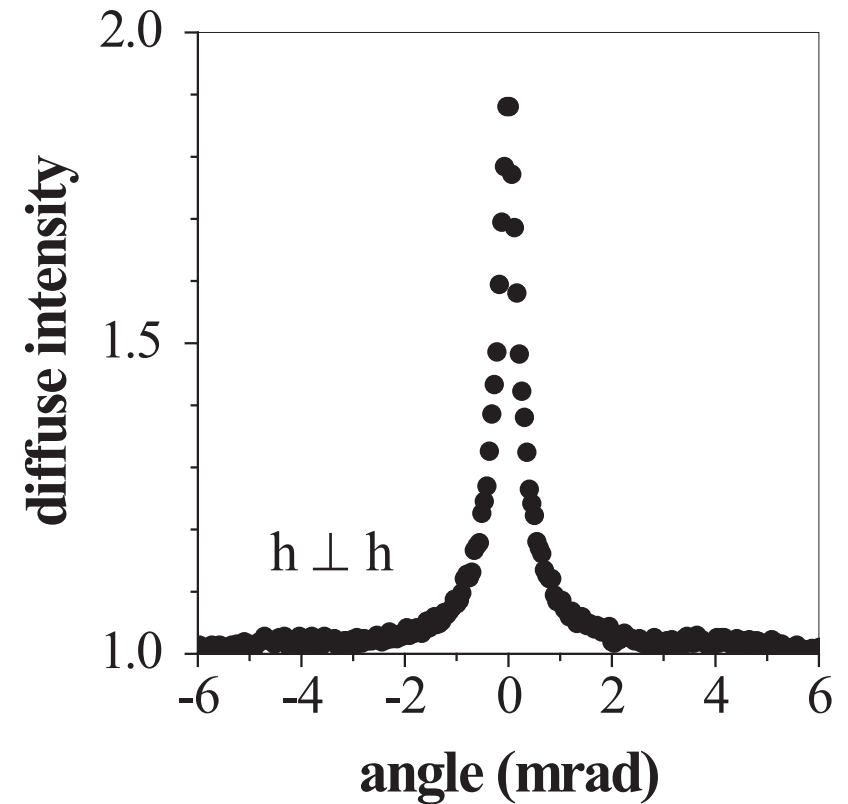
[Labeyrie et al., 2003, and Chanelière et al, 2004]

Rb^{85}



- $N \sim 10^{10}$ atoms
- optical thickness $b \simeq 40$

Sr^{88}

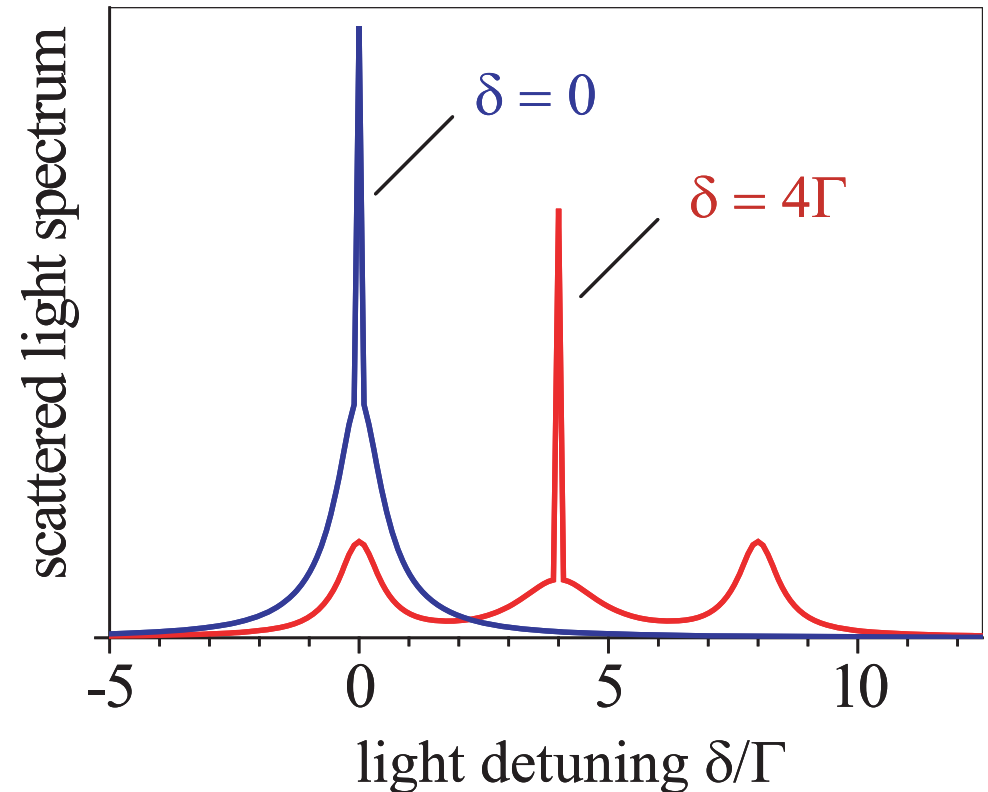


- $N \sim 10^7$ atoms
- optical thickness $b \simeq 4$

Coherence loss at high injected intensities

- at low intensities and resonant laser-atom interaction, i.e., at $\omega_L = \omega_0$: elastic photon scattering
- at high intensities and finite detuning $\delta = \omega_L - \omega_0$: *inelastic scattering*
- ratio of inelastically vs. elastically scattered photons controlled by **saturation parameter**

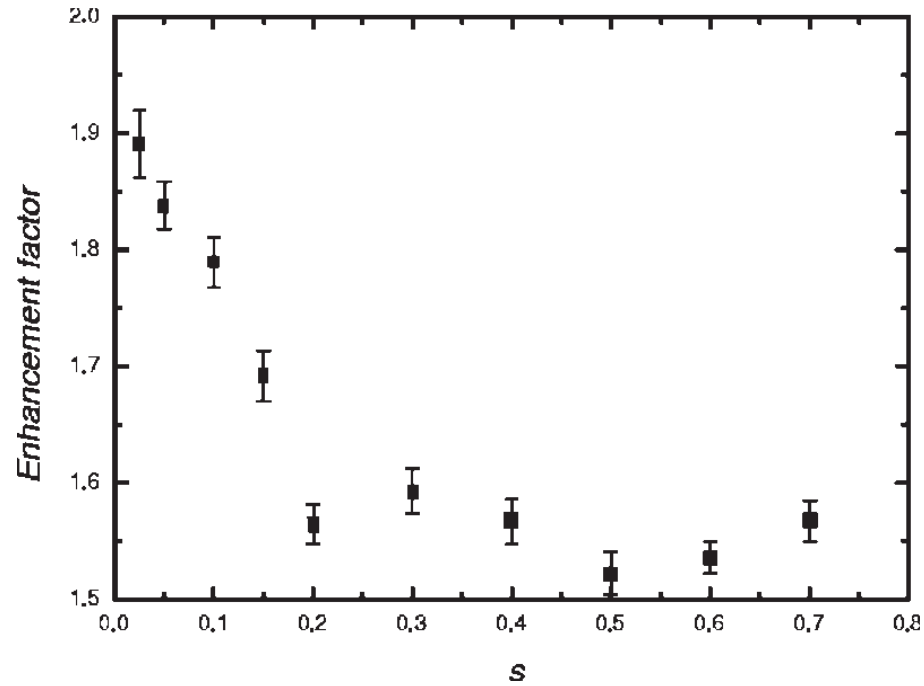
$$s = \frac{\Omega^2}{2(\delta^2 + \gamma^2)}$$



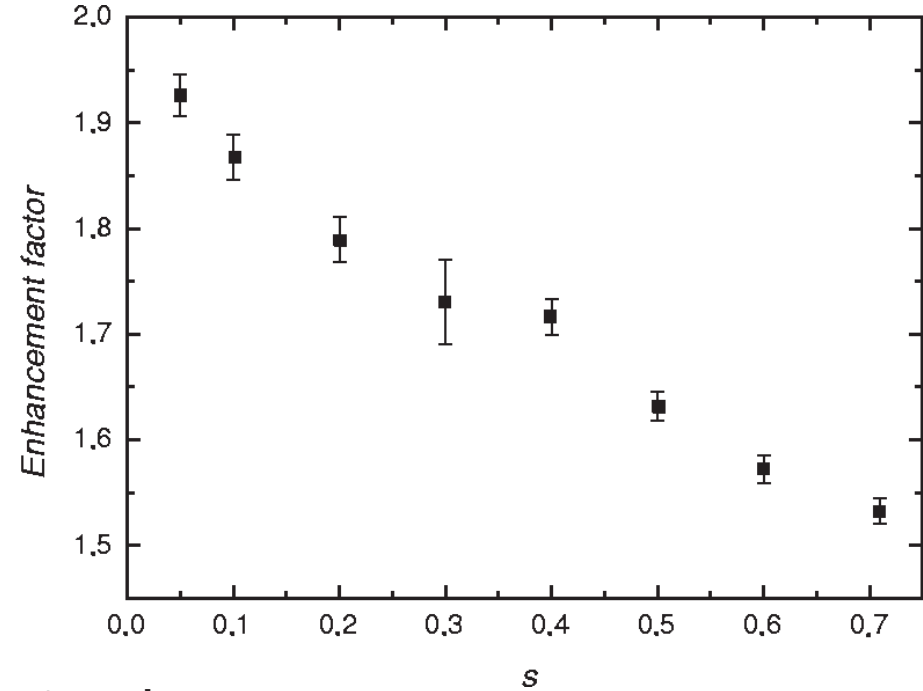
spectral signature for a photon scattered off a single two-level atom: **Mollow triplet** exhibits trident shape, at large intensities, i.e., large Rabi frequencies Ω , with spectral lines separated by Ω [Mollow 1969]

Experimental observations on Sr

finite detuning, $\delta > 0$



on resonance, $\delta = 0$



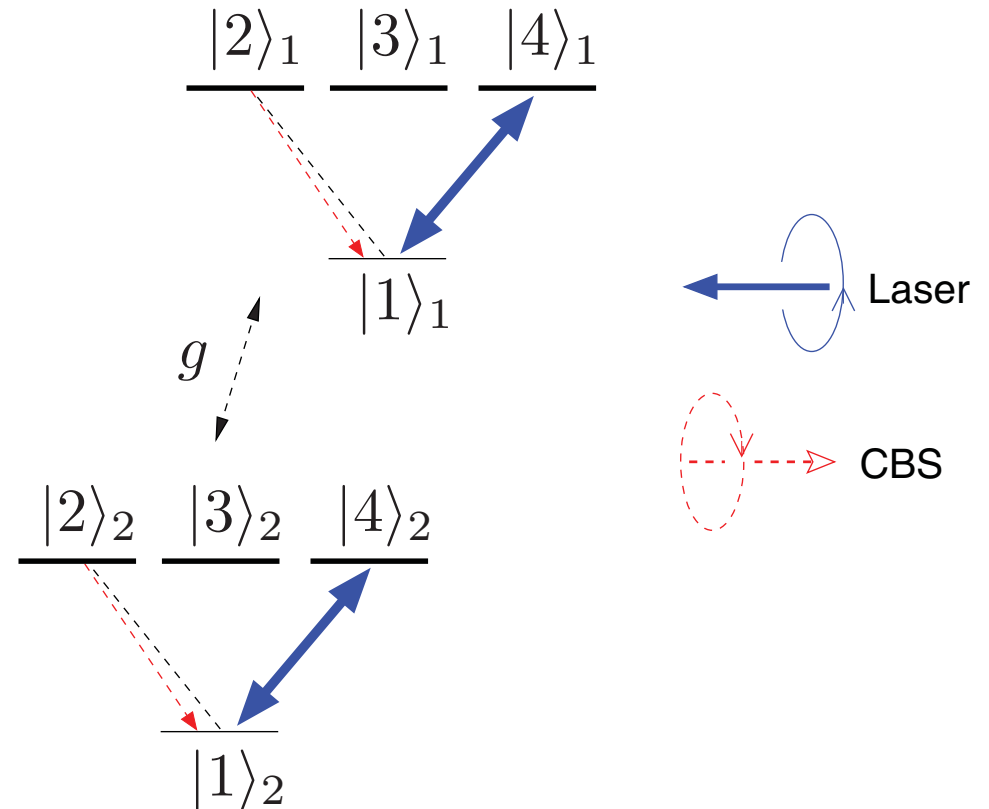
[Chanelière et al., 2004]

dramatic suppression of the signal at high saturation parameters

Modelling CBS in the regime of nonlinear, inelastic scattering

The model

- scattering off two atoms at distance r_{12}
- far field approximation $r_{12} \gg \lambda = 2\pi k_L$
- polarization selective detection
- disorder mimicked by suitable average over atomic position



small parameter: far field atom-atom coupling constant g

The fundamental evolution equation

The stationary backscattered intensity is derived from the steady state solutions for the atomic dipole operators and their correlation functions.

These steady state solutions are obtained from the master equation

$$\langle \dot{Q} \rangle = \sum_{\alpha=1}^{N=2} \langle \mathcal{L}_{\alpha} Q \rangle + \sum_{\alpha \neq \beta=1}^{N=2} \langle \mathcal{L}_{\alpha\beta} Q \rangle ,$$

with

$$Q \in \{\sigma_{11}^1, \dots, \sigma_{44}^1\} \otimes \{\sigma_{11}^2, \dots, \sigma_{44}^2\}$$

(256 operators)

The Liouvillians \mathcal{L}_{α} (independent atoms) and $\mathcal{L}_{\alpha\beta}$ (interacting atoms) account for the interactions between atoms, injected laser field, and environment modes (including the polarization degree of freedom).

CBS intensity from the source dipoles

Stationary backscattering intensity in terms of atomic dipoles and dipole-dipole correlators (helicity preserving channel)

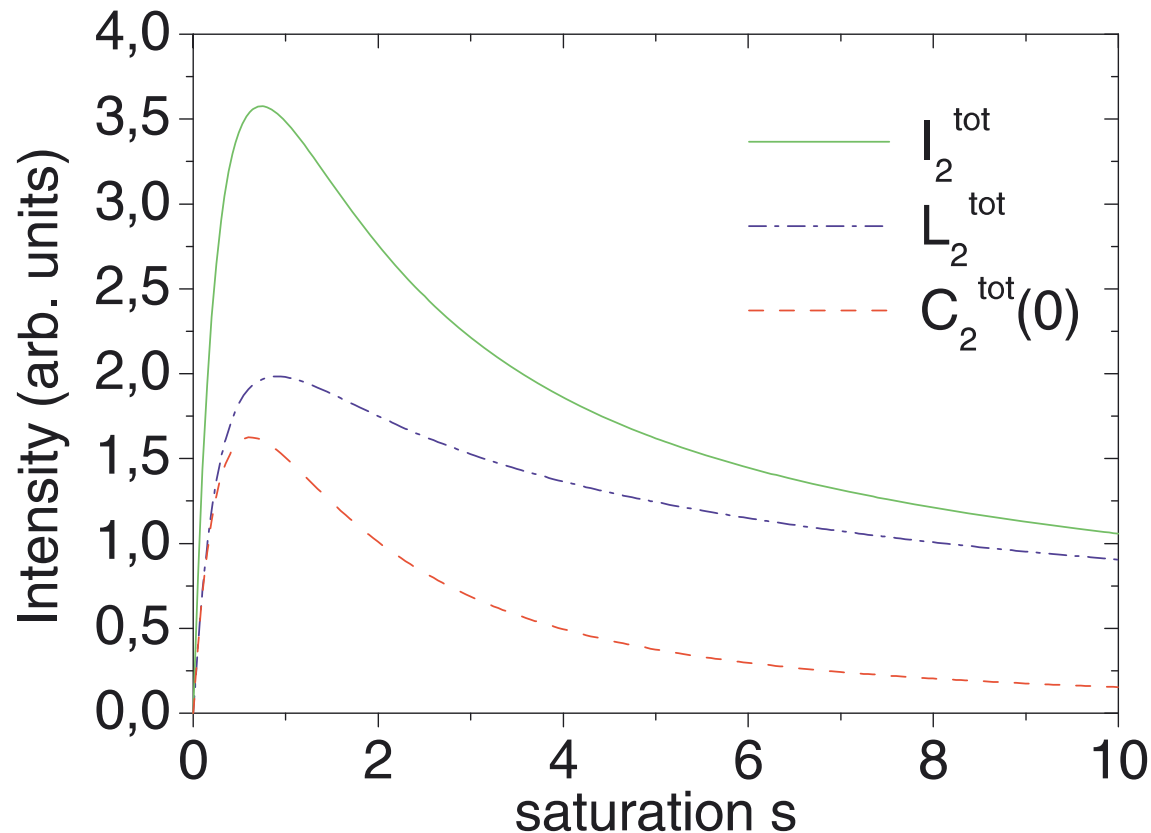
$$\langle I \rangle_{\text{ss}} = \langle \sigma_{22}^1 \rangle_{\text{ss}} + \langle \sigma_{22}^2 \rangle_{\text{ss}} + 2\text{Re} \left(\langle \sigma_{21}^1 \sigma_{12}^2 \rangle_{\text{ss}} e^{i\mathbf{k} \cdot \mathbf{r}_{12}} \right)$$

- expansion to second order in the atom-atom coupling constant
- tantamount to restriction to contributions from double scattering (two photons exchanged between both atoms)
- configuration average of the orientation of \mathbf{r}_{12} with respect to the backscattering direction, and of the distance r_{12} over an interval of order λ

$$\begin{aligned} I_{\text{ss}}^{\text{tot}[2]}(\theta) &= L^{\text{tot}} + C^{\text{tot}}(\theta), \\ L^{\text{tot}} &= \langle \langle \sigma_{22}^1 \rangle_{\text{ss}}^{[2]} + \langle \sigma_{22}^2 \rangle_{\text{ss}}^{[2]} \rangle_{\text{conf}}, \\ C^{\text{tot}}(\theta) &= 2\text{Re} \langle \langle \sigma_{21}^1 \sigma_{12}^2 \rangle_{\text{ss}}^{[2]} e^{i\mathbf{k} \cdot \mathbf{r}_{12}} \rangle_{\text{conf}} \end{aligned}$$

CBS intensity in the helicity preserving channel

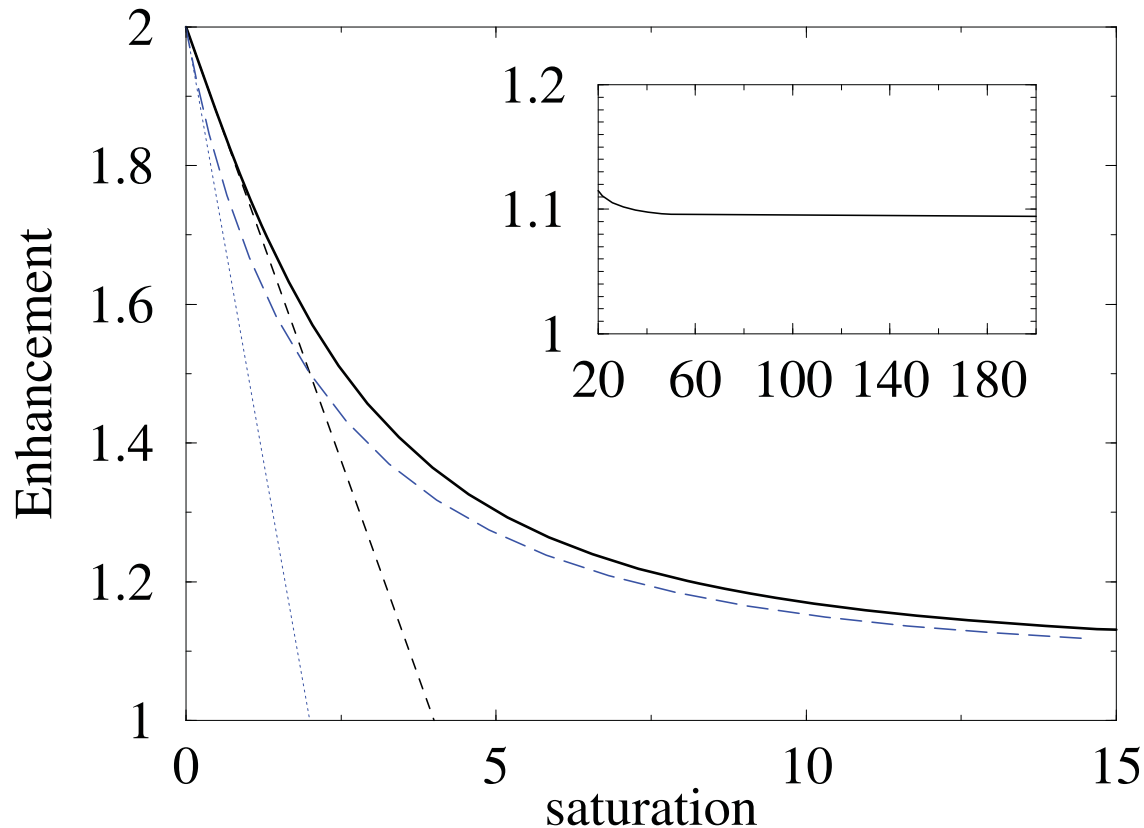
CBS signal for arbitrary saturation parameters ($\delta = 0$)



- $I_{ss}^{\text{tot}[2]}$ exhibits maximum at $s \simeq 0.7$, and asymptotic decay $\sim s^{-1}$
- in strong contrast to scattering intensity from an isolated atom, $\sim s/(1+s)$
- drop of C^{tot} below L^{tot} at finite s indicates loss of coherence

CBS enhancement factor vs. saturation

solid curve: $\delta = 0$ – dashed: $\delta = \gamma$



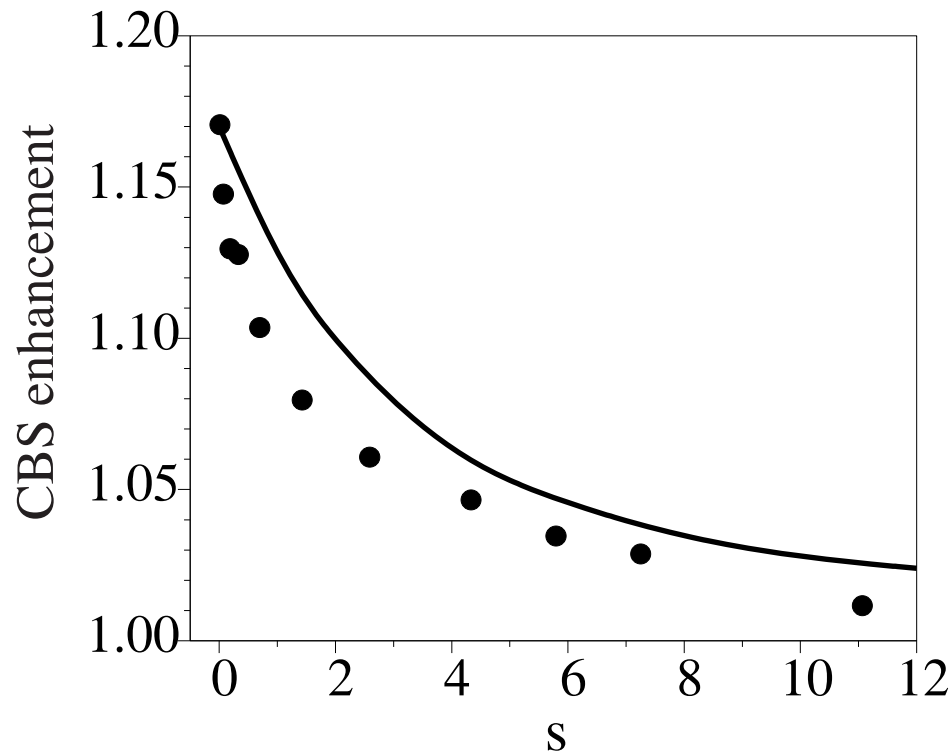
- rapid decrease of CBS contrast with s
- decay faster for finite detuning, in qualitative agreement with experiment
- in the limit of small intensities, agreement with scattering theoretical treatment (perturbative in s) [Wellens et al., 2004]

nonvanishing residual CBS contrast in the deeply inelastic limit

– due to self-interference of *inelastically* scattered photons!

$$\alpha_{\infty} = 23/21$$

Comparison Rb experiment vs. two-atom Sr theory

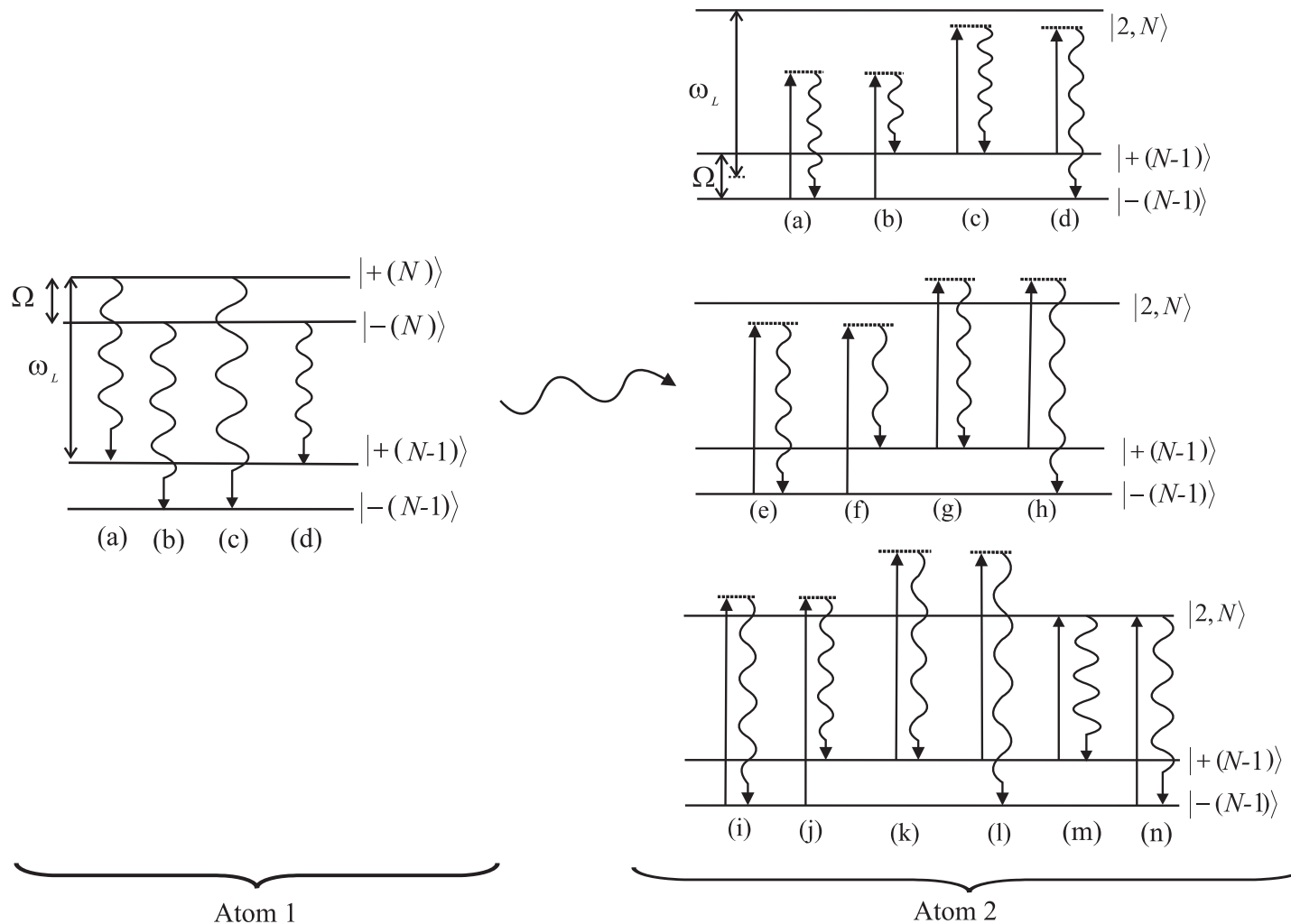


- surprising agreement, *despite* degeneracy of Rb ground state
- rather *due to* degeneracy, since the latter implies strongly suppressed contribution from higher than second order scattering processes
- indeed, agreement even better with theoretical result for small nonvanishing detuning

solid curve: rescaled theory at resonance (fit initial value at small s)

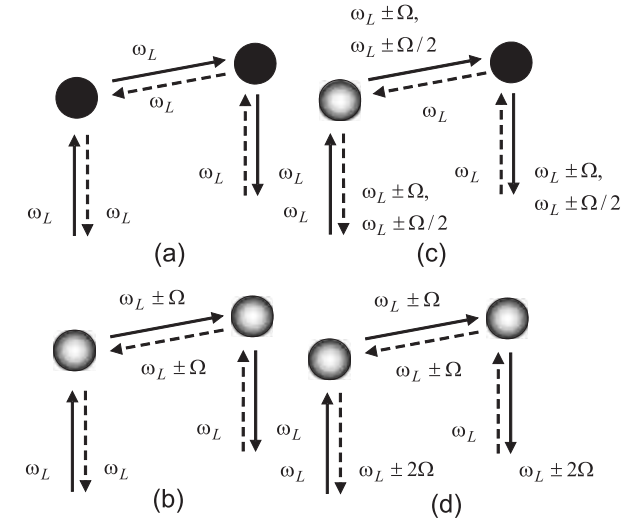
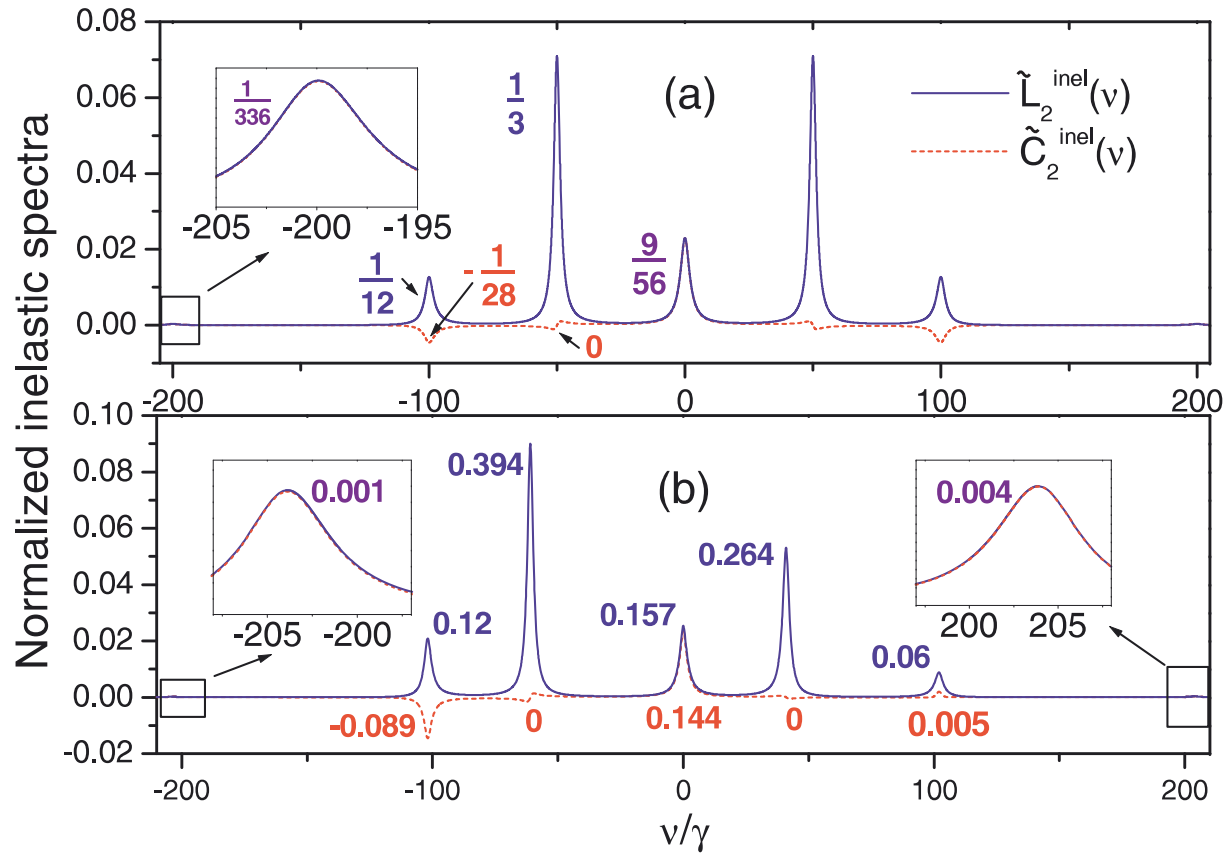
filled circles: experiment on Rb

Exchanging photons between dressed states



The photon scattered by atom one probes the laser-dressed transition $1 \leftrightarrow 2$ of atom 2

Dressed state CBS spectrum

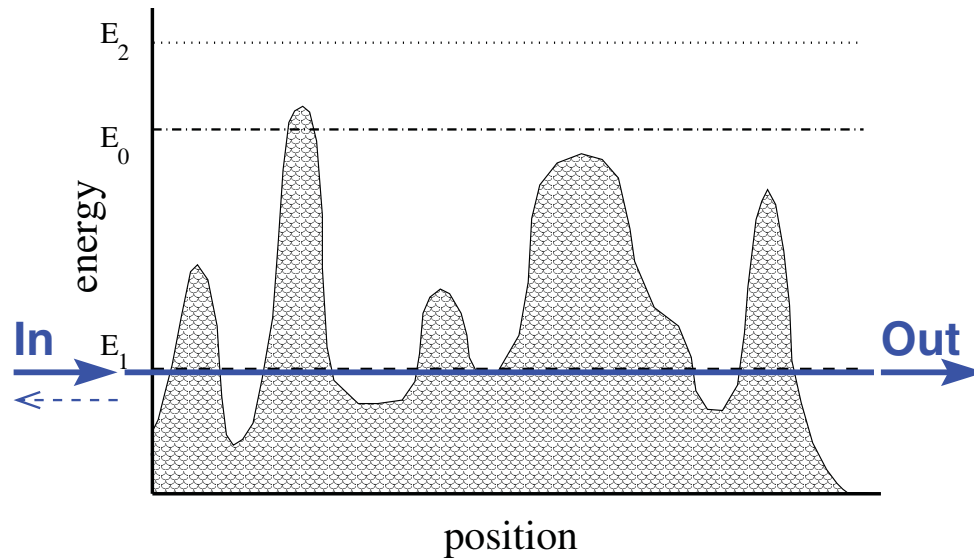


Double scattering leaves a clear (and detectable) signature in the CBS spectrum

Roadmap

- **Nonlinear resonances: from helium to Bose-Hubbard**
Peter Schlagheck & Javier Madroñero & Pierre Lugan & Klaus Zimmermann & Soeren Roerden & Maximilian Schmidt & Celsus Bouri
- **Matter wave transport in periodic optical potentials**
Alexey Ponomarev & Javier Madroñero & Hannah Venzl & Alexej Schelle & Andrey Kolovsky & Stefan Hunn & Moritz Hiller & Tobias Zech & Lewin Stein & Sandro Wimberger & Dominik Hörndlein & Vivian Franca
- **Photon transport in disordered atomic samples**
Vyacheslav Shatokhin & Thomas Wellens & Cord A. Müller & Tobias Geiger & Felix Eckert & Nicolas Cherroret & Jochen Zimmermann & Scott Sanders
- **Energy transport in strongly driven Rydberg systems**
Andreas Krug & Sandro Wimberger & Javier Madroñero & Alexej Schelle
- **Quantum transport in biological functional units**
Torsten Scholak & Thomas Wellens & Simeon Sauer & Florian Mintert & Fernando de Melo & Markus Tiersch

Anderson localization



DISORDER-INDUCED

tight binding Hamiltonian

$$E_n^0 c_n + V(c_{n-1} + c_{n+1}) = E c_n$$

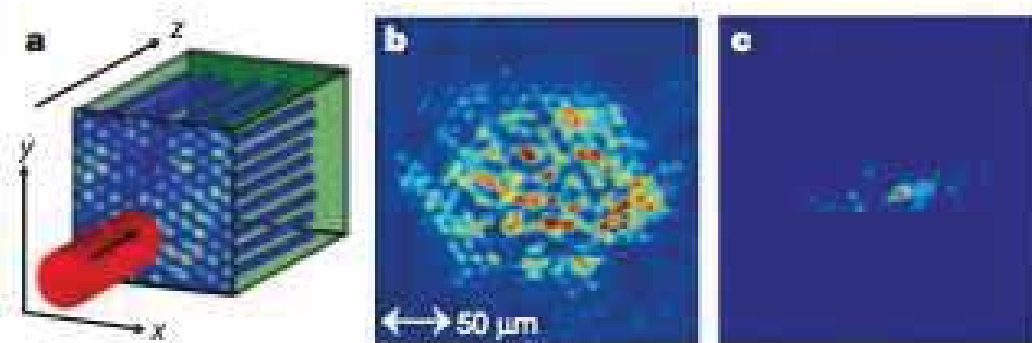
- metal-insulator transition in disordered solids [Anderson 1958]
- only exponentially localized states in 1D – localization length ξ , sample length L
- relevant parameter: ξ/L determines conductance g
- generally relevant for transport in disordered/chaotic/complex systems

[Chirikov, Shepelyansky, Izrailev, Casati 1979/1980;

Jensen et al. 1989; Saraceno et al. 1989]

Anderson localization in complex systems

– light in material potentials – matter in light-potentials – energy in matter and light –



Transport and Anderson localization in disordered two-dimensional photonic lattices

Tal Schwartz¹, Guy Bartal¹, Shmuel Fishman¹ & Mordechai Segev¹

PRL 96, 063904 (2006)

PHYSICAL REVIEW LETTERS

week ending
17 FEBRUARY 2006

Observation of the Critical Regime Near Anderson Localization of Light

Martin Störzer, Peter Gross, Christof M. Aegerter, and Georg Maret

PRL 102, 183001 (2009)

PHYSICAL REVIEW LETTERS

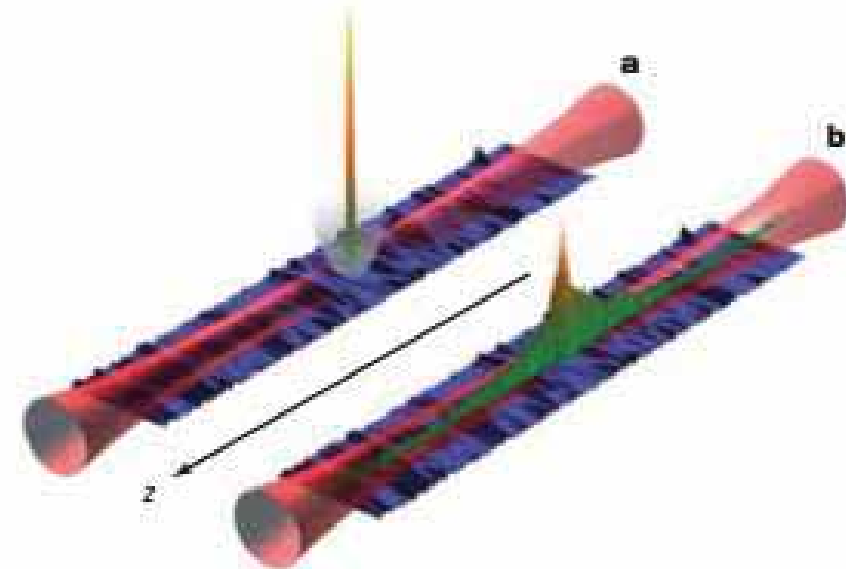
week ending
8 MAY 2009

Microwave-Driven Atoms: From Anderson Localization to Einstein's Photoeffect

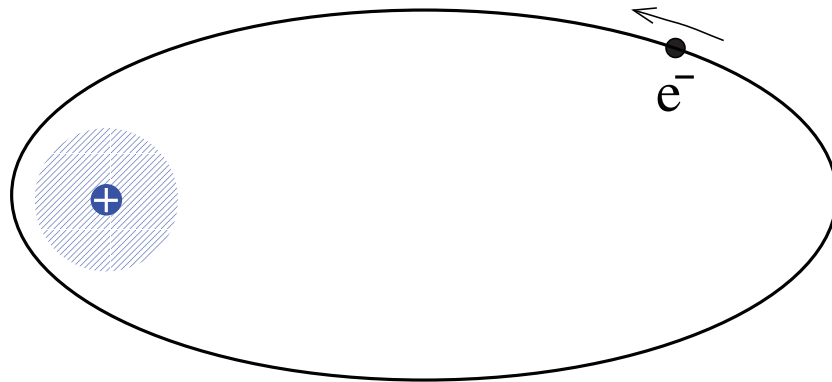
Alexej Schelle,^{1,2} Dominique Delande,² and Andreas Buchleitner¹

Direct observation of Anderson localization of matter waves in a controlled disorder

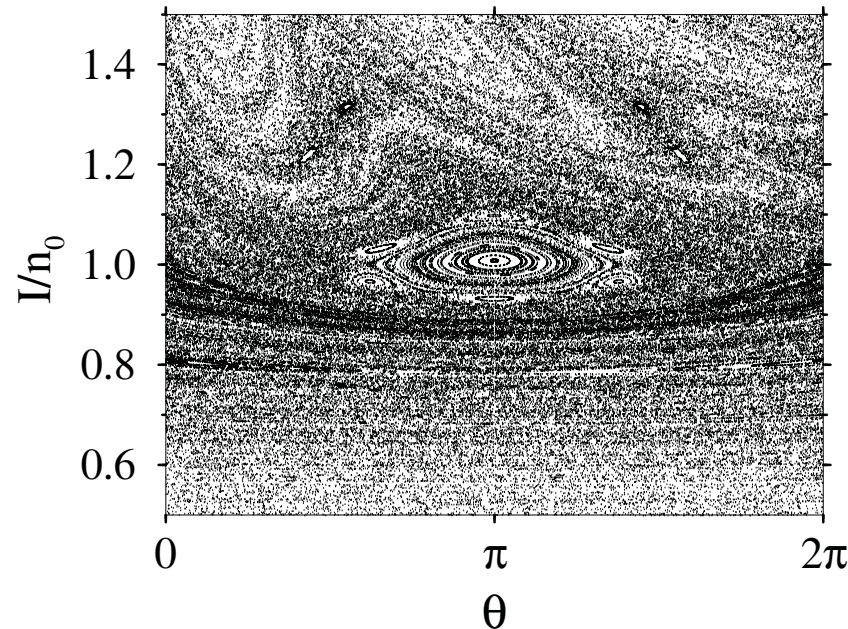
Juliette Billy¹, Vincent Josse¹, Zhanchun Zuo¹, Alain Bernard¹, Ben Hambrecht¹, Pierre Lugan¹, David Clément¹, Laurent Sanchez-Palencia¹, Philippe Bouyer¹ & Alain Aspect¹



Periodically driven one electron Rydberg states



← regular, Kepler like motion of Rydberg electron in semiclassical regime (quantum numbers $n_0 \geq 60$)

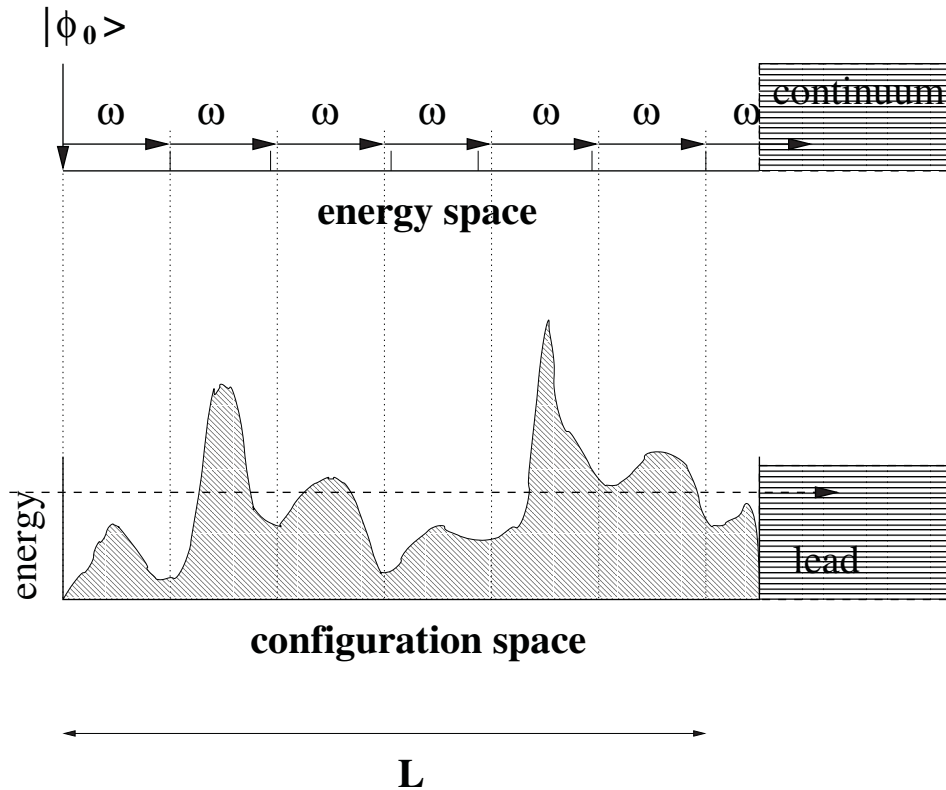


← near resonant (microwave) driving induces

- mixed phase space –
- chaotic/complex dynamics
- decay/ionization

[Koch et al. 1988; Bayfield et al. 1989; Walther et al. 1989; Gallagher et al. 1991, 2004]

Mapping atoms on the Anderson model

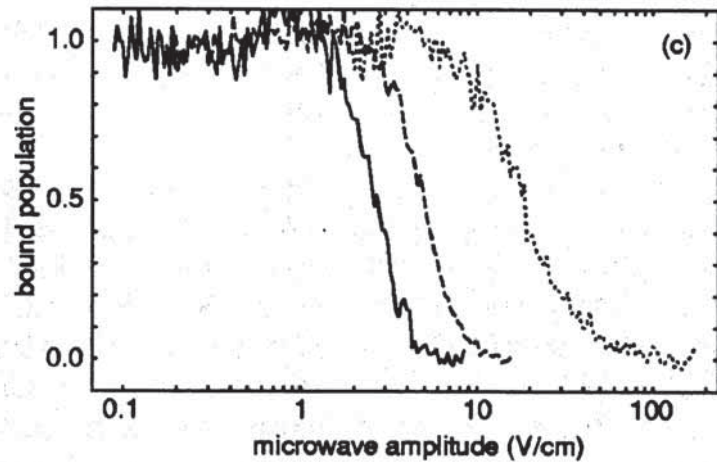


- Anderson: subsequent transmission and reflection events
- atom:
 - transmission \rightarrow absorption
 - reflection \rightarrow emission
 - disorder \rightarrow detuning
 - configuration space \rightarrow energy
 - sample length \rightarrow # photons to ionize

expect quantum suppression of chaotic ionization
= Anderson localization of energy flow
 (due to quasirandomly distributed one-photon coupling matrix elements)

[Fishman, Grepel, Prange 1982; Krug, Wimberger, - 2003]

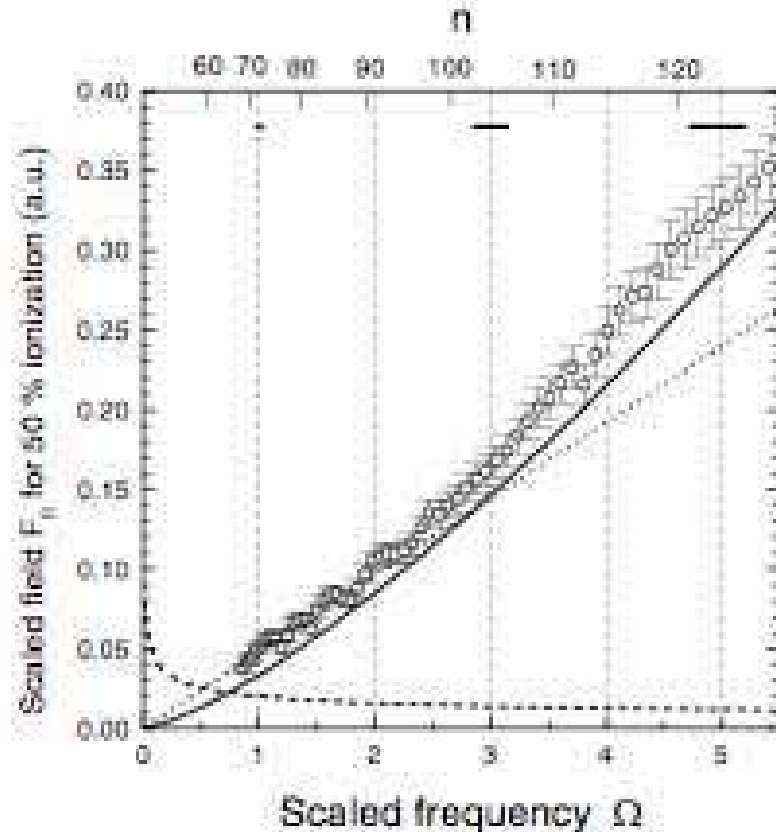
Experimental facts



← ionization yield P_{ion} vs. field amplitude F exhibits ionization threshold

[Noel, Griffith and Gallagher, 2000]

- density of states $\sim n_0^4$
- up to 50 photons absorbed for ionization



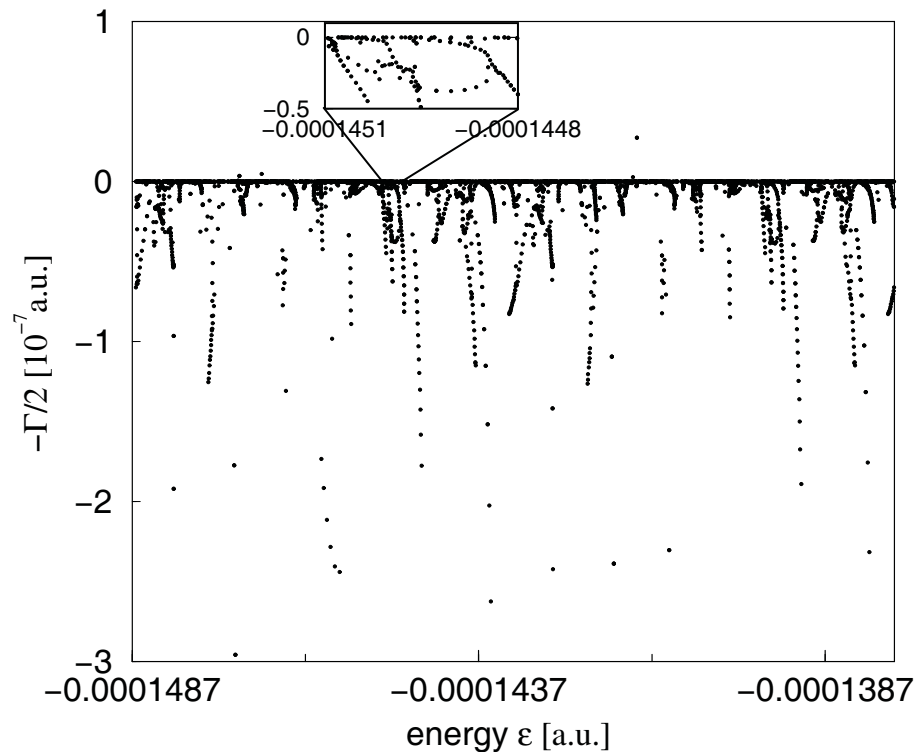
← Anderson vulgo dynamical localization suppresses classically chaotic ionization

[Maeda & Gallagher et al., 2004]

- $\Omega = \omega \times n_0^3$, $F_0 = F \times n_0^4$

the atom ceases to absorb photons!

Ionization yield from poles of the resolvent operator



[A. Krug, PhD thesis (2001)]

- Ionization signal from the initial state $|\phi_0\rangle$:

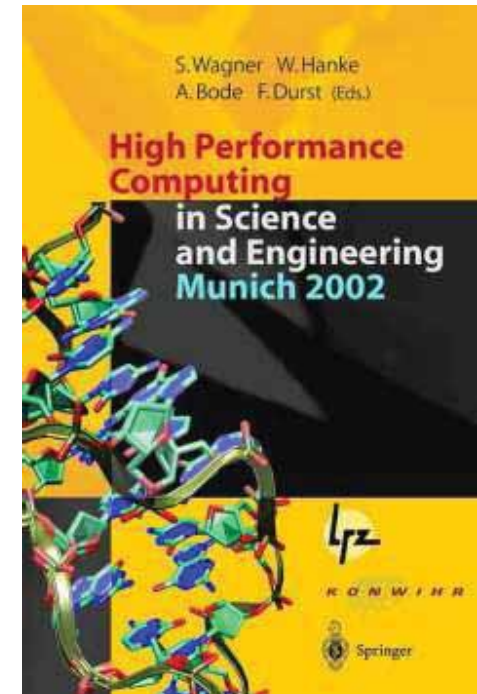
$$P_{\text{ion}}(t) = 1 - \sum_{\epsilon} |\langle \phi_0 | \epsilon \rangle|^2 \exp(-\Gamma_{\epsilon} t)$$

- approx. 4000 poles contribute!

Our lab



also see



Funding by Bayerische Akademie der Wissenschaften as a “Grand Challenge Project”

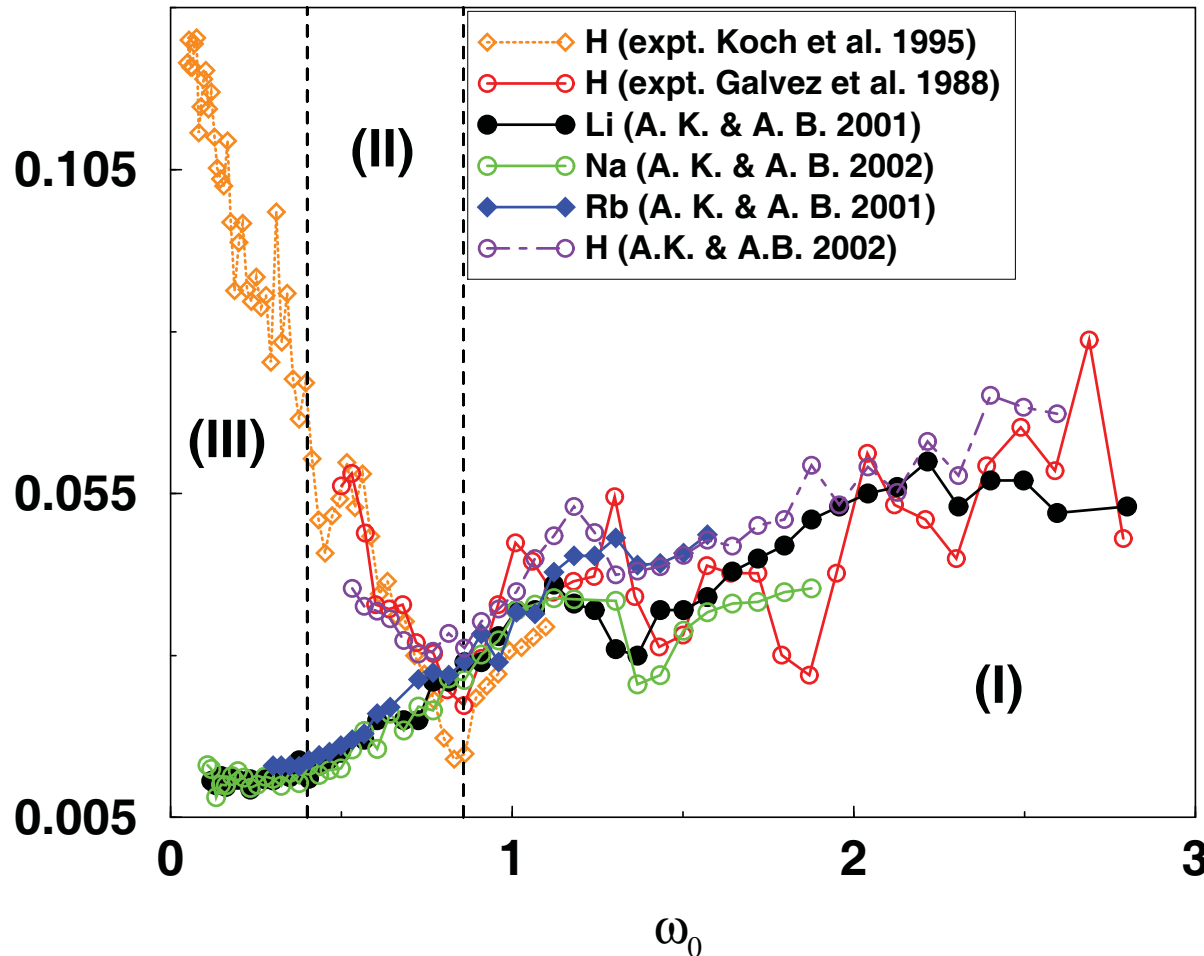


Universal ionization threshold

Identical parameters in theory and experiment – for H, Li, Na, Rb

$$n_0 = 28 \dots 80, \omega/2\pi = 36 \text{ GHz}, t = 327 \times 2\pi/\omega$$

[E.J. Galvez et al., 1988; P.M. Koch et al., 1995; A. Krug & A.B., PRL 2001]



→ Coulomb/Kepler scaled variables
 $F_0 = F \times n_0^4$ and $\omega_0 = \omega \times n_0^3$!

- experimental evidence of universal threshold in T.F. Gallagher's group! [invited talk Bad Honnef (2003)]

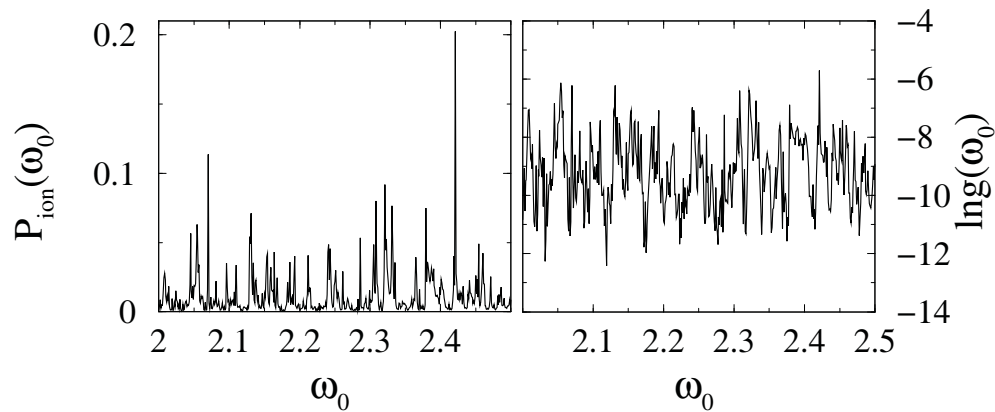
universal hydrogenlike ionization in (I)
enhanced ionization in (II) – nonresonant ionization in (III)

Atomic conductance fluctuations

Large fluctuations of the atomic conductance!

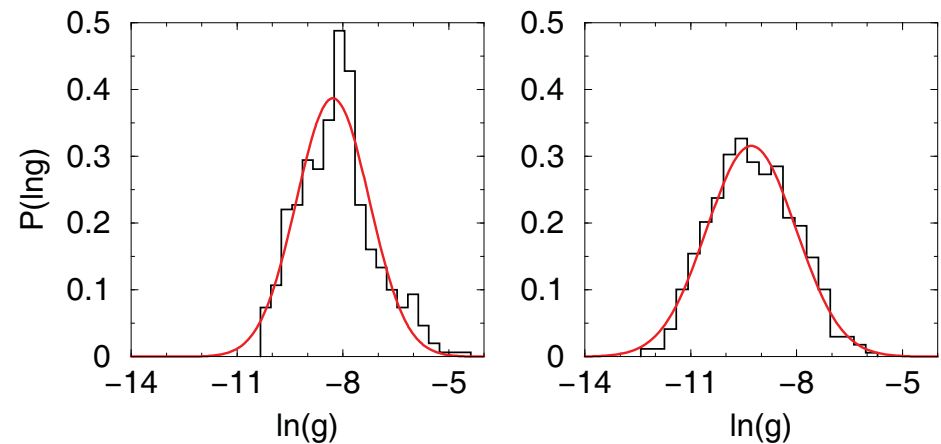
$$g \sim dP_{\text{ion}}/dt |_{t=0} \sim \sum_{\epsilon} |\langle \psi_0 | \epsilon \rangle|^2 \Gamma_{\epsilon}$$

Statistical distribution in quantitative agreement with 1D Anderson!



$n_0 = 100$

[S. Wimberger, diploma thesis (2000)]



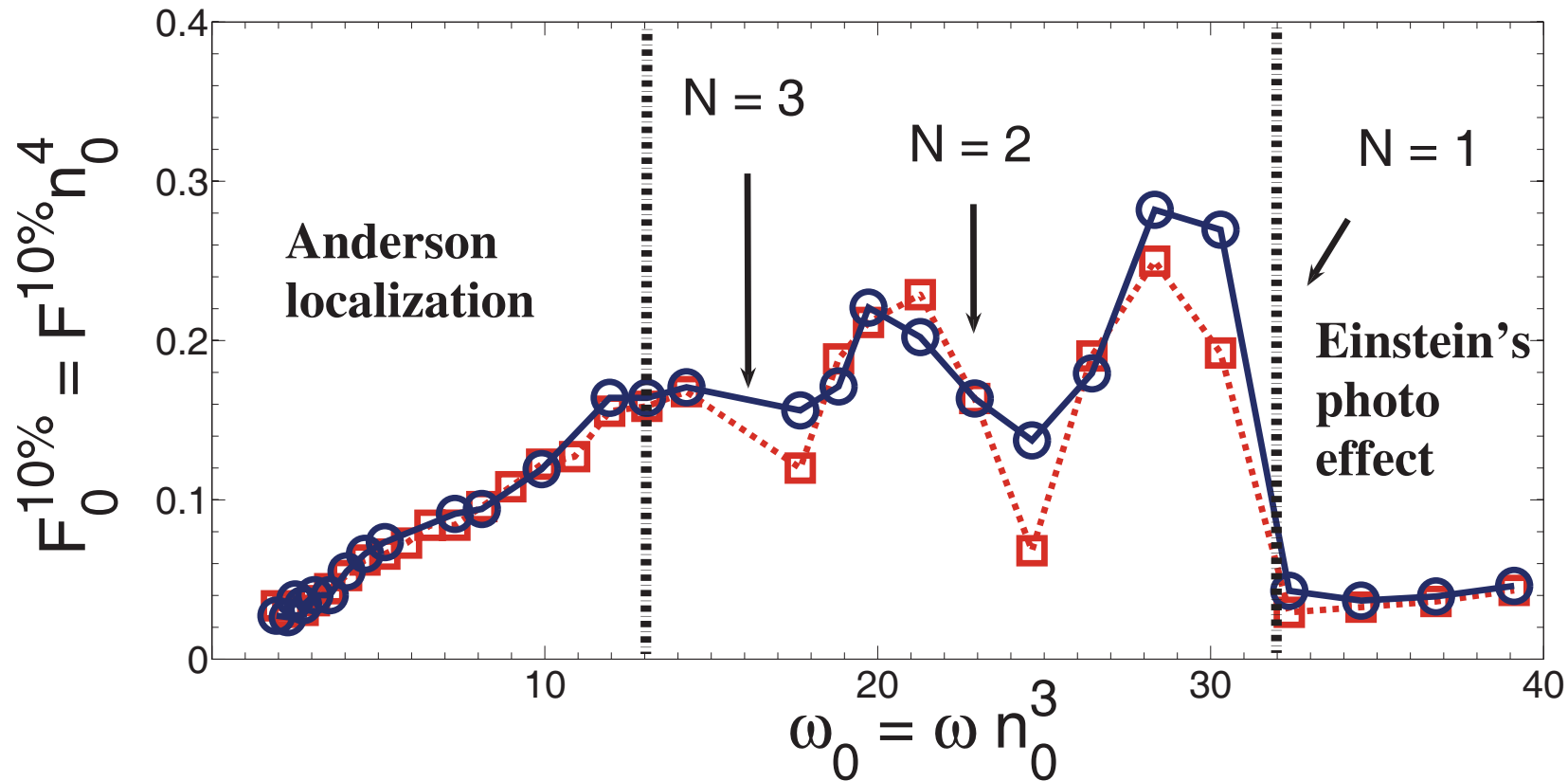
$n_0 = 40 \dots$

100

But what about Einstein's photo effect???

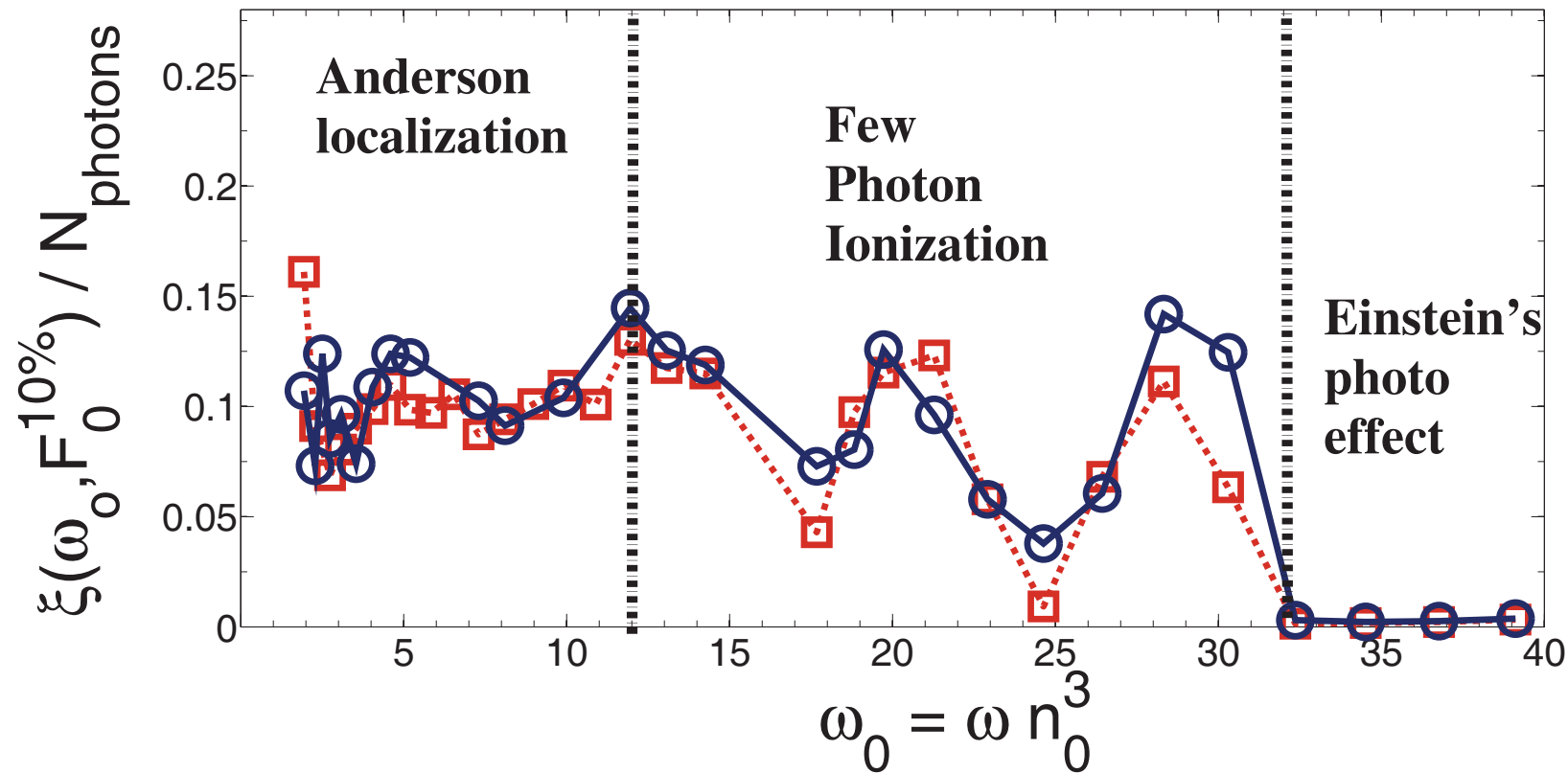
- ? multiphoton signal **originally considered in contradiction** to Einstein
- ? **intensity** threshold rather than frequency threshold
- ? **but one and the same physical system**
- ! **continuous transition from Anderson to Einstein**
 - **fix** laboratory frequency ω
 - **sweep** initial principal quantum number $n_0 = 90 \dots 245$
 - **reduce number of photons/sample size** required for ionization down to one (at $n_0 = 230$)

From Anderson to Einstein – hydrogen and lithium



- regime I ($\omega_0 = 1.9 \dots 13.1$): universal ionization threshold (Anderson)
- regime II ($\omega_0 = 13.1 \dots 31.5$): open direct N -photon ionization channels
- regime III ($\omega_0 > 31.5$): Einstein's realm

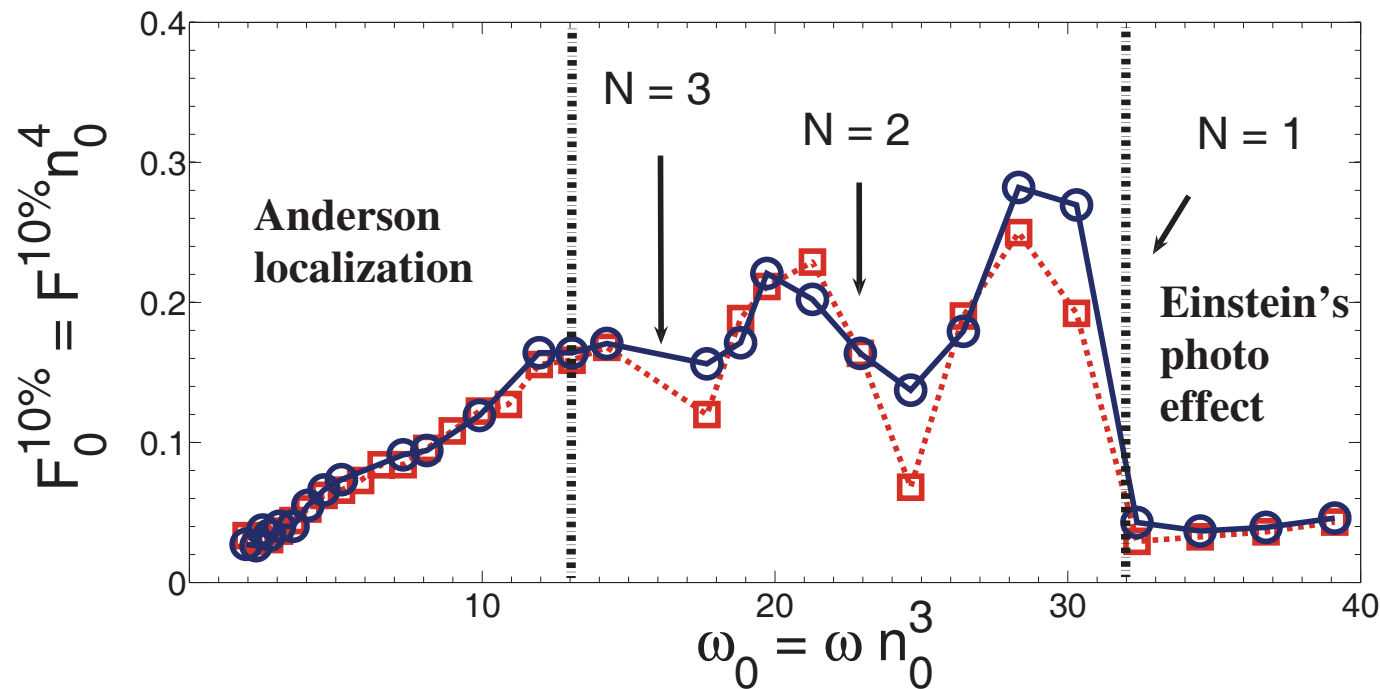
Anderson localization prevails up to one photon threshold



- **localization length ξ roughly constant** up to one photon channel (at $F_0^{10\%}$ — — $\xi \simeq 3.33[F_0^{10\%}]^2 \omega_0^{-10/3} n_0^2$)
- modulations for $13 \leq \omega_0 \leq 32$ due to **granularity of lattice = opening of N-photon channels** (jargon community-specific!!!)

Discussion

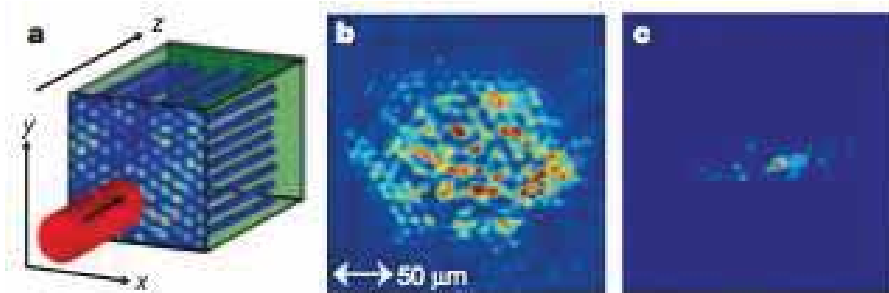
- for increasing sample size (i.e., starting out from regime III)
 - rapid emergence of **Anderson localization**
 - due to **rapid increase of # of transmission amplitudes**
 - though garnished (in regime II) by **finite size effects**
 - which atomic physicists call **direct multiphoton channel opening**
- reminiscent of **rapid emergence of thermodynamic limit** in many particle, e.g., Bose-Hubbard dynamics



Roadmap

- **Nonlinear resonances: from helium to Bose-Hubbard**
Peter Schlagheck & Javier Madroñero & Pierre Lugan & Klaus Zimmermann & Soeren Roerden & Maximilian Schmidt & Celsus Bouri
- **Matter wave transport in periodic optical potentials**
Alexey Ponomarev & Javier Madroñero & Hannah Venzl & Alexej Schelle & Andrey Kolovsky & Stefan Hunn & Moritz Hiller & Tobias Zech & Lewin Stein & Sandro Wimberger & Dominik Hörndlein & Vivian Franca
- **Photon transport in disordered atomic samples**
Vyacheslav Shatokhin & Thomas Wellens & Cord A. Müller & Tobias Geiger & Felix Eckert & Nicolas Cherroret & Jochen Zimmermann & Scott Sanders
- **Energy transport in strongly driven Rydberg systems**
Andreas Krug & Sandro Wimberger & Javier Madroñero & Alexej Schelle
- **Quantum transport in biological functional units**
Torsten Scholak & Thomas Wellens & Simeon Sauer & Florian Mintert & Fernando de Melo & Markus Tiersch

Disorder and transport



Transport and Anderson localization in disordered two-dimensional photonic lattices

Tal Schwartz¹, Guy Bartal¹, Shmuel Fishman¹ & Mordechai Segev¹

PRL 96, 063004 (2006) PHYSICAL REVIEW LETTERS week ending 17 FEBRUARY 2006

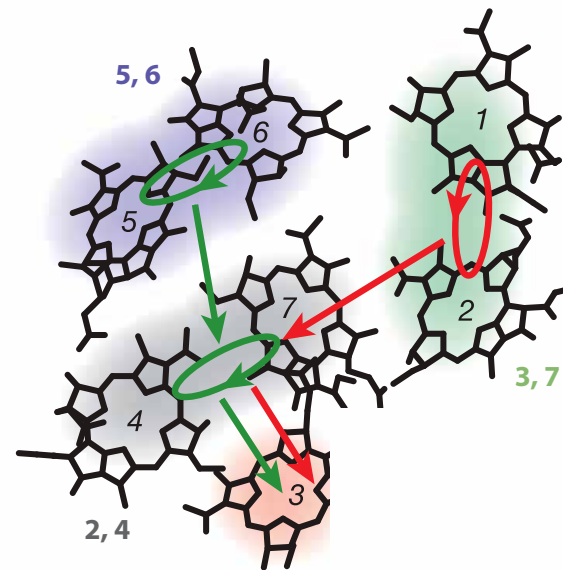
Observation of the Critical Regime Near Anderson Localization of Light

Martin Störzer, Peter Gross, Christof M. Aegerter, and Georg Maret

PRL 102, 183001 (2009) PHYSICAL REVIEW LETTERS week ending 8 MAY 2009

Microwave-Driven Atoms: From Anderson Localization to Einstein's Photoeffect

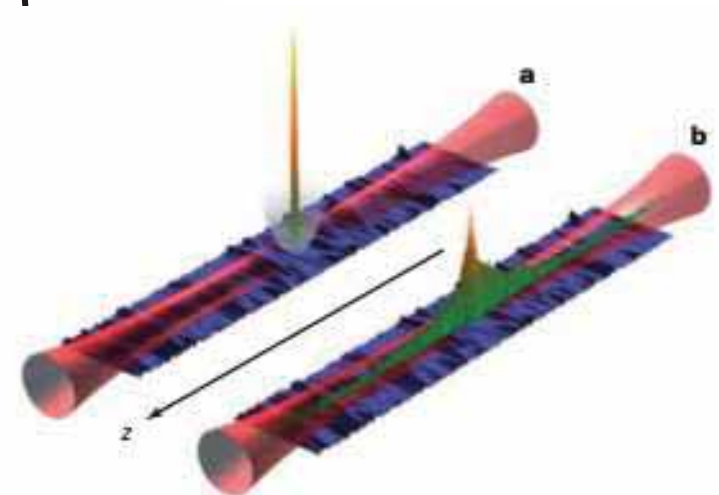
Alexej Schelle,^{1,2} Dominique Delande,² and Andreas Buchleitner¹



Quantum-Coherent Electronic Energy Transfer: Did Nature Think of It First?

Gregory D. Scholes*

Department of Chemistry, Institute for Optical Sciences and Centre for Quantum Information and Quantum Control, University of Toronto, 80 St. George Street, Toronto, Ontario, M5S 3H6 Canada



Direct observation of Anderson localization of matter waves in a controlled disorder

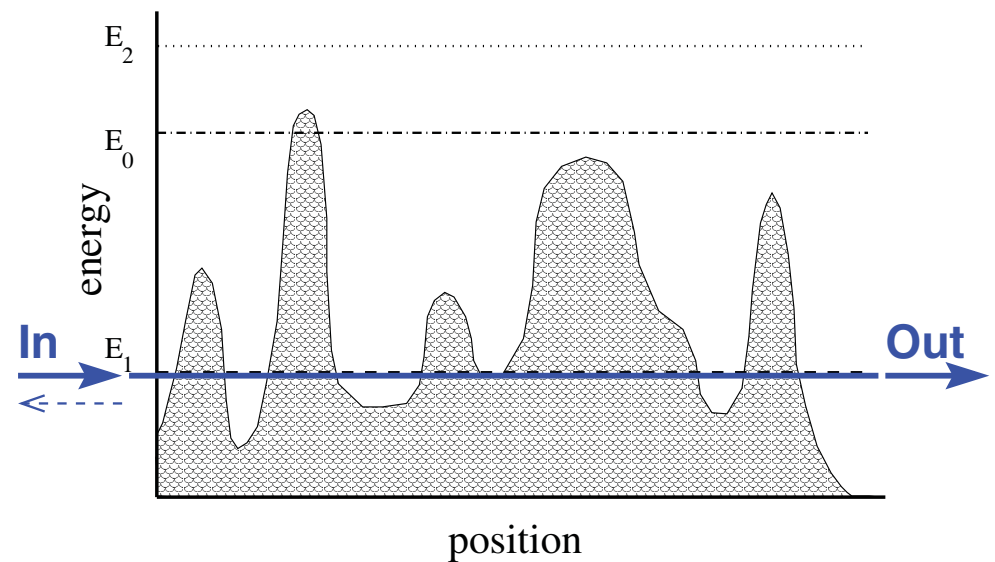
Juliette Billy¹, Vincent Josse¹, Zhanchun Zuo¹, Alain Bernard¹, Ben Hambrecht¹, Pierre Lukan¹, David Clément¹, Laurent Sanchez-Palencia¹, Philippe Bouyer¹ & Alain Aspect¹

(Quantum) Transport in complex systems . . .

. . . strongly affected by

- **disorder** (Anderson)
- **interaction** (Mott)
- **coherence** (photons, BEC)
- **decoherence** (chemistry, biology)

disorder-induced localization



interference effect

exponential suppression
of (diffusive) transport

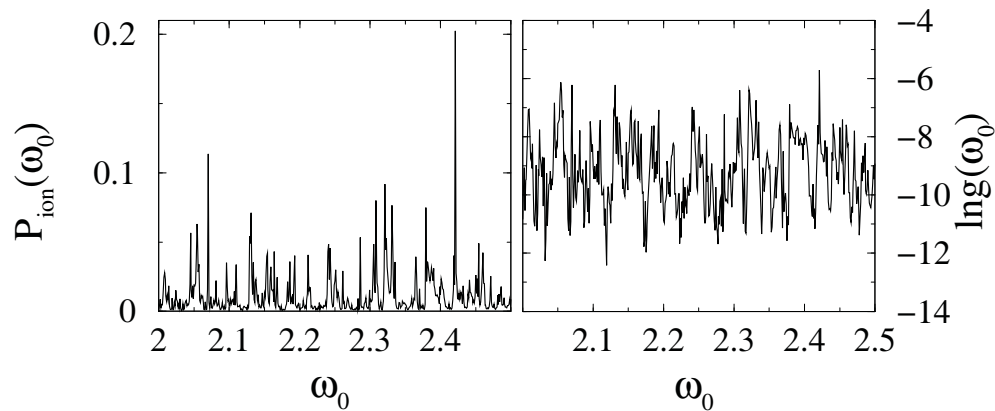
in thermodynamic limit, $L \rightarrow \infty$!

Hallmark: (atomic) conductance fluctuations

Large fluctuations of the atomic conductance!

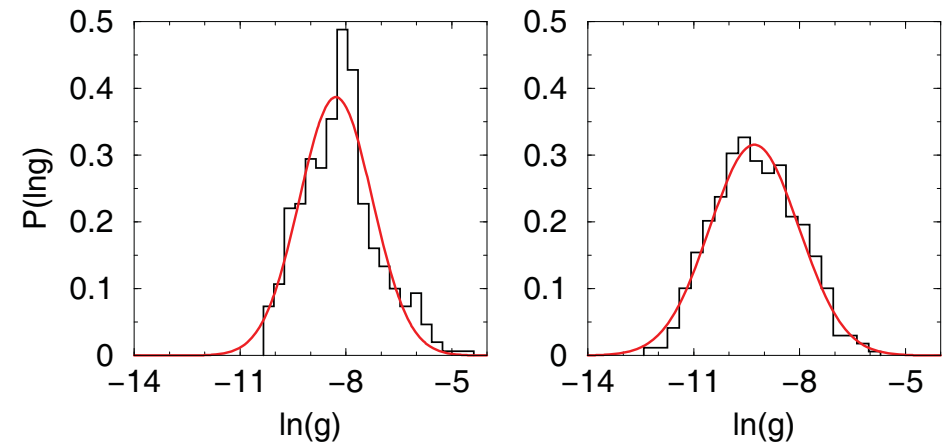
$$g \sim dP_{\text{ion}}/dt |_{t=0} \sim \sum_{\epsilon} |\langle \psi_0 | \epsilon \rangle|^2 \Gamma_{\epsilon}$$

Statistical distribution in
quantitative agreement with 1D
Anderson!



$n_0 = 100$

[S. Wimberger, diploma thesis (2000)]

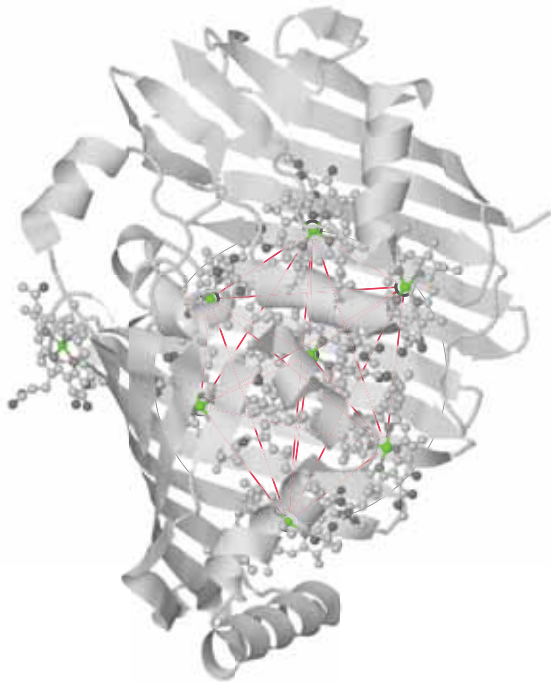


$n_0 = 40 \dots$

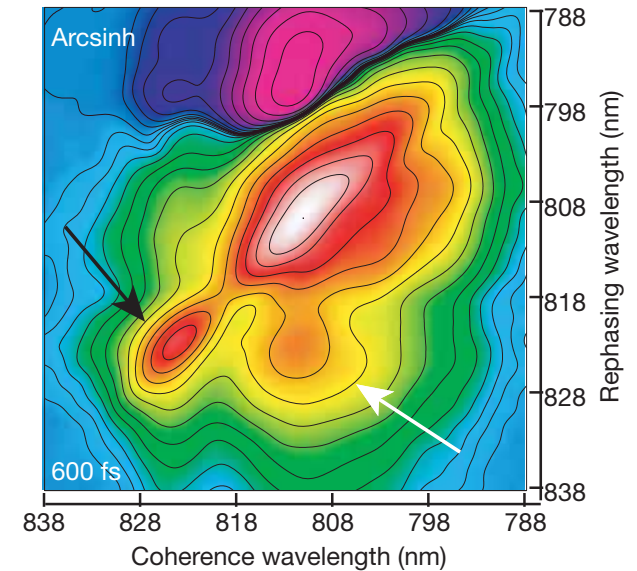
100

Quantum coherence in photosynthesis

photosynthetic complex



2D spectroscopy



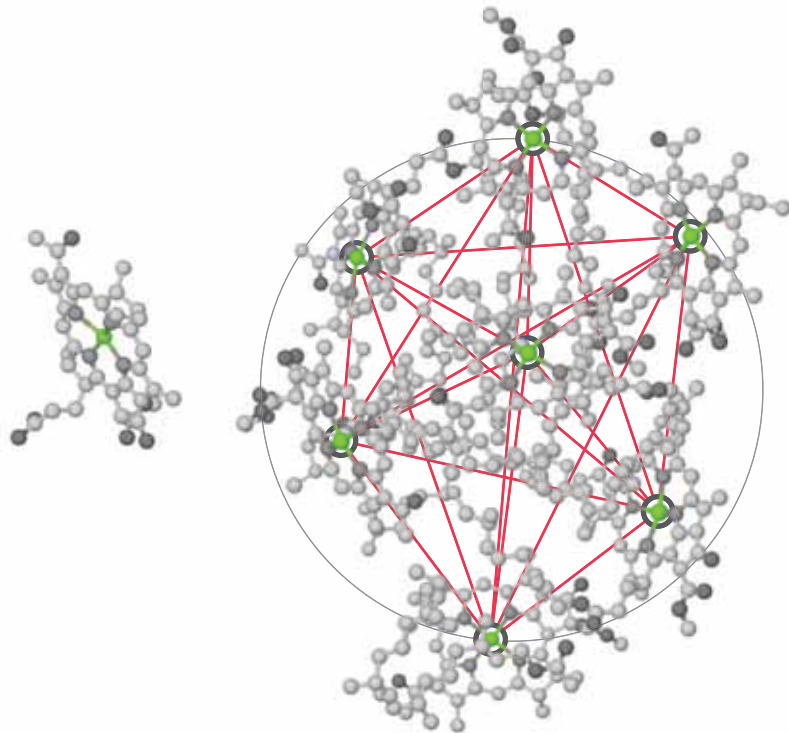
light harvesting antenna complexes (e.g., “FMO”) funnel excitations from receptor to reaction center with $\geq 95\%$ quantum efficiency

at ambient temperature [Engel et al., Nature 446, 782 (2007); Collini et al., Science 323, 369 (2009)]

in noisy, multi-hierarchical environment

??? ORIGIN OF THIS EFFICIENCY ???

Coherent vs. incoherent causes of efficiency – under debate



- **noise-induced efficiency**

[Wolynes, Breuer, Graham, Dittrich et al., 1980-1999]

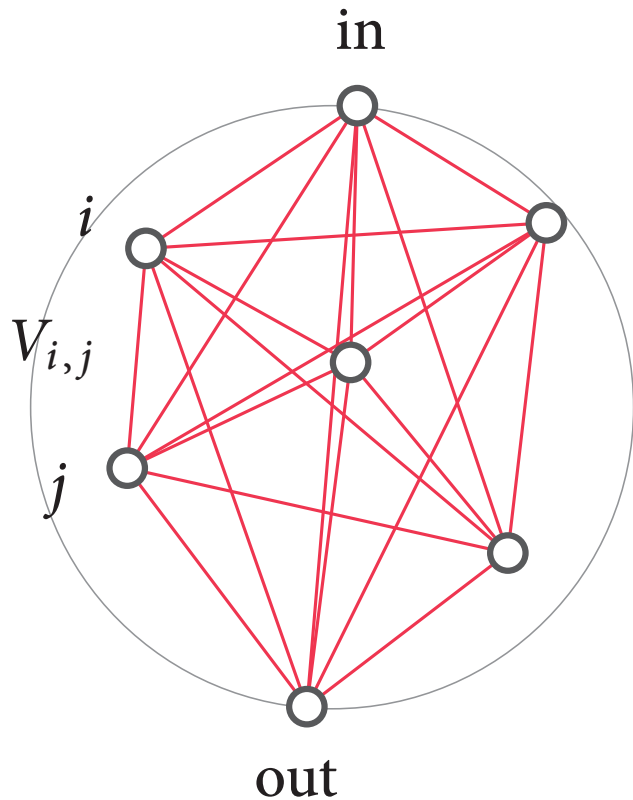
- **decoherence “breaks” disorder-induced localization of transport** [Whaley et al., Aspuru-Guzik et al.]
- **“optimal” environment coupling** [Briegel et al., Plenio et al.]
- **noise restores *classical* transport!**
- **quantum if non-Markovian** [Thorwart et al., Fleming et al.]

- **HERE: fully coherent transport**

- **on optimal molecular conformations** [Scholak et al.]
- **“selected” by evolution from statistical sample**

Physical abstraction

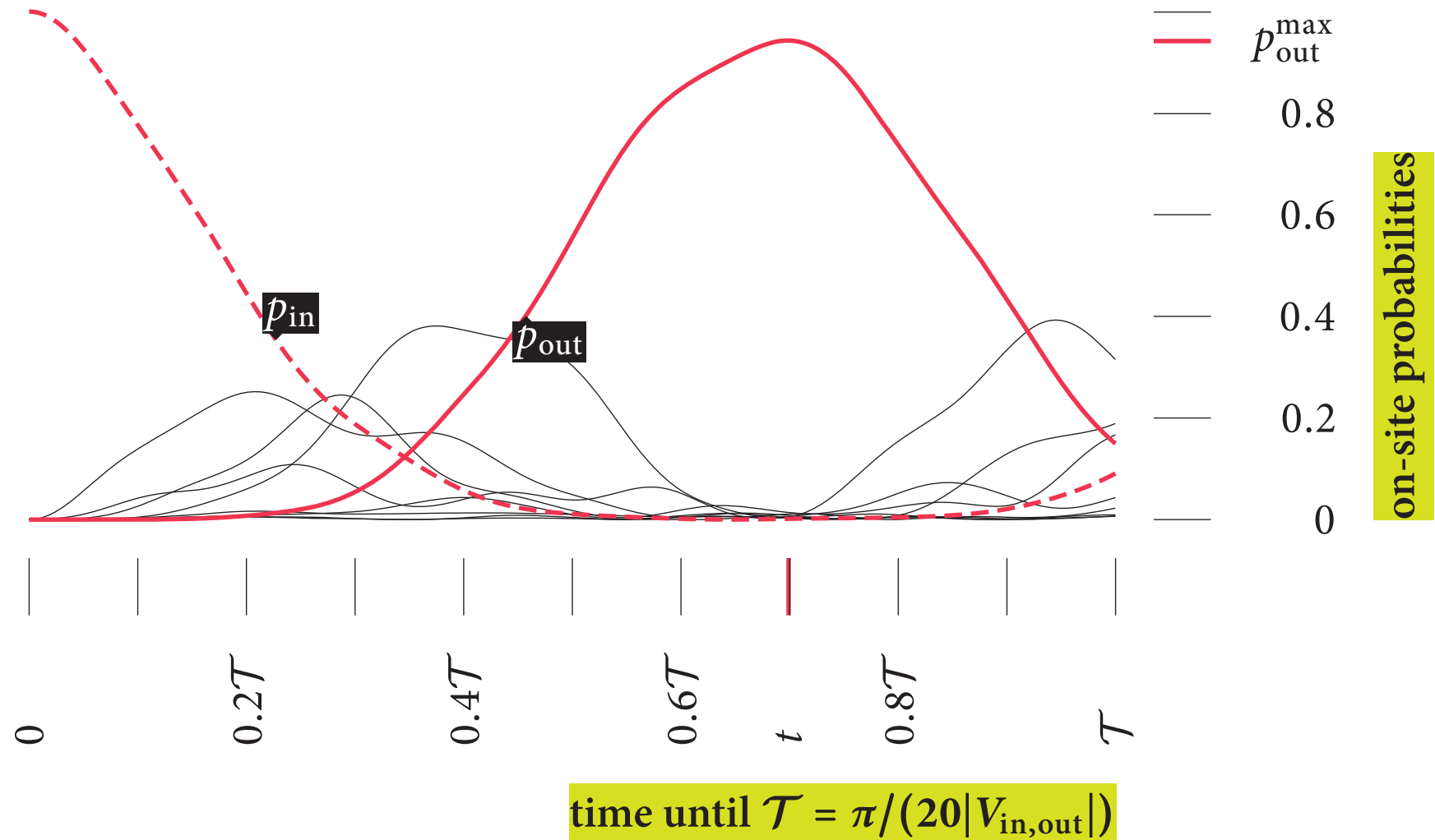
- FMO as a 3D network of sites –
- coherent dynamics on finite, fully connected, random graph –



- intersite coupling $V_{i,j} \sim r_{i,j}^{-3}$
- excitation injected at “in”
- excitation delivered at “out”
- remaining sites randomly placed within sphere
- **efficient** \equiv large p_{out} , after short times

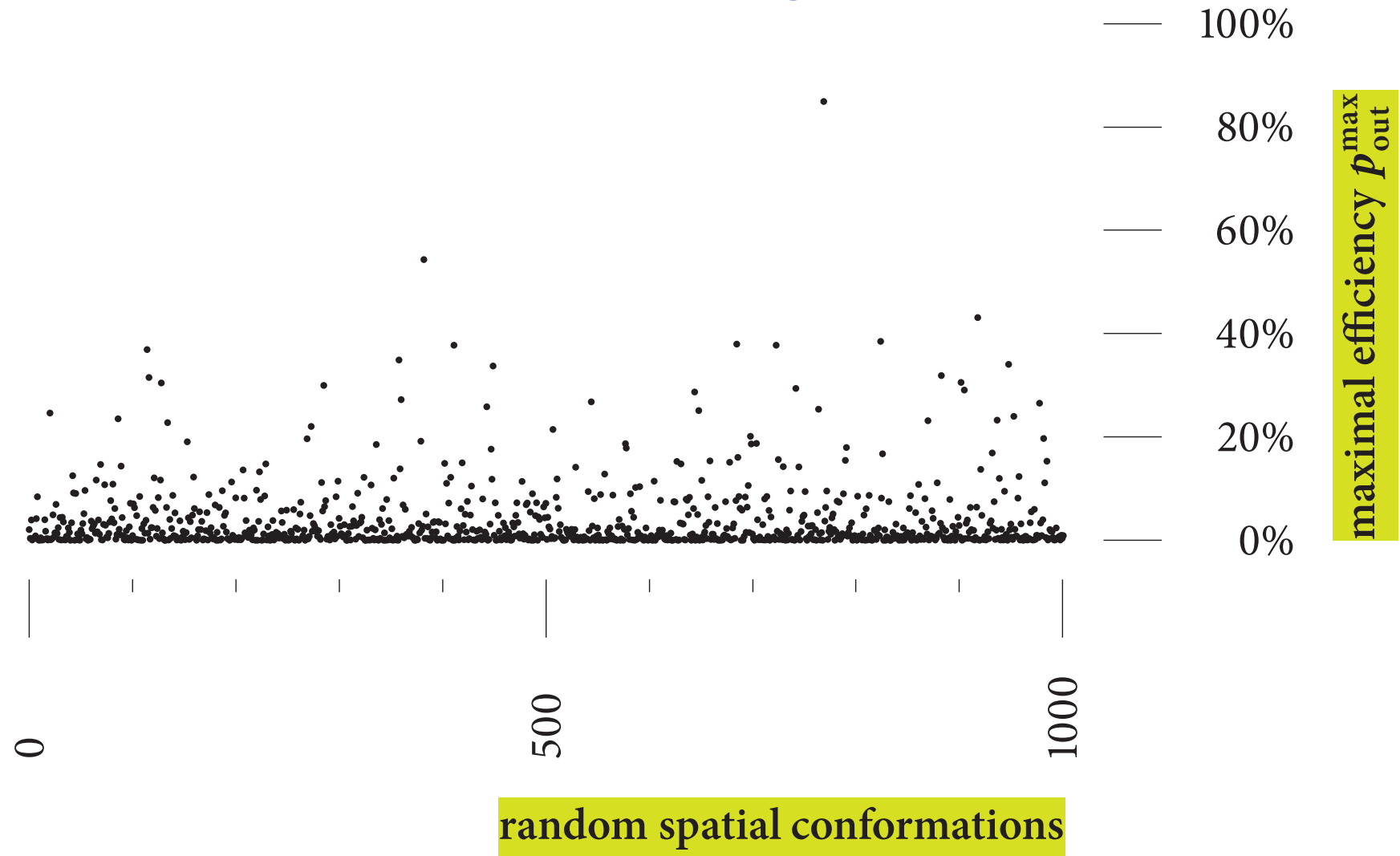
Transport efficiency

time evolution of on-site probabilities $p_i = |\langle i|U(t)|\text{in}\rangle|^2$



Transport efficiency vs. configuration

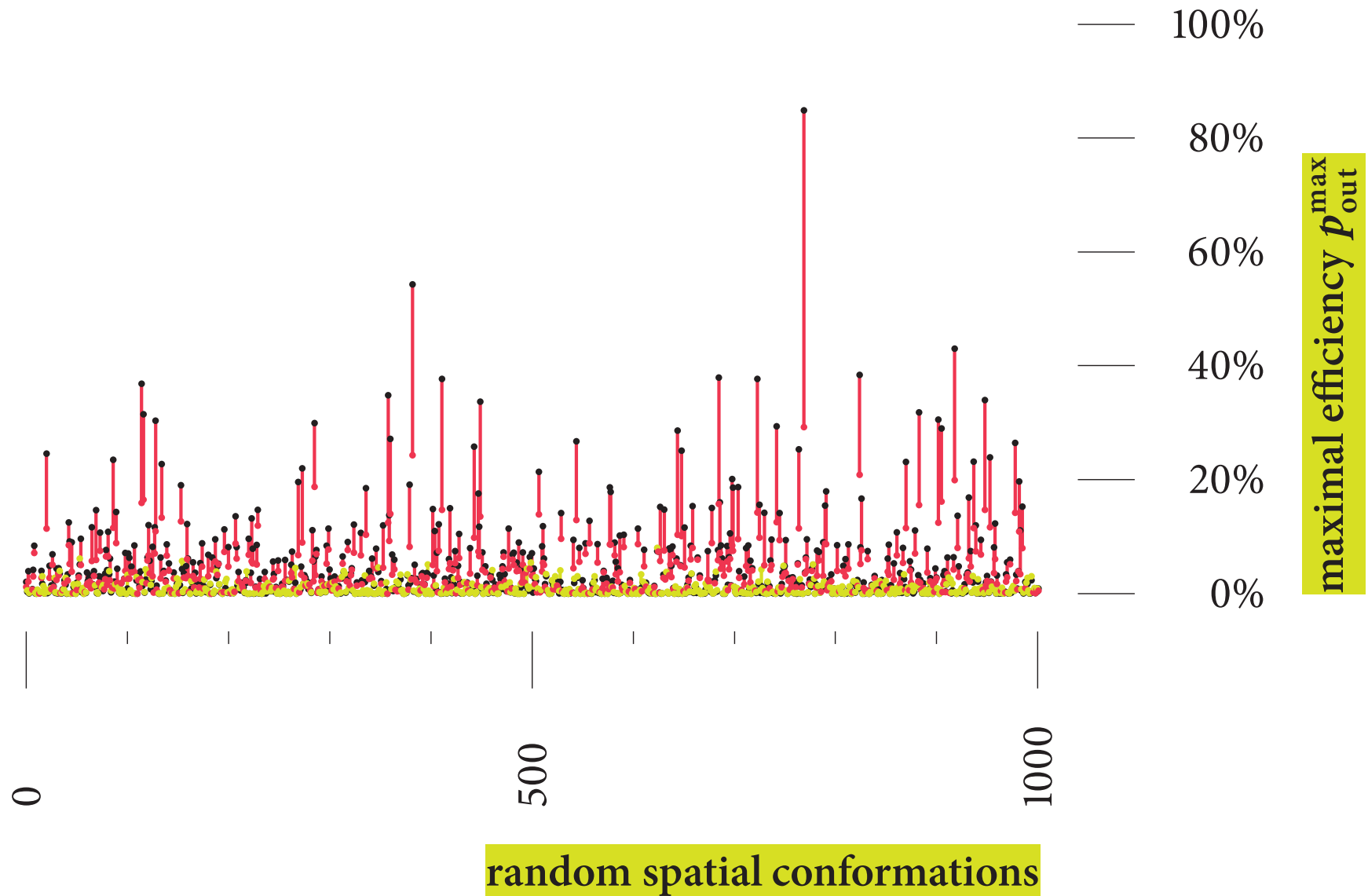
characteristic and **LARGE** fluctuations!



→ rare, optimal configurations – mostly localized transport ←

Transport under dephasing at rate $\gamma = 0.6/\mathcal{T}$

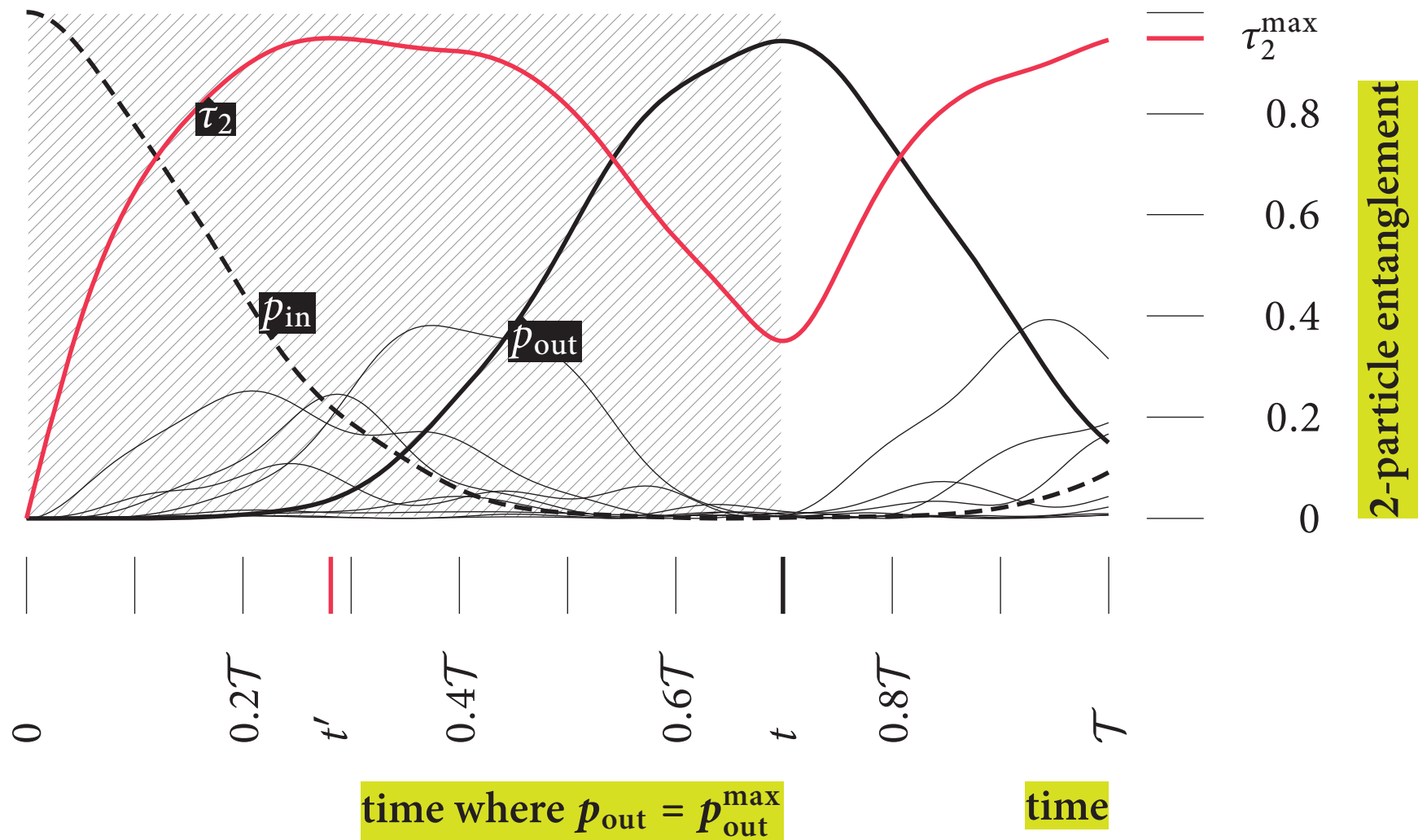
efficient/inefficient configurations remain efficient/inefficient under decoherence!!



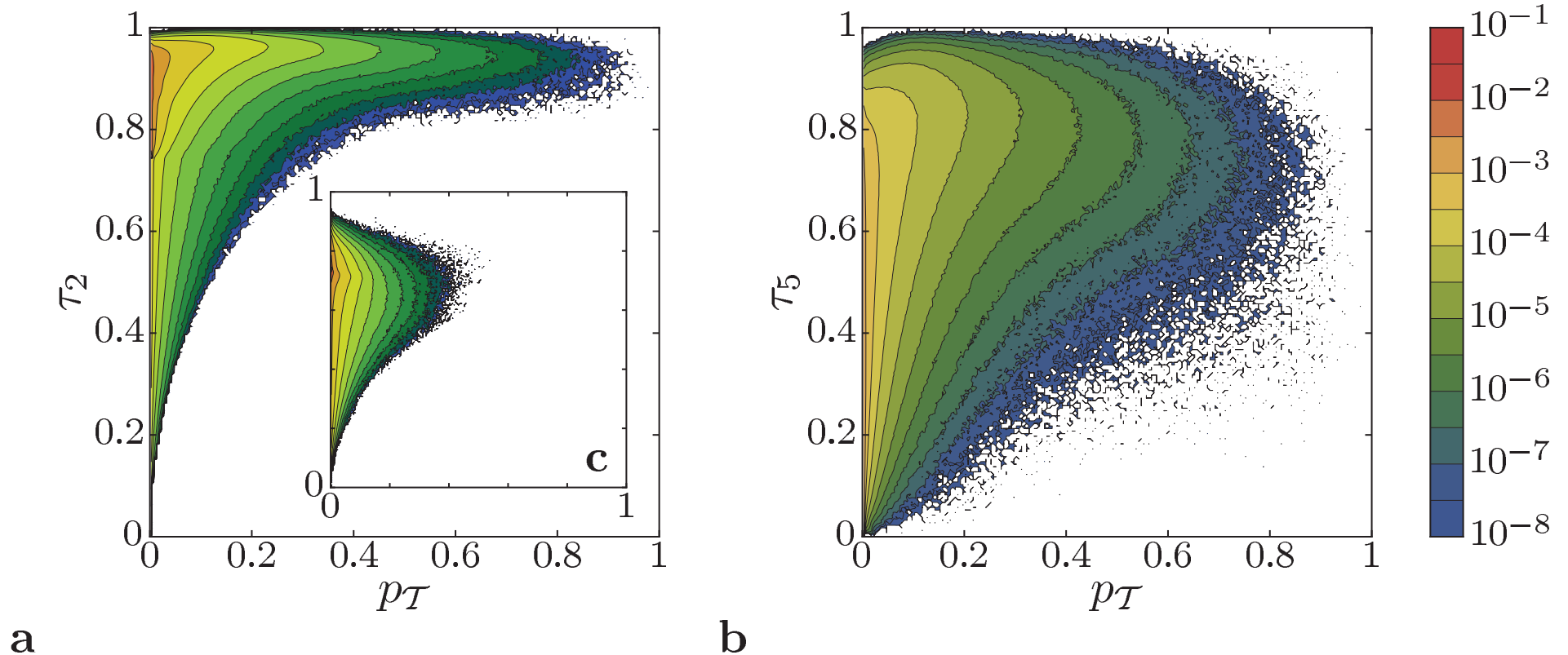
Functional rôle of entanglement?

time evolution of global two-particle entanglement

$$\tau_2(\psi(t)) = \sqrt{\left(1 - \sum_{i=1}^N p_i^2(t)\right) / \left(1 - 1/N\right)}$$



Transport efficiency vs. entanglement



no efficient transport without many-particle entanglement

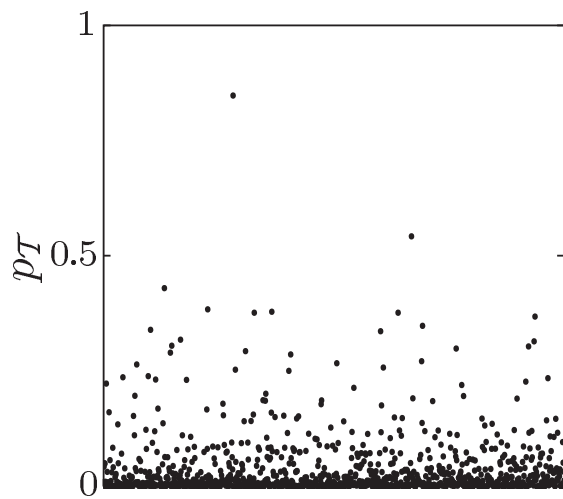
left: two-particle – right: five-particle entanglement

strong correlation prevails under dephasing

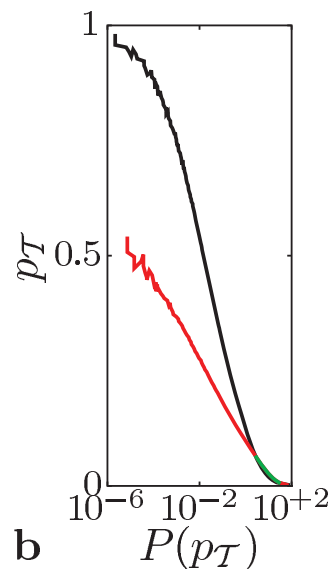
inset left (as above)

Discussion

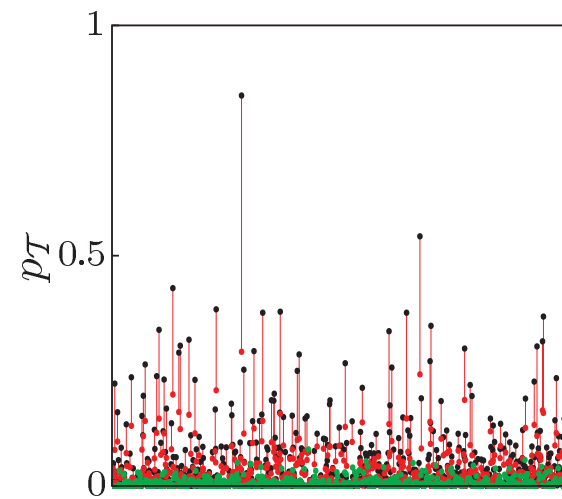
- the efficiency of excitation transport in the FMO complex is
 - due to RARE, constructive, multi-path quantum interference
 - across a finite-size sample
 - with statistics which define cost function!
- dephasing
 - improves the performance of the bad conformations
 - degrades the performance of the good conformations
 - but does NOT render the bad ones better than the good!



a random configurations



b

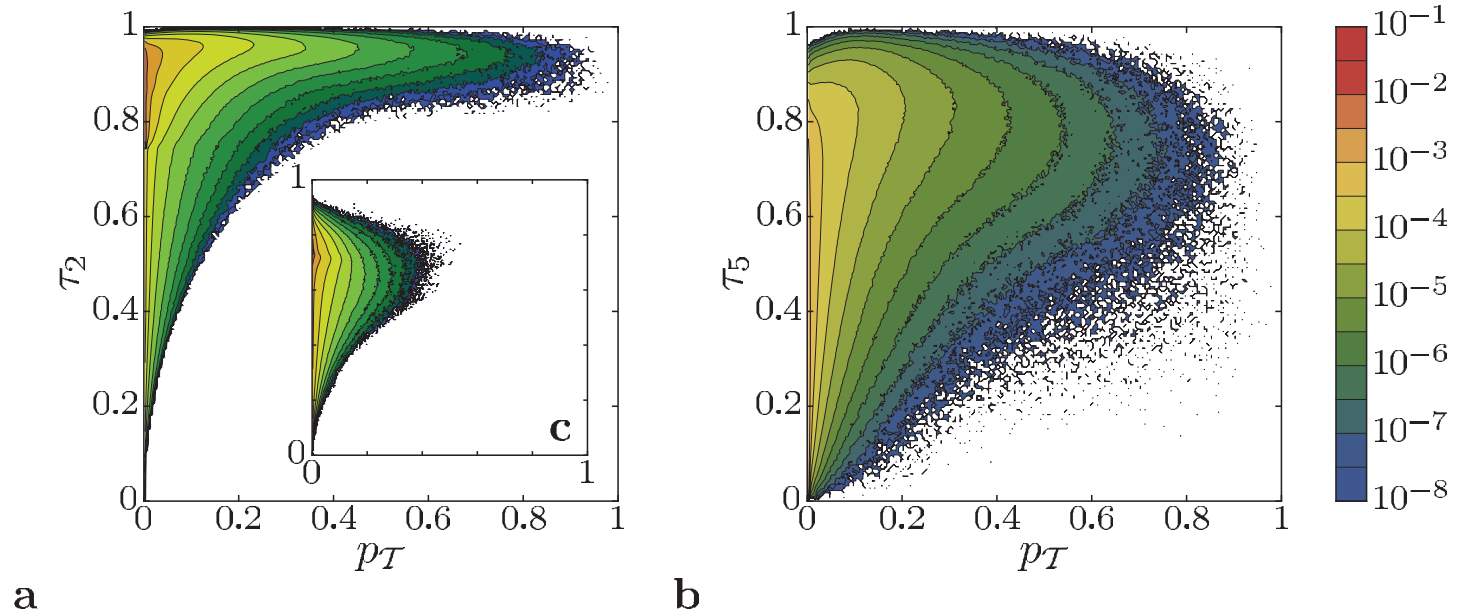


c

random configurations

Open questions – Perspectives

- the rôle of entanglement



- necessary *and* sufficient?
- physical characteristics of the efficient configurations?
- quantitative theory/sensitive experimental tests!

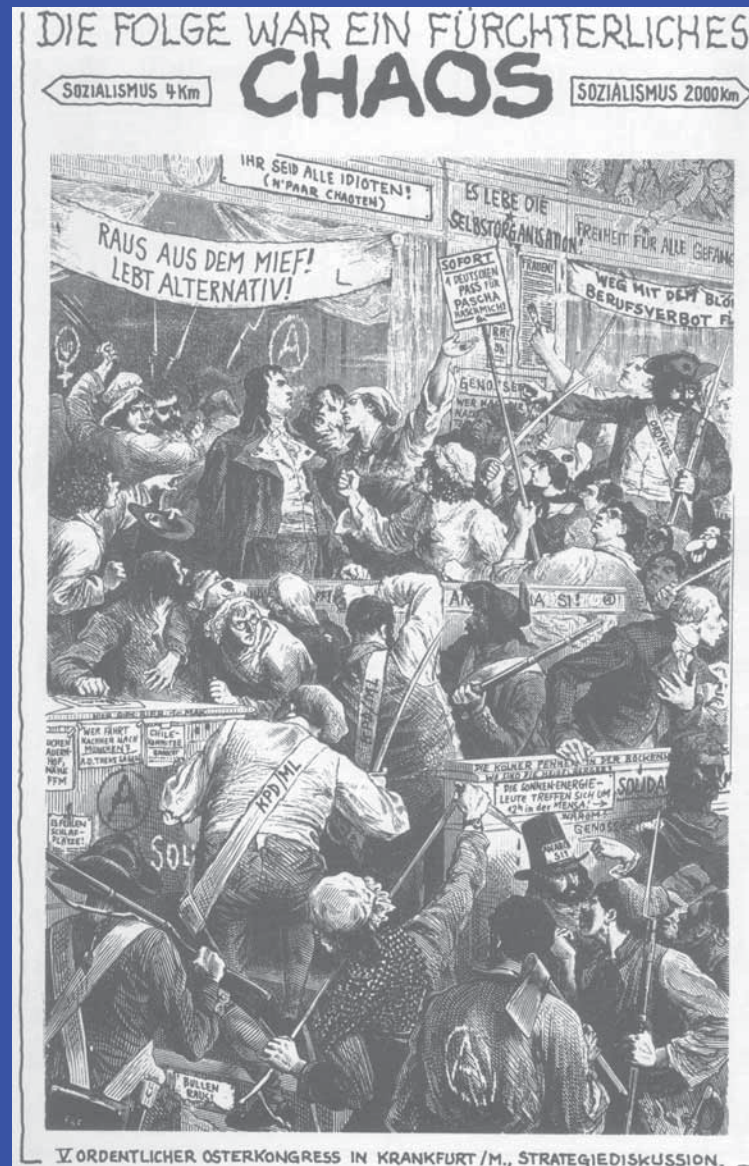
- hallmark of entanglement beyond coherence, in these systems?
- evolutionary advantage of entanglement?

Literature - School 2011 - etc

- more in – **T. Scholak et al., arXiv:0912.3560** –
- School and Workshop on
”**New Trends in Quantum Dynamics and Quantum Entanglement**”
at ICTP Trieste, February 14-25, 2011
- **Freiburg M.Sc. in Physics – fully taught in English**, starting winter term 2011/2012
- **Freiburg Research Focus on Quantum Efficiency** – tenure track Junior Professor (assistant professor) position to come up soon

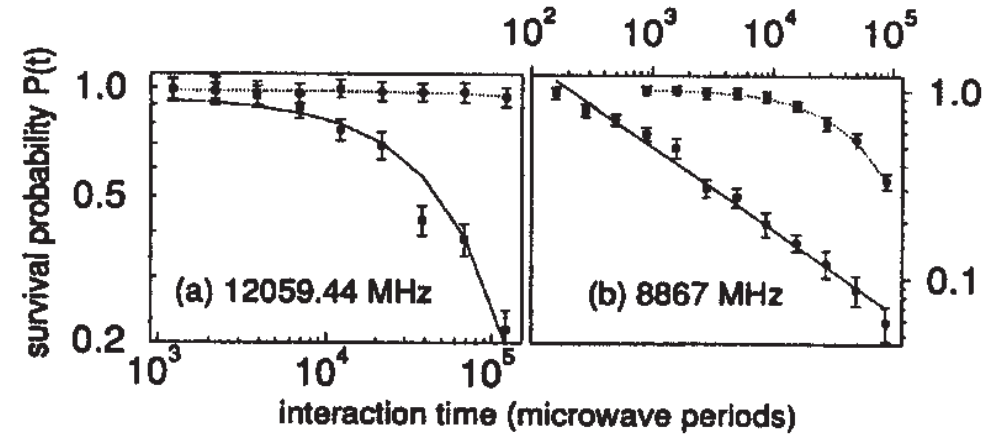
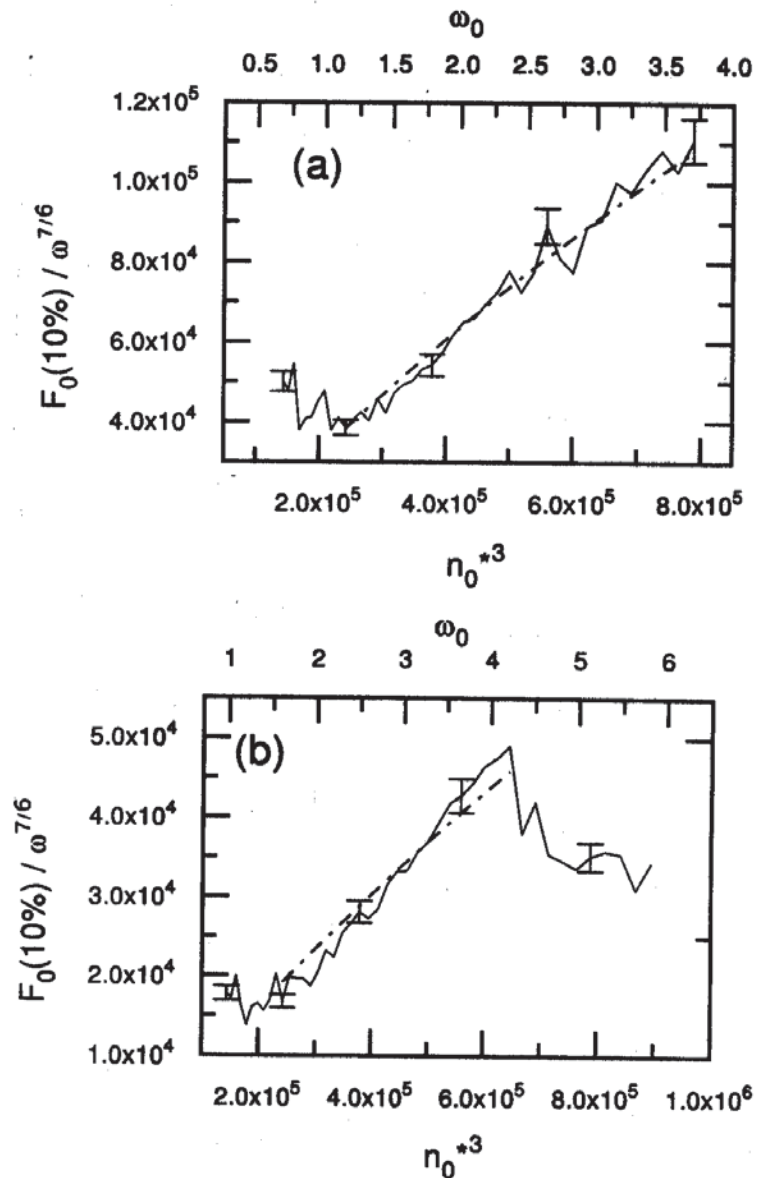
www.quantum.uni-freiburg.de

Complex quantum dynamics bear beautiful surprises



Welcome, if you want to join us!

Open questions – a Grand Challenge project



↑ algebraic decay of survival probability, for appropriate driving frequency and intensity, $P_{\text{surv}} \sim t^{-0.44}$

[A.B. et al., 1995; see also Fu et al., 1990]

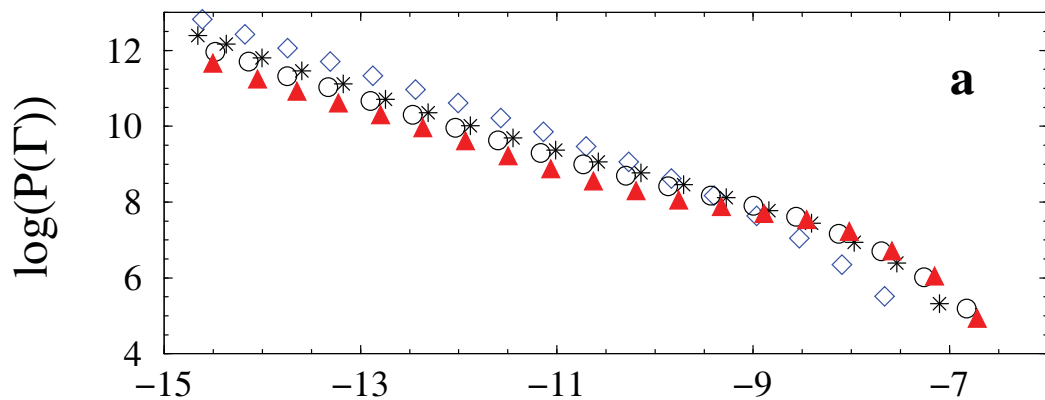
← apparently enhanced ionization of alkali Rydberg states

[O. Benson et al., 1995]

Statistics of decay rates (global)

(a) 1D hydrogen, $n_0 = 100$, $\omega/2\pi = 13.16 \dots 16.45$ GHz, $\xi/N = 0.25$
 (diamonds), 0.5 (stars), 1.0 (circles), 2.0 (pyramids)

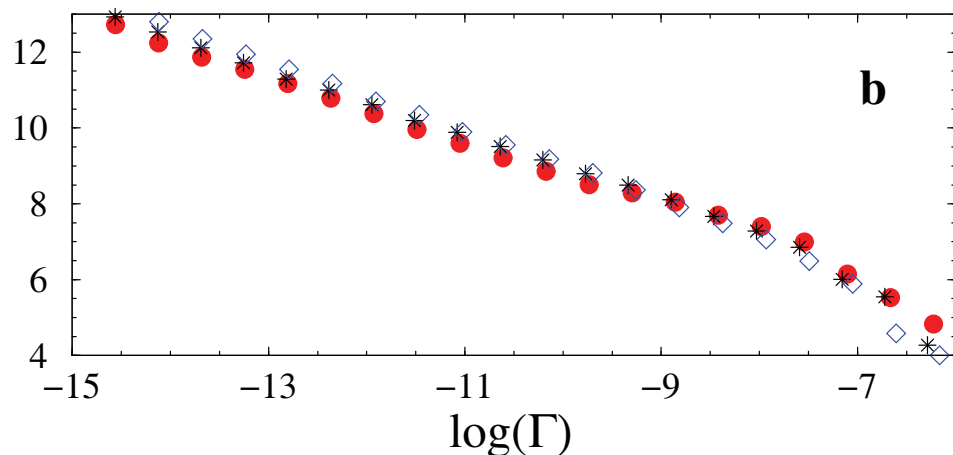
(b) 3D hydrogen, $n_0 = 70$, $\omega/2\pi = 35.5 \dots 36.1$ GHz, dito [S. Wimberger et al. 2002]



→ 1D and 3D exhibit $p(\Gamma) \sim \Gamma^{-1}$, for $\xi/N = 0.25$, in quantitative agreement with 1D Anderson!

→ emerging knee for increasing ξ/N (→ elliptic and separatrix states)

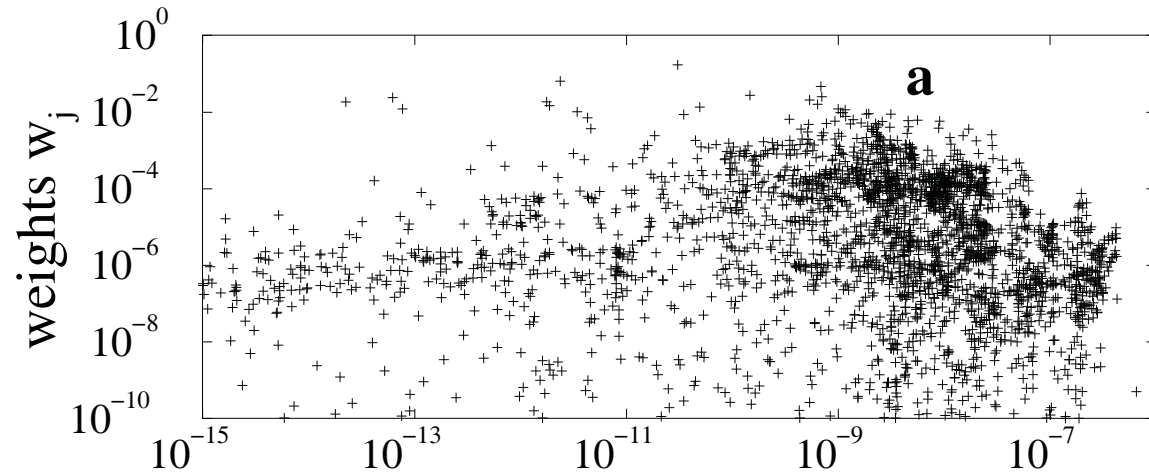
[Geisel et al. 1986, AB & Delande 1995, Ketzmerick et al. 2000]



→ l -dependent phase space structure for 3D!

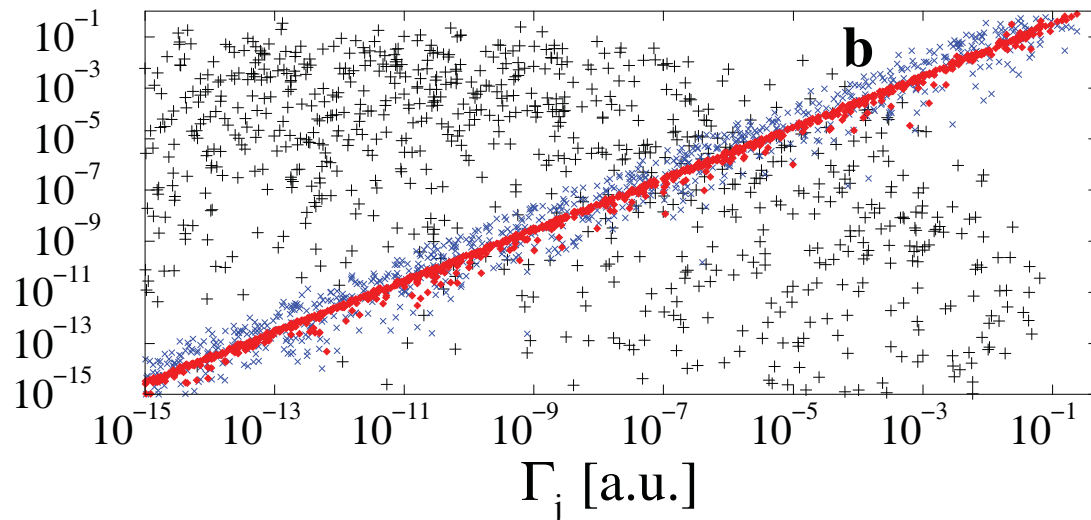
Weight distribution (local)

3D atom (top) vs 1D Anderson model (bottom)



→ 3D atom:

$$n_0 = 70, \ell_0 = 0, m_0 = 0, \\ n_{\text{edge}} \simeq 100$$

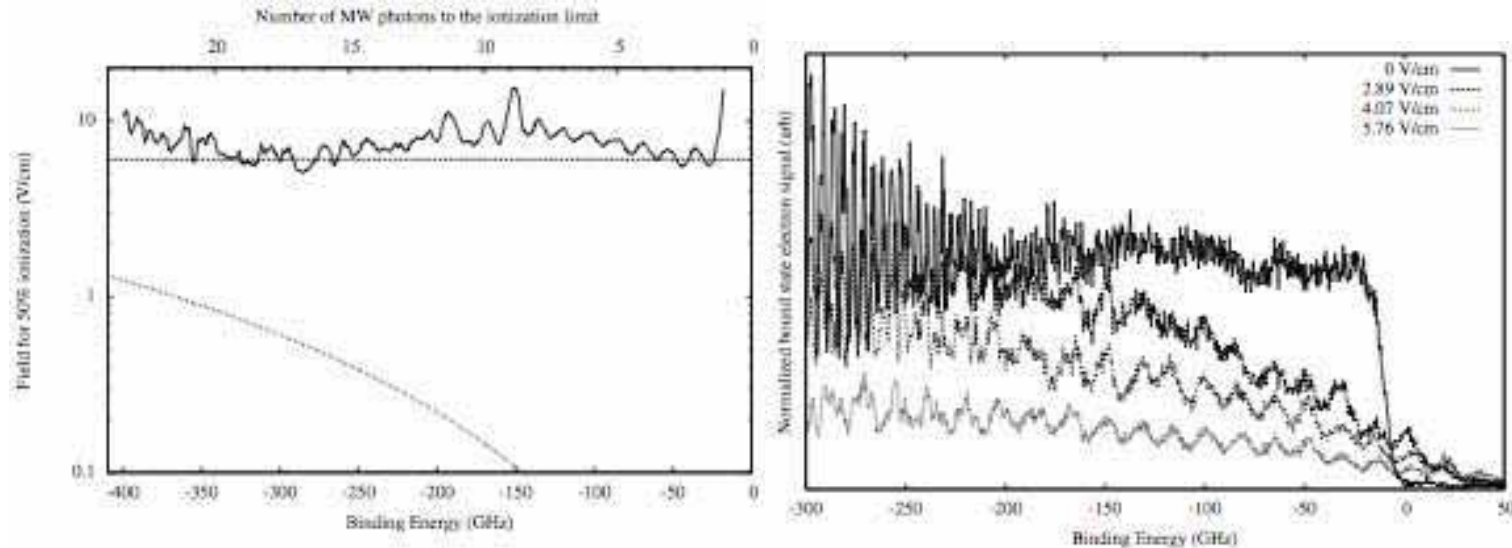


→ 1D Anderson: half open 1D
sample of length $N = 1000$,
decay from $n_{\text{edge}} \simeq 1000$,
 $n_0 = 900$, $n_0 = 999$,
 $n_0 = 1000$

– generically $w_j \approx \Gamma_j$ –

Conclusion – Perspectives

- experimental verification
(Gurian, Maeda & Gallagher, preprint 3rd April 2009)



- why wasn't that done before???
- could not excite atoms up to $n_0 > 130$ – now: reach $n_0 \simeq 450$!!!
- experiments appear to suggest microwave-assisted recombination from the continuum
- is there any signature of the large size of the atomic initial state at one-photon threshold? $n_0 = 230 \rightarrow \langle r \rangle \simeq 2 \times n_0^2 \simeq 10 \mu m$

A. Schelle, D. Delande, -, PRL 102, 183001 (2009)